



"BABEŞ-BOLYAI" University from Cluj-Napoca
Faculty of Chemistry and Chemical Engineering
Department of Chemistry



Laboratory of Fine Organic and Heterocyclic Stereosynthesis

<http://chem.ubbcluj.ro/~darab>



Ing. Maria Cristina MORAR (married HĂDĂREAN)

"Novel (hyper)conjugated (oxazolidin)thiazolidine and melamine-dendritic compounds obtained by diastereoselective or iterative synthesis, with potential biomedical or electrochemical applications and as organic materials"

PhD Thesis Abstract

Committee Members:

President	Prof. Habil. Dr. Ing. PAIZS Csaba	Universitatea "Babeş-Bolyai" Cluj-Napoca
Reviewer	Prof. Dr. Ionel MANGALAGIU	Universitatea "A. I. Cuza" Iaşi
Reviewer	Conf. Habil. Dr. Ileana FĂRCĂŞANU	Universitatea din Bucureşti
Reviewer	Conf. Dr. Ana Maria TEREÇ	Universitatea "Babeş-Bolyai" Cluj-Napoca
Scientific advisor	Prof. Dr. Ing. Mircea Darabantu (HDR)	Universitatea "Babeş-Bolyai" Cluj-Napoca

Cluj-Napoca
Iunie 2018

GENERAL CONTENTS

Abbreviations

Chapter I

Synthesis and stereochemistry of new 1,3-thiazolidine systems based on 2-amino-2-(mercaptomethyl)propane-1,3-diol: 4,4-bis(hydroxymethyl)-1,3-thiazolidines and c-5-hydroxymethyl-3-oxa-7-thia-r-1-azabicyclo[3.3.0]octanes

Abstract

Introduction

Results and Discussion

1. Synthesis and structure of novel 2-aryl-1,3-thiazolidine series
 - 1.1. Synthesis
 - 1.2. Structural assignments
 - (a) Preferred arrangement of the Ar C-2-ligand
 - (b) Assignment of the relative configuration at the N-3 position by means of ¹H RMN spectra.
 - (c) The anomeric effect occurring in the >N-C-S- sequence
 - (d) The ring chain-tautomerism in case of 2 aril-1,3 thiazolidine compounds
2. Synthesis and structure of novel c-5-hydroxymethyl-3-oxa-7-thia-r-1-azabicyclo[3.3.0]octanes
 - 2.1. Synthesis
 - 2.2. Rationalisation of the synthetic results
 - 2.3. Additional structural evidence

Conclions

Experimental Section

References

Annexes

Chapter II

New p-aminophenol based dendritic melamines. Iterative synthesis, structure and electrochemical characterisation

Abstract

Introduction

Results and Discussion

1. Synthesis
2. Preliminary structural assignments
3. Electrochemical characterisation
 - 3.1. Cyclic voltammetry
 - 3.2. Influence of the starting potential
 - 3.3. Reproducibility
 - 3.4. Influence of repetitive potential cycling

Conclions

Experimental Section

References

Annexes

Chapter III

Design, synthesis and structure of novel G-2 melamine-based dendrimers incorporating 4-(n-octyloxy)aniline as a peripheral unit

Abstract

Introduction

Results and Discussion

1. Synthesis

1.1. Design

1.2. Synthesis of *N*-substituted tripoded melamine with phenyl-4-oxyalkanoate units, C1 and C3, as central dendritic building blocks

1.3. Synthesis of G-1 dendrons

1.4. *Synthesis of G-2 dendrimers*

2. Structural assignments

2.1. Assignments based on DFT calculations of G-0 and G-1 dendrons: optimal geometry and solvation effects

2.2. Assignments by means of NMR and IR spectroscopy

2.2.1. Rotational diastereomerism at dendritic level

2.2.2. Dendritic solvation

2.2.3. Assignment of ionic interactions in dendrimers **12**, **13** and **14**

2.2.4. Assignments by means of 2D-1H-DOSY NMR in tandem with DFT calculations at dendritic level

2.3. Assignments by means of TEM analyses

Conclusions

Experimental Section

References

Annexes

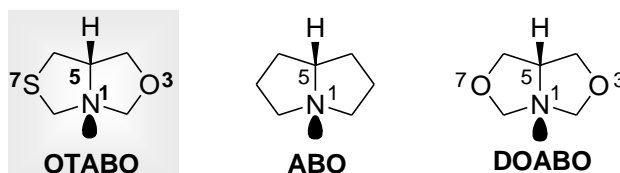
Keywords: anomeric effect, cysteinols, 1,3-oxazolidines, ring-chain tautomerism, 1,3-thiazolidines, *p*-aminophenol, cyclic voltammetry, dendrimers, DFT, melamines, amination, nano-aggregates, 4-(*n*-octyloxy)aniline

Chapter I

Synthesis and stereochemistry of new 1,3-thiazolidine systems based on 2-amino-2-(mercaptomethyl)propane-1,3-diol: 4,4-bis(hydroxymethyl)-1,3-thiazolidines and *c*-5-hydroxymethyl-3-oxa-7-thia-*r*-1-azabicyclo[3.3.0]octanes

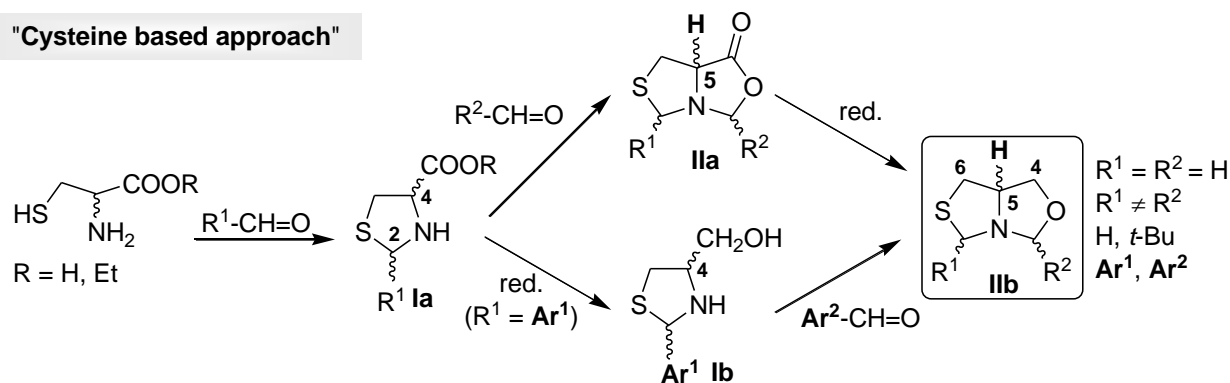
INTRODUCTION

The heterocyclic saturated *cis*-fused system 3-oxa-7-thia-*r*-1-azabicyclo[3.3.0]-*c*-5-octane (OTABO) has been known since the 1970s.¹ This compound can be viewed as a chiral (1*R**,5*S**) 3-oxa-7-thia analogue of the core alkaloid pyrrolizidine, *r*-1-azabicyclo[3.3.0]-*c*-5-octane (ABO), as well an *S*-analogue of the much better documented 3,7-dioxa-*r*-1-azabicyclo[3.3.0]-*c*-5-octane (DOABO) (Scheme 1).²



Scheme 1

Currently, there are two known routes by which the thiazolidin-oxazolidine skeleton of type OTABO can be built. In the method we named the “Cysteine based approach” (Scheme 2),² one of its enantiomers (optionally as ethyl cysteinate) is sequentially cyclo-condensed with aldehydes, proceeding via 1,3-thiazolidines **1a**, to yield thiazolidin-azalactones of type **11a**.^{1, 3}



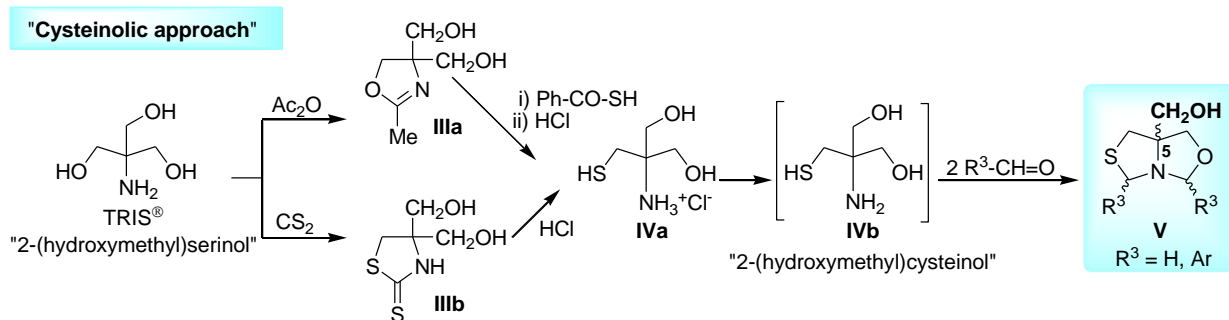
Scheme 2

Their reduction provides series OTABO **11b**, including the parent system: $R^1 = R^2 = H$.^{1b} In the 1980s, the above chemistry was developed by Seebach et al.^{3c, 3d} as an *R*-cysteine diastereoselective cyclisation (**11a**, $R^1 = t\text{-Bu}$, $R^2 = H$) toward the benefit of subsequent asymmetric functionalisation *via* metallation at the C-5 position of **11a**.⁴ The same methodology was applied to obtain 2,4-disubstituted-1,3-thiazolidines **1a** with impact upon the stereochemistry of saturated five-membered rings⁵ and notable bioactivity.⁶

Recently, Saiz et al.^{7, 7a} reported an alternative pathway directed toward optically active derivatives of OTABO **11b**, specifically *via* 1,3-thiazolidines **1b** (Scheme 2). This strategy also uses a two-step manipulation with different aryl-aldehydes, $\text{Ar}^{1(2)}\text{-CH=O}$. The successful preparation of series (4*S*)-**1a**, **-b** and (5*S*)-**11b** was claimed to access a potential DCL (Dynamic Combinatorial Library) because, depending on the electrophilicity of $\text{Ar}^{1(2)}\text{-CH=O}$, thia- vs. oxaminalisation equilibrium distributions were observed.

The synthesis of the first thiazolidin-oxazolidine condensed system OTABO (Scheme 1), which was singly functionalised at the C-5 position with a hydroxymethyl group, was reported by us based on the “Cysteinolic approach” (Scheme 3, compound **V**, $R^3 = H$).²

The key intermediate in this approach is the thioamino-1,3-diol **IVb**, which is otherwise known as a “2-(hydroxymethyl)cysteinol” (stable as its hydrochloride **IVa** only)^{2a, 2b} and has either the 1,3-oxazoline **111a** or the 1,3-thiazolidin-2-thione **111b** as precursors; the latter was proposed by Saiz et al.^{7b} recently.



Scheme 3

One must examine the essential differences between the two series of bicycles OTABO known so far, which are **IIb** (Scheme 2) and **V** (Scheme 3). While compounds **IIb** are optically active with no further developments regarding the chemistry on the C-(4)-C-(5)-C-(6) sequence, series **V**, although a racemate, still contains an exploitable functionality at C-5.

The increased interest in thiazolidin-oxazolidines OTABO impelled us to enlarge the “*Cysteinolic approach*” by targeting new compounds in series **V**, which arise from the consecutive cyclocondensation of “2-(hydroxymethyl)cysteinol” **IVb** with two different aldehydes. In this regard, the previously unreported tandem reaction using first Ar-CH=O and then H₂C=O was interesting to us because of the very distinct reactivity of these electrophiles against the triple nucleophile **IVb**. No similar synthetic or structural approaches have been reported to date.

RESULTS AND DISCUSSION

1. Synthesis and structure of novel 2-aryl-1,3-thiazolidine series

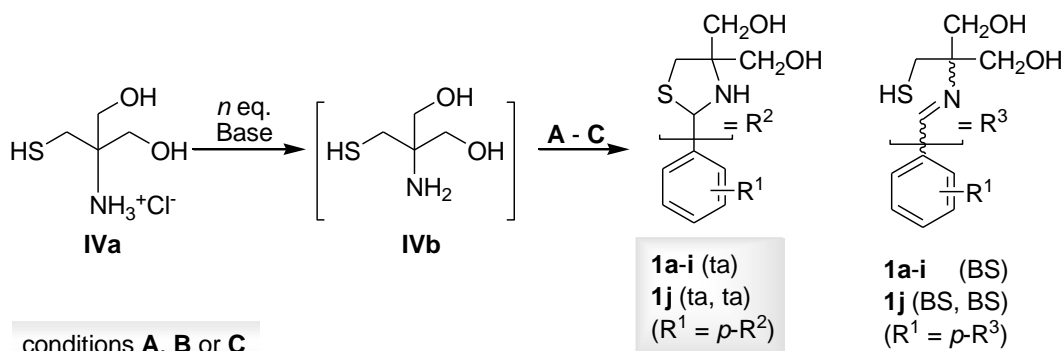
Initially, we examined the thiaminalisation of the free base **IVb**, which is derived from **IVa** (Scheme 3), via reaction with various aryl-(di)aldehydes to enact a classically disfavoured Baldwin’s 5-*endo-trig* cyclisation.⁸ We chose to explore a larger diversity of carbonyl electrophiles than were investigated in the synthesis of 1,3-thiazolidines **Ia** (Scheme 2). In this context, the use of thionated (*pseudo*)ephedrine⁹ or the much simpler 2-aminoethanethiol (*cysteamine*) were reported.¹⁰ The resulting cyclocondensates were investigated via conformational analysis,^{10a} as biomolecules^{10b, 10c} and ring-chain tautomers.¹¹

The aim of this section is to report the synthesis of a new family of 2-aryl-4,4-bis(hydroxymethyl)-1,3-thiazolidines and examine the structure of these molecules in terms of configurational analysis, anomeric effects and ring-chain tautomerism. These properties would be used as the basis for the next ring closure to generate new thiazolidin-oxazolidine derivatives **V** (Scheme 3).

1.1. Synthesis

Scheme 4 depicts our first step, which was thiaminalisation, and the isolated yields from reactions using a range of aryl-(di)aldehydes under three different sets of conditions.

In the presence of a stoichiometric amount of aryl-(di)aldehyde (**a-i**), the free base **IVb** was generated in situ from **IVa** via acid-base interchange. Because **IVb** exhibited high redox instability,² three types of reaction conditions, **A-C**, were tested. All three conditions employed mild conditions and an inert atmosphere. We previously reported^{2a, 2b} the isolation of a type DOABO dimeric *S,S-cis*-fused oxazolidine (Scheme 1) as a side product of the reaction between **IVb** (6% partial conversion) and two molar equivalents of formaldehyde, yielding derivative **V** (R³ = H, 94% conversion, Scheme 3). Therefore, we have been cautious ever since because formaldehyde acted not only as an electrophile, but also as an oxidant acting on **IVb**. Therefore, it was clear to us that the thiaminalisations depicted in Scheme 4 “trapped” **IVb** using our carbonyl electrophiles with moderate success. The lowest yield was in the case of *p*-nitrobenzaldehyde, which contained a nitro group that can act as another oxidant for the thiol group (compound **1a**, method **A**),^{7c} and the results confirmed the above suspicion. Even if milder conditions were applied, e.g., **C**, the result was almost the same. All of the other investigated aryl-(di)aldehydes, **b-i**, demonstrated that our protocols were viable for generating the product in medium to satisfactory yields.



conditions **A, B** or **C**

1 eq. (*o*-, *m*-, *p*-) R¹-C₆H₄-CH=O **a-h** (→ **1a-h**); 0.5 eq. *p*-C₆H₄(CH=O)₂ **i** (→ **1i, 1j**)

A: 0.5 eq. K₂CO₃ aq. / Benzene / Dean-Stark trap / reflux / 6-8 h / N₂

B: 1.0 eq. Et₃N / EtOH / reflux / 8 - 10 h / N₂

C: 1.0 eq. Et₃N / EtOH / r.t. / 48 h / N₂

No.	R ¹	Method	Yield (%)	Isolation	Assigned as:
1a	<i>p</i> -O ₂ N	A	15	c.c. ^a	ta ^b
1b	<i>p</i> -Cl	C	36	d.c. ^c	ta
1c	<i>p</i> -Br	C	55	d.c.	ta
1d	H	A	51	c.c.	ta
		C	52	d.c.	ta
1e	<i>m</i> -HO	B	40	c.c.	ta
1f	<i>p</i> -HO	B	40	c.c.	ta
1g	<i>o</i> -HO	B	50	c.c.	72:28 / (ta):(BS) ^d
1h	<i>p</i> -Me ₂ N	B	44	c.c.	ta
1i^e	<i>p</i> -O=CH	C	-	-	ta
1j	<i>p</i> -R ²⁽³⁾	C	74 ^f	d.c.	94:1:5 / 1j (ta, ta): 1j (BS, BS): 1i (ta)

^acolumn chromatography. ^b1,3-thiazolidina (NMR, DMSO-*d*₆). ^cdirect crystallisation. ^dSchiff Base (NMR, DMSO-*d*₆).

^eSide product in the synthesis of **1j**. ^fAs total conversion of **IVa** into **1j+1i**

Scheme 4

Because the dimeric compound **1j** exhibited a low solubility in common solvents, it was isolated as a material contaminated with 5% of its precursor, the mono-thiazolidine **1i**.

1.2. Structural assignments

Our structural investigations were based on NMR (in solution) and IR spectroscopy (in solid state) in tandem with DFT calculations.

The NMR spectra of condensates **1a-j** established their identity (Scheme 4) as exclusively (**1a-f**, **1h**, **1i**) or largely (**1g**, **1j**) the 1,3-thiazolidine forms (Table 1).

The 2D-¹H,¹H-NOESY chart for compound **1a** (Figure 1, dashed red lines) revealed that the thiazolidine-ring faces were sterically non-equivalent (*cis* vs. *trans*) (Scheme 5) because only one nOe interaction H-2 / CH₂OH was observed.

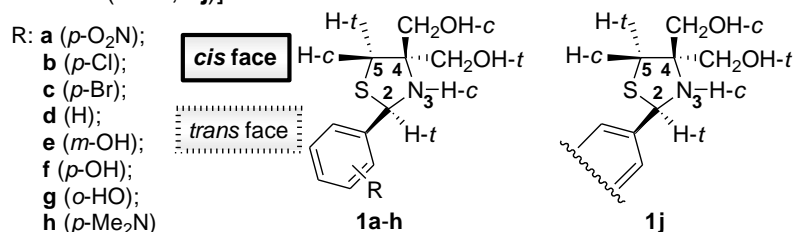
Therefore, the saturated heterocyclic skeleton was heterofacial,¹² with two stereogenic centres located at C-2 and N-3. In contrast to the other 1,3-thiazolidines, e.g., of type **1a** (Scheme 2)^{6b} or those built on thionated (*pseudo*)ephedrine,⁹ no epimerisation occurred at C-2. Therefore, we could adopt the Ar-ligand at C-2 position as a fiducial substituent.¹² The remaining exocyclic ligands, N-H, C(5)-H and C-CH₂OH are henceforth referred to with the use of descriptors: -*c* (*cis*) and -*t* (*trans*).

(a) Preferred arrangement of the Ar C-2-ligand

The Ar C-2 ligand was placed in a *pseudo*-equatorial position, as in conformers **1a** (*Ec*-₂) ⇌ **1a** (*En*), with a dominant bisectonal orientation. This stereochemistry promoted the lower field absorption of the CH₂OH-*c* protons relative to the CH₂OH-*t*. Mutatis-mutandis, δ(OH-*c*) was higher than δ(OH-*t*) by approximately 0.2-0.3 ppm.

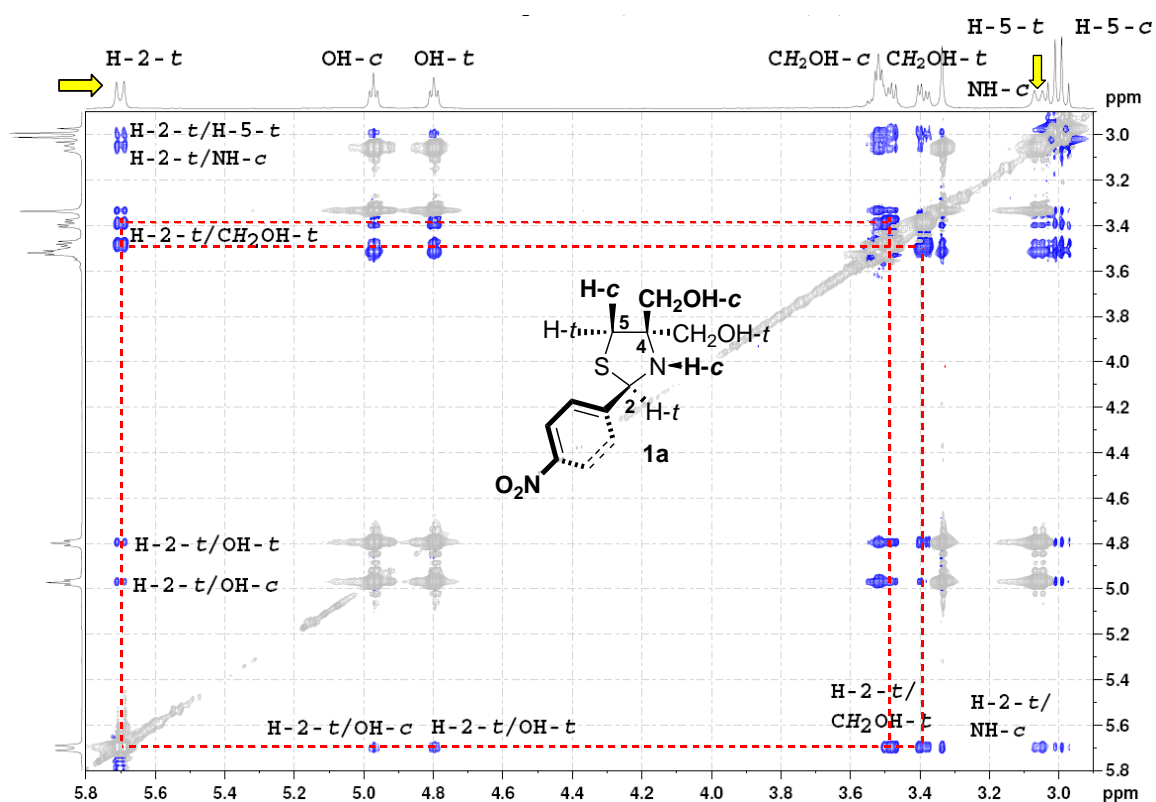
(b) Assignment of the relative configuration at the N-3 position

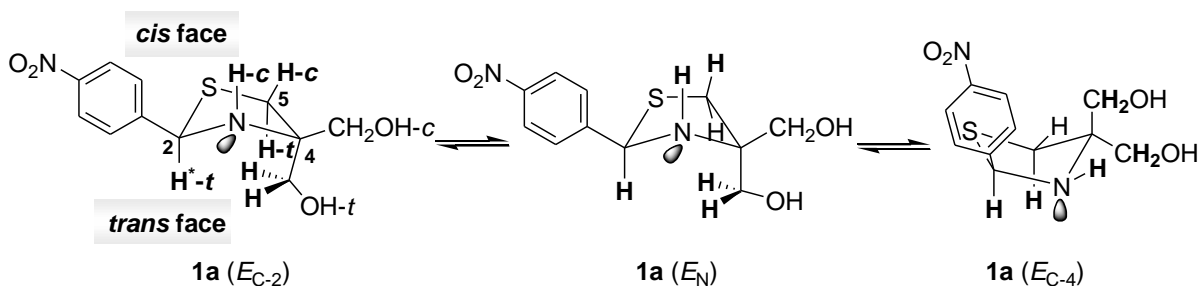
Table 1. Relevant ^1H NMR data of compounds **1a-h** and **1j** [DMSO- d_6 , 298 K, on 500 MHz timescale (**1a**), 300 MHz timescale (**1b-h**, **1j**)]



No.	Face	H-2- <i>t</i>	NH- <i>c</i>	CH $_2$ OH- <i>c</i> , - <i>t</i>	OH- <i>c</i> , - <i>t</i>	H-5- <i>c</i> , - <i>t</i>
1a	<i>cis</i>		3.06 (d, 11.5) ^a	3.54 (dd), 3.51 (dd)	4.97 (t) ^b	2.99 (d)
	<i>trans</i>	5.70 (d, 11.0) ^a		3.48 (dd), 3.39 (dd)	4.80 (t)	3.02 (d)
1b	<i>cis</i>		Not detected	3.57 (d), 3.53 (d)	4.90 (bs)	2.97 (d)
	<i>trans</i>	5.54 (s)		3.45 (d), 3.33 (d)		3.01 (d)
1c	<i>cis</i>		2.87 (d, 11.4)	3.57 (d), 3.53 (d)	4.99 (bs)	2.96 (d)
	<i>trans</i>	5.52 (d, 10.5)		3.45 (d), 3.33 (d)		3.01 (d)
1d	<i>cis</i>		2.86 (d, 12.0)	3.63 (d), 3.57 (d)	5.07 (t)	2.99 (d)
	<i>trans</i>	5.54 (d, 12.0)		3.47 (dd), 3.34 (dd)	4.77 (t)	3.04 (d)
1e	<i>cis</i>		2.79 (d, 12.0)	3.59 (s)	5.07 (bs)	2.98 (s)
	<i>trans</i>	5.44 (d, 12.0)		3.42 (s), 3.33 (s)	4.75 (bs)	
1f	<i>cis</i>		2.70 (d, 12.3)	3.59 (dd), 3.55 (dd)	5.04 (t)	2.94 (d)
	<i>trans</i>	5.42 (d, 12.0)		3.42 (dd), 3.29 (dd)	4.71 (t)	2.99 (d)
1g^c	<i>cis</i>		3.30 (d, 12.3)	3.59 (bs)	5.04 (bs)	2.90 (d)
	<i>trans</i>	5.70 (d, 9.9)		3.45 (bd), 3.34 (bd)	4.75 (bs)	2.96 (d)
1h	<i>cis</i>		2.70 (bd, 11.7)	3.61 (bd), 3.56 (bd)	5.05 (t)	2.95 (bd)
	<i>trans</i>	5.42 (bd, 10.5)		3.43 (bdd), 3.26 (bdd)	4.71 (bdd) ^d	3.00 (bd)
1j^e	<i>cis</i>		2.85 (d, 11.7)	3.60 (d), 3.54 (d)	5.04 (t)	2.97 (d)
	<i>trans</i>	5.53 (d, 11.1)		3.45 (dd), 3.33 (dd)	4.76 (t)	3.01 (d)

^aNon-averaged $^3J_{\text{H,H}}(\text{NH-CH})$ values; ^bDoublet of doublets as a triplet. ^cAs the main ring-chain tautomer, 72% 1,3-thiazolidine **1g**, see later discussion. ^dbdd: broad doublet of doublets. ^eAs the main ring-chain tautomer, 99% double 1,3-thiazolidine *meso*-, *rac*-**1j** see discussion.





***bold face**: nOe interactions between protons in a given conformer as disclosed by the 2D- ^1H , ^1H -NOESY Chart of compound **1a** (Figure 2)

Scheme 5

Except for compound **1b**, a noteworthy vicinal $^3J_{\text{H,H}}$ (NH-CH) coupling pattern, which was approximately 11.5 Hz, was observed (e.g., thiazolidine **1a**, Figure 1, yellow arrows). Due to the fast pseudorotation of the pentaheterocycle, this was an averaged J value, mediating the environments illustrated in Scheme 5. However, the magnitude of the $^3J_{\text{H,H}}$ (NH-CH) coupling pattern allowed us to estimate the NH proton life time of its spin state, τ (s), where $\tau > 1 / ^3J [\text{Hz}, \text{s}^{-1}] \sim 0.09$ s.^{13, 13a} The size of the τ value precluded the N -pyramidal inversion,^{9, 13b} as well as an acid-base interchange, implying the existence of an NH group.^{13c} The same shape of the NH resonance (in CDCl_3) in epimeric 2-aryl-1,3-thiazolidines **1a** and **1b** (Scheme 2, $\text{R}^1 = \text{Ar}$) was listed, with no comments, by Saiz et al.^{7a} To our knowledge, to the above unusual splitting of an amine proton (Figure 1),^{13a, 13b} no attention was paid by other authors,^{3e, 5a, 5b, 6a, 9, 10a, 11b, 11c} including those investigating 2-aryl-1,3-thiazolidines.^{3e, 6a, 11b} Based on the $^3J_{\text{H,H}}$ (NH-CH) value and the NOESY Chart for compound **1a**, we ascertained a *pseudo-trans* (ax-ax \rightleftharpoons ax-eq) relationship between H-2-*t* / NH-*c* (Scheme 5), in spite of the inadequacy of the Karplus equation^{10a, 14} for this fluctuation of the H-N-C-H dihedral angle magnitude in a five-membered saturated heterocycle.^{15a-c} In addition to the C-2 (R^*), a N (R^*) relative configuration, which is stable for at least 0.09 s, can be assigned.

(c) The anomeric effect occurring in the $>\text{N-C-S-}$ sequence

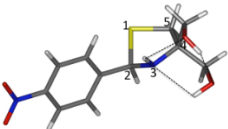
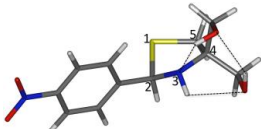
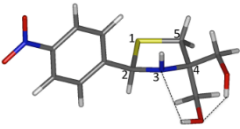
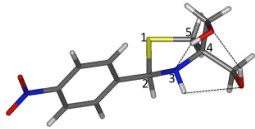
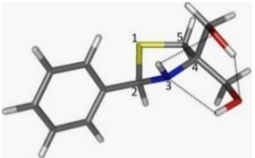
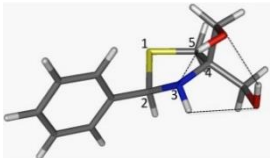
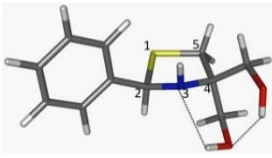
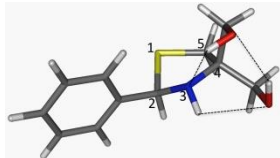
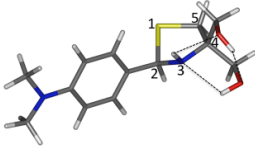
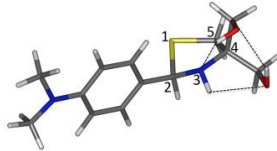
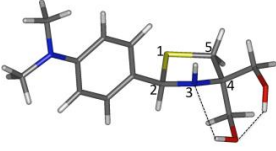
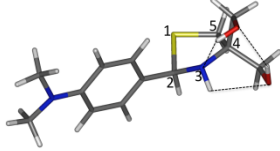
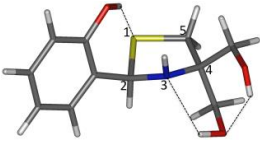
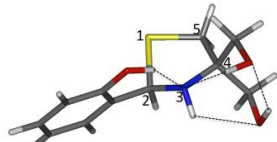
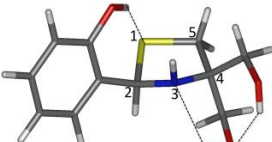
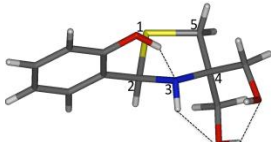
We mention the related configurational analysis of Sélambaron et al.^{5a} concerning the molecular structure of a dimeric N,N' -methylenebis-1,3-thiazolidine of type **1a** (Scheme 2). The *pseudo-axial* orientation of its N,N' -methylene exocyclic ligand against the *pseudo-equatorial* orientation of the nitrogen lone pair (lpN-eq) were put in conjunction with the following: i) the decrease in the bond length of N-C(2) (-0.019 Å) vs. N-C(4) and ii) the increase of the S-C(2) bond length (+0.035 Å) against S-C(5). These findings provide evidence for an *endo* anomeric effect arising from a well-positioned donor, lpN-eq, overlapping with an appropriately oriented acceptor, which is the antiperiplanar antibonding $\sigma^*(\text{C-S})$ orbital. According to literature,^{16a} this is a general behaviour occurring in saturated 1,3- X,N pentaheterocycles ($X = \text{O}^{2b, 15c, 16, 17, \text{S}^{2b, 5, 10c}$), i.e., in those containing the $>\text{N-C-X-}$ sequence. The 1,3-thiazolidine system is, however, much less explored.

Because we were unable to obtain single crystals for a similar X-ray analysis of series **1**, we performed DFT calculations on compounds **1a**, **1d**, **1h** and **1g**; these compounds were chosen as representative due to the different electronic and steric influence of the Ar-ring R^1 -substituents (Chart 1, Table 2, Chart 2).

From several molecular arrangements, the optimised geometries, which were predicted by these calculations, agreed with the conformations of the envelope $E_{\text{C-2}}$, E_{N} and $E_{\text{C-4}}$ types described by ^1H NMR data analysis (Scheme 5, Chart 1). The two most stable conformers were differentiated by the steric relationship between ligands H-2 and NH. The *pseudo-trans* arrangement of the NH-*c* / H-2-*t* in 2-aryl-1,3-thiazolidines **1a**, **1d** and **1h**, conferred more stability than the alternative *pseudo-cis* arrangement in the gas phase, as well as in solution (Table 2). The differences in stability $\Delta(E, H \text{ or } G_{298}) < 0$, *pseudo-trans* against *pseudo-cis*, increased with the increasing electron donating character of the $p\text{-R}^1$ substituent $\text{NO}_2 < \text{H} < \text{NMe}_2$ (Table 2).

The noticeable “reversed” stabilisation in the case of compound **1g**, $\Delta(E, H \text{ or } G_{298}) > 0$, *pseudo-trans* against *pseudo-cis*, was not surprising because of the expected intramolecular hydrogen-bonding,

Chart 1. Optimised geometries of 2-aryl-1,3-thiazolidines **1a**, **1d**, **1h** and **1g** in the gas phase and in DMSO^a at the B3LYP/6-311++G** level of theory

Gas phase	DMSO		
1 (<i>pseudo-trans</i>) ^b	1 (<i>pseudo-cis</i>) ^b	1 (<i>pseudo-trans</i>)	1 (<i>pseudo-cis</i>)
a			
			
90.8 ^c	-157.4	89.5	-155.8
d			
			
90.3 ^c	-157.6	87.8	-156.0
h			
			
90.1 ^c	-157.4	88.4	-156.4
g			
			
90.2 ^c	-163.5	87.7	-161.5

^aPCM calculation using the CPCM polarisable conductor continuum model. ^bThe lpN and the proton H-2 are the references for the descriptors *pseudo-trans* and *pseudo-cis*. ^cThe H-N / C(2)-S dihedral angle (in degrees)

bisectonal-phenol α -(O)-H...lpN-ax (thiazolidine).

In the “thiaminalic zone” (>N-C-S-) of the selected compounds, the shortening of the N-C(2) bond with respect to N-C(4) [\sim (- 0.029 Å) in gas phase, \sim (- 0.025 Å) in DMSO] alongside the increased length of the C(2)-S bond relative to S-C(5) [\sim (+ 0.065 Å) in gas phase, \sim (+ 0.077 Å) in DMSO] were more pronounced in conformers **1** (*pseudo-trans*).

To examine these geometric fluctuations with respect to the manifestation of an anomeric effect we performed NBO and $^3J_{H,H}(\text{NH-CH})$ coupling constant analyses for 1,3-thiazolidine **1d** at the B3LYP/6-311++G** level of theory (Chart 2).

The E_{del} values for the hyperconjugation of lpN-eq $\rightarrow \sigma^* \text{C}(2)\text{-S}$ in **1d** (*pseudo-trans*) were the highest encountered in our investigation [50.12 kJ/mol (gas phase), 55.35 kJ/mol (DMSO)] and are in line with the modifications of the bond distances in the same region. We were able to assign the structures of our 1,3-thiazolidines using “bonding / non-bonding” formulations (Scheme 6).¹⁷

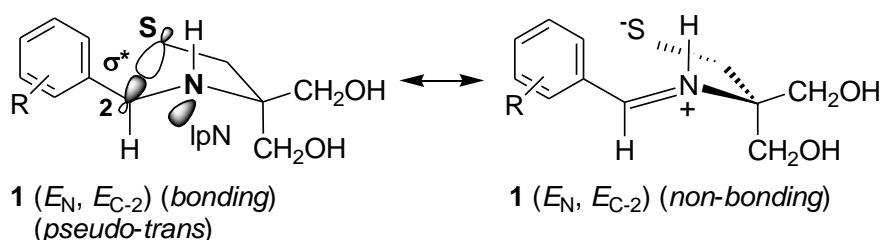
To this end, the **1d** (*pseudo-trans*) calculated value of the $^3J_{H,H}(\text{NH-CH})$ coupling in solution (11.7 Hz, Table 2) validated our experimental data, which was 11.5 Hz (Table 1).

Additionally, these $^3J_{H,H}(\text{NH-CH})$ constants are typically found in motifs such as >CH-NH-(C=X)- \leftrightarrow >CH-NH⁺=(C-X)⁻, (X = O, S, NH, C< etc.),^{13a, 13b} i.e., in those containing the nitrogen involved in partial double bonds formed because of a *stabilising* lpN $\rightarrow\pi$ conjugation. According to our data, a lpN $\rightarrow\sigma^*$ hyperconjugative relationship in >N-C-X- (X = S, O) sequences, symbolised as -NH-CH-X- \leftrightarrow -NH⁺=CH] [X⁻ can be deduced as well; this deduction requires a $^3J_{H,H}(\text{NH-CH})$ value. This diagnosis also applies for compound **1g**, in which the (*pseudo-trans*) conformer, which displays identical $^3J_{H,H}(\text{NH-CH}) = 11.1$ Hz values (calculation vs. experiment, Table 1) was less stable than the (*pseudo-cis*) one.

Table 2. Computed energies of 2-aryl-1,3-thiazolidines **1a**, **1d**, **1h** and **1g** in the gas phase and in DMSO^a (at the B3LYP/6-311++G** level of theory)

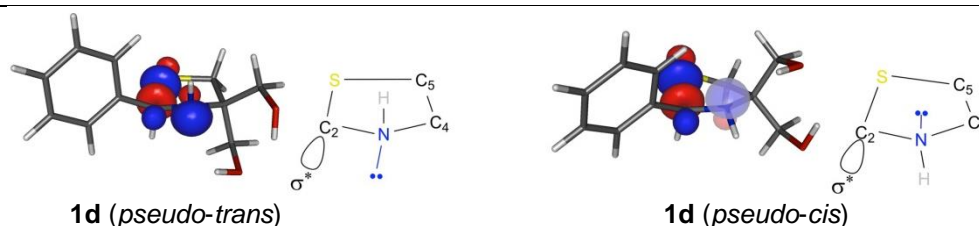
Stability, (kJ/mol) as 1 (<i>pseudo-trans</i>) ^b - 1 (<i>pseudo-cis</i>) ^b			Selected bond distances, d (Å) Contractions Δd (Å) as [N-C(2)] - [N-C(4)] < 0 Elongations Δd (Å) as [S-C(2)] - [S-C(5)] > 0				Selected hydrogen bond distances, d (Å) ^{c, d}		bond
ΔE	ΔH	ΔG_{298}	N-C(4)	N-C(2)	S-C(5)	S-C(2)	(N)H...O	(O)H...N	o-OH...X ^e
Gas phase									
			1a, 1d, 1h, 1g (<i>pseudo-trans</i>)						
- 6.44 a	- 5.40 a	- 6.01 a	1.482 a	1.449 a	1.829 a	1.885 a	2.369 a	2.441 a	-
- 8.55 d	- 7.69 d	- 9.21 d	1.480 d	1.451 d	1.829 d	1.887 d	2.409 d	2.381 d	-
- 9.45 h	- 8.49 h	- 9.51 h	1.479 h	1.452 h	1.828 h	1.891 h	2.437 h	2.371 h	-
+ 0.10 g	- 0.12 g	- 1.04 g	1.468 g	1.443 g	1.836 g	1.919 g	2.797 g	2.308 g	2.259 g
			- 0.033 a		+ 0.056 a				
			- 0.029 d		+ 0.058 d				
			- 0.027 h		+ 0.063 h				
			- 0.025 g		+ 0.083 g				
			1a, 1d, 1h, 1g (<i>pseudo-cis</i>)						
			1.488 a	1.464 a	1.832 a	1.850 a	2.372 a	2.402 a	-
			1.486 d	1.467 d	1.832 d	1.851 d	2.395 d	2.351 d	-
			1.485 h	1.470 h	1.831 h	1.855 h	2.411 h	2.321 h	-
			1.489 g	1.478 g	1.833 g	1.854 g	2.328 g	2.718 g	1.838 g
			- 0.024 a		+ 0.018 a				
			- 0.019 d		+ 0.019 d				
			- 0.015 h		+ 0.024 h				
			- 0.011 g		+ 0.021 g				
DMSO									
			1a, 1d, 1h, 1g (<i>pseudo-trans</i>)						
- 6.89 a	- 5.97 a	- 7.64 a	1.471 a	1.445 a	1.838 a	1.908 a	2.938 a	2.430 a	-
- 9.86 d	- 8.85 d	- 10.89 d	1.471 d	1.446 d	1.837 d	1.910 d	2.936 d	2.381 d	-
- 11.22 h	- 10.33 h	- 11.80 h	1.470 h	1.448 h	1.836 h	1.917 h	2.932 h	2.372 h	-
+ 7.39 g	+ 6.92 g	+ 4.53 g	1.470 g	1.444 g	1.838 g	1.923 g	2.901 g	2.427 g	2.236 g
			- 0.026 a		+ 0.070 a				
			- 0.025 d		+ 0.073 d				
			- 0.022 h		+ 0.081 h				
			- 0.026 g		+ 0.085 g				
			1a, 1d, 1h, 1g (<i>pseudo-cis</i>)						
			1.489 a	1.464 a	1.832 a	1.852 a	2.440 a	2.382 a	-
			1.488 d	1.467 d	1.832 d	1.853 d	2.450 d	2.339 d	-
			1.487 h	1.471 h	1.832 h	1.858 h	2.456 h	2.314 h	-
			1.480 g	1.474 g	1.844 g	1.874 g	2.464 g	3.002 g	1.798 g
			- 0.025 a		+ 0.020 a				
			- 0.021 d		+ 0.021 d				
			- 0.016 h		+ 0.026 h				
			- 0.006 g		+ 0.030 g				

^aPCM calculation using the CPCM polarisable conductor continuum model. ^bThe IpN and the proton H-2 are the references for the descriptors *pseudo-cis* and *pseudo-trans*. ^cIntramolecular hydrogen bonds involving the geminal hydroxymethyl groups only are not listed for reason of simplicity. ^d Σr_{vdw} (O, H) (sum of the van der Waals radii) = 2.60 Å. ^eX = S in **1g** (*pseudo-trans*), X = O in **1g** (*pseudo-cis*).



Scheme 6

Chart 2. Relevant energies ($E_{\text{del.}}$) of the NBO hyperconjugative interactions and $^3J_{\text{H,H}}(\text{NH-CH})$ coupling constant in the gas phase and in DMSO^a (at the B3LYP/6-311++G** level of theory) in 1,3-thiazolidine **1d**

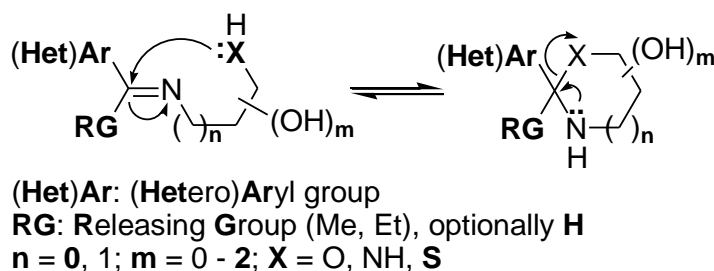


Stabilisation energies $E_{\text{del.}}$ as $\text{lpN-eq} \rightarrow \sigma^*$ (kJ/mol)							$^3J_{\text{H,H}}(\text{NH-CH})$ (Hz) ^b
State	C(2)-S	C(4)-C(5)	C(2)-H	C(4)-C(H ₂ OH-t)	C(4)-C(H ₂ OH-c)	C(2)-C(Ph)	
Gas phase	1d (pseudo-trans)						
	50.12	15.27	15.31	17.36	3.68	-	11.5
DMSO	1d (pseudo-cis)						
	-	5.82	26.44	17.41	11.88	9.79	5.0
DMSO	1d (pseudo-trans)						
	55.35	28.41	14.06	11.63	-	-	11.7
DMSO	1d (pseudo-cis)						
	-	6.40	24.89	17.36	11.05	10.21	5.3

^aPCM calculation using the CPCM polarisable conductor continuum model. ^bGIAO (Gauge-Independent Atomic Orbital) method for NMR chemical shift calculations was used.

(d) The ring chain-tautomerism

The ring-chain tautomerism of Schiff Bases derived from (hetero)aryl carbonyl compounds and amino(poly)(thi)ols involves the reversible nucleophilic addition of an XH group to an imine double bond and is well established (Scheme 7).¹¹ The situations in which X = S and n = 0, have received little attention.^{6a, 10c, 11b, 11c} To examine the condensates of **IVb** with aryl-(di)aldehydes **a-i** (Scheme 4), our studies utilized a combination of IR (in solid state) with NMR (in solution) data.

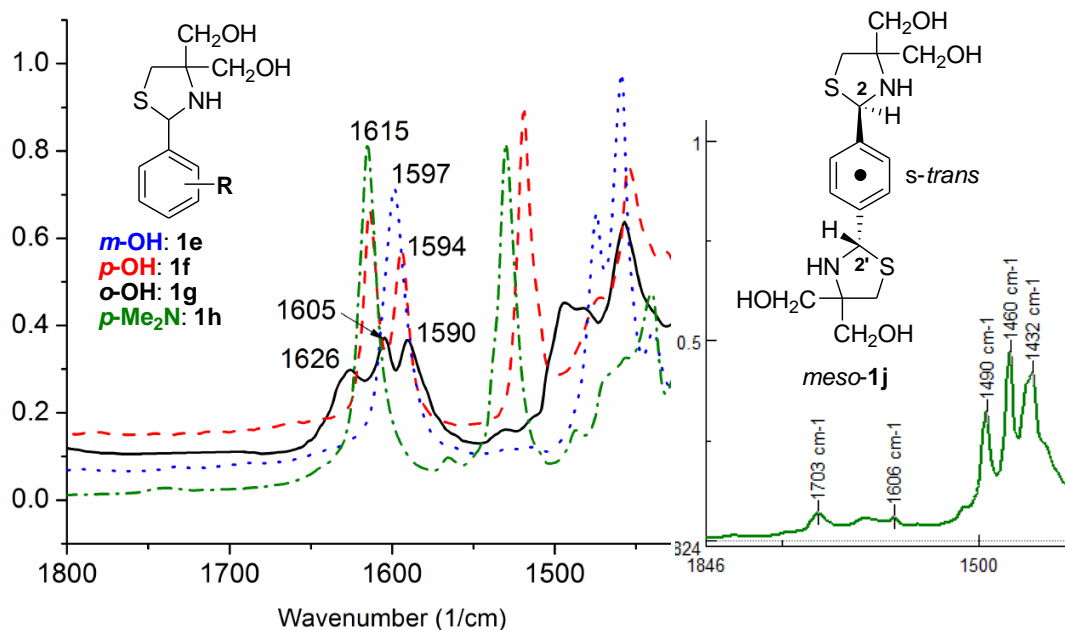


Scheme 7

In the solid state (Chart 3), the IR spectra of the mono-condensates **1a-h** displayed a typical band located in the aromatic region at approximately 1600 cm^{-1} ; we assigned this resonance to a conjugated $\nu_{\text{C}=\text{C}^{\text{sk}}}$ absorption and not to a $\nu_{\text{C}=\text{N}^{\text{sk}}}$ one.^{13b} The dimeric condensate **1j** exhibited the same band at 1606 cm^{-1} (Chart 3), but it was very weak (almost flat) and therefore consistent with the presence of a major C_i symmetric *meso-1j s-trans* form in the solid state. The signal observed at 1703 cm^{-1} ($\nu_{\text{C}=\text{O}^{\text{sk}}}$) indicated the previously mentioned contamination of compound **1j** with **1i** (Scheme 4).

In solution (Scheme 4, Figure 1 and Table 1), the NMR spectra identified the “cysteinolic” mono-condensates of aryl-aldehydes **a-f**, **h** and **i** as 1,3-thiazolidine ring-forms only. Meanwhile, the mono-condensate of salicylaldehyde **g**, was a mixture with a constant composition: **1g** (ta) (1,3-thiazolidine) 72% vs. **1g** (BS) (Schiff Base) 28%. Therefore, the ring-chain tautomerism in series **1a-i** existed only in the case of **1g** and manifested as a spontaneous equilibration attained when passing from the solid state to solution, i.e., a partial (28%) ring opening of **1g** (ta) towards **1g** (BS). In line with the literature data,^{11b-d} this general behaviour of series **1a-i** is not surprising considering the much higher nucleophilicity of the SH group relative to the OH group.

Chart 3. Details from IR Spectra (KBr) of condensates **1a-h** and **1j** indicating their thiazolidine nature



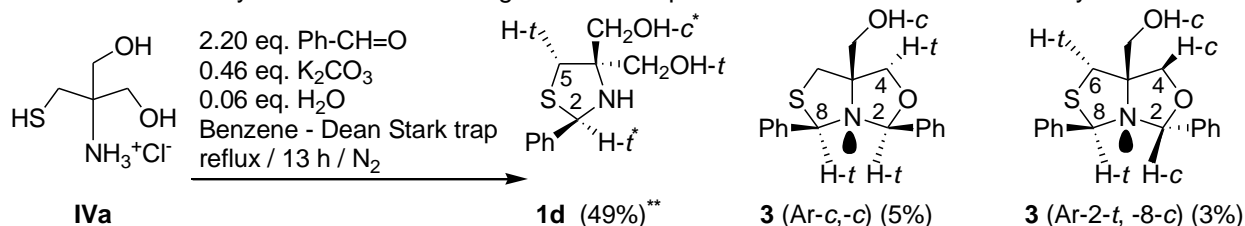
R	<i>p</i> -O ₂ N	<i>p</i> -Cl	<i>p</i> -Br	H	<i>m</i> -HO	<i>p</i> -HO	<i>o</i> -HO	<i>p</i> -Me ₂ N
Compd.	1a	1b	1c	1d	1e	1f	1g	1h
ν (cm ⁻¹)	1608 (m)	1634 (m)	1592 (w)	1602 (w)	1597 (s)	1614 (s)	1626 (m)	1615 (s)

2. Synthesis and structure of novel *c*-5-hydroxymethyl-3-oxa-7-thia-*r*-1-azabicyclo[3.3.0]octanes

2.1. Synthesis

When we attempted the one-pot double ring-closure of the in situ-generated thioamino-1,3-diol **IVb** with two molar equivalents of benzaldehyde, our results were very disappointing (Chart 4). In addition to

Chart 4. Results of the cyclocondensation of “2-(hydroxymethyl)cysteinol” **IVb** with 2 mol. eq. of benzaldehyde and the NMR assignment of the product nature and stereochemistry



*Stereochemical descriptors *c* (*cis*) and *t* (*trans*) are referred with respect to the fiducial substituents (*t*): Ph (in **1d**) and the lone pair at N-1 in **3**. **Partial conversions of **IVa**

Compd.	1d	3 (Ar-<i>c</i>, -<i>c</i>)		3 (Ar-2-<i>t</i>, -8-<i>c</i>)	
H-Positions	H-2- <i>t</i>	H-8- <i>t</i> ⇌ ^a	⇌ ^a H-2- <i>t</i>	H-8- <i>t</i>	H-2- <i>c</i>
δ_{H} (ppm)	5.55 (s)	5.32 (s)	5.39 (s)	5.27 (s)	5.63 (s)
	↗↘ ^a	↖↗	↕↔ ^a	↕↔	↗↘
	CH ₂ OH- <i>t</i>		H-4- <i>t</i>	H-6- <i>t</i>	H-4- <i>c</i>
	3.93 (d)		3.90 (d)	3.10 (d)	3.91 (d)
					CH ₂ OH- <i>c</i>
					3.86 (d), 3.77 (d)
C-Positions	C-2	C-8	C-2	C-8	C-2
δ_{C} (ppm) ^b	70.5	74.1	99.2	70.0	95.6

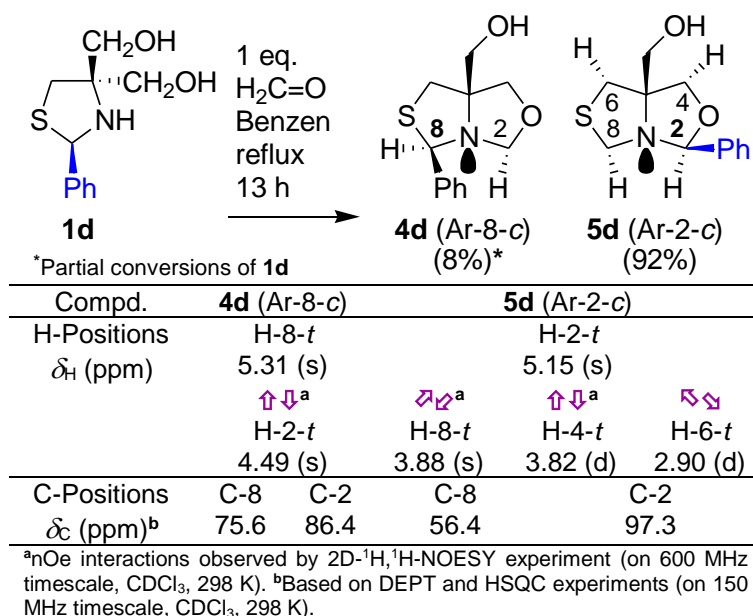
^anOe interactions observed by 2D-¹H,¹H-NOESY experiment (on 600 MHz timescale, CDCl₃, 298 K). ^bBased on DEPT and HSQC experiments (on 150 MHz timescale, CDCl₃, 298 K)

the oxidative alteration of **IVb**, its partial conversion also indicated intermediate **1d** was surprisingly unreactive toward benzaldehyde. Diastereomers **3** were previously investigated via DFT by Saiz et al.,^{7b} but there was no synthesis to support the calculations. In our hands, the experimental difference in stability, $\Delta G_{298} = G_{298}[\mathbf{3}(\text{Ar-}c, -c)] - G_{298}[\mathbf{3}(\text{Ar-}2-t, -8-c)]$, was about -1.31 kJ/mol, which was much smaller than the value provided by the computations (-7.10 kJ/mol). The mixture of **1d**+**3** could only be isolated by column

chromatography as a single mixed fraction. If we increased the electrophilicity of the aryl-aldehyde partner, i.e., by using two molar equivalents of *p*-nitrobenzaldehyde, under the same conditions (Chart 4), then only the thiaminalisation process took place to furnish thiazolidine **1a** (Scheme 4). We deduced that the nucleophilicity of the NH group on the 2-aryl-1,3-thiazolidines **1a** and **1d** might have been diminished by the anomeric effect (Section 1.2. c, Scheme 6).^{5b}

Therefore, we changed our strategy; a stoichiometric amount of *p*-formaldehyde was used as the oxaminalisation electrophile with the isolated members of the series: **1a-h**, **1j**. In a test experiment, no reaction occurred between **1d** and formaldehyde in ethanol at room temperature within 24 h. With heating, monitoring by TLC detected an near complete trans-thiaminalisation, producing the known derivative **V** (Scheme 3, R³ = H).^{2a, 2b} In contrast, the synthesis performed in benzene, which utilized a Dean-Stark trap for the continuous removal of water, provided both positive and surprising results (Chart 5).

Chart 5. Results of the cyclocondensation of 1,3-thiazolidine **1d** with 1 mol. eq. of formaldehyde and the NMR assignment of the product nature and stereochemistry



The quantitative conversion of **1d** produced a mixture of the regioisomers, **4d** (Ar-8-c) and **5d** (Ar-2-c), which were isolated by column chromatography as a mixture (single fraction). The starting material **1d** did not act as an a priori *N*-, *S*- protected form of **IVb** because the reaction also resulted in an almost complete “migration” of the benzaldehyde, -S-(Ph)CH-N< (1,3-thiazolidine) → >N-(Ph)CH-O- (1,3-oxazolidine).

This behaviour has not yet been reported in the literature.

Our results prompted us to screen, the rest of the 2-aryl-1,3- thiazolidines, **1a-c**, **1e-h** and **1j** (Chart 6), under identical conditions (Chart 5).

According to our data, the above reactivity of the benzaldehyde-based 1,3-thiazolidine **1d** was the exception rather than the rule. The repeated failures to obtain thiazolidin-oxazolidine condensed systems based on the tandem *p*-chlorobenzaldehyde (**b**) or *m*-hydroxybenzaldehyde (**e**) / formaldehyde systems should be viewed exceptions, as well; the explanation for these systems is still obscure to us. These observations led us to consider the influence of the aryl-ring substituent R¹ over not only the regioselectivity of the cyclocondensations, Ar-8 (series **4**) vs. Ar-2 (series **5**) but also the diastereoselectivities, Ar-8(2)-*c* vs. Ar-8(2)-*t*. In this context, when using a long reaction time (13 h), we observed a thermodynamic distribution of the products.

First, the regioselectivity was elucidated using ¹³C as *J*_{mod}, DEPT and 2D-¹H,¹³C-HSQC NMR experiments [compounds **4d** (Ar-8-c), **5d** (Ar-2-c)]. The spectral data for the 1,3-thiazolidine ring displayed condensed δ_{C} (-S-CH₂-N<) ~ 56 ppm but ~ 75 ppm in a -S-CH(Ar)-N< motif; meanwhile, in the

Chart 6. Results of the cyclocondensation of 1,3-thiazolidine **1a-c**, **1e-h** and **1j** with formaldehyde and the ¹H NMR assignment of the product nature and stereochemistry

Expected									
<p>$n = 1.0$ eq. 1a-c, 1e-h → 4a-c, 4e-h; 5a-c, 5e-h; $R^1 = \text{a}$ (<i>p</i>-O₂N); b (<i>p</i>-Cl); c (<i>p</i>-Br); e (<i>m</i>-HO); f (<i>p</i>-HO); g (<i>o</i>-HO); h (<i>p</i>-Me₂N)</p> <p>$n = 0.5$ eq. 1j ($R^1 = \text{p-R}^2$) → 4j ($R^1 = \text{p-R}^4$, $R^1 = \text{p-R}^4$); 5j ($R^1 = \text{p-R}^5$, $R^1 = \text{p-R}^5$)</p> <p>*Represented as 1<i>R</i>,5<i>S</i>* relative configurations of the unsubstituted <i>cis</i>-fused thiazolidin-oxazolidine skeleton; for the inversion of these configurations 1<i>R</i>,5<i>S</i>* → 1<i>S</i>,5<i>R</i>* see discussion and Schemes 8-12.</p>									
Found									
Partial and / or total conversions (%) ^a	Isomeric compositions (%) ^b	Relevant ¹ H NMR δ (ppm) values							
		H-2 ^{c-c}	H-2 ^{-t}	H-8 ^{d-c}	H-8- ^t	H-4 ^{e-c}	H-4 ^{-t}	H-6 ^{f-c}	H-6 ^{-t}
1a → 4a : 75	4a (c) 82 4a (t) 8	4.38	4.50		5.56	3.74	3.65	3.13	3.02
1a → 5a : 8	5a (c) 6 5a (t) 4		5.37						
Total 83		5.86							
1b → complex reaction mixture									
1c → 4c : 92	4c (c) 96 4c (t) 4	4.30	4.41		5.34	3.72	3.66	3.12	2.97
1e → complex reaction mixture									
1f → 4f : 79	4f (c) 93 4f (t) 7	4.20	4.32		5.18		3.68	3.14	2.93
1f → 5f : 15	5f (c) 85 5f (t) 15		4.85	3.94	3.75	4.19	3.52	3.01	2.86
Total 94		5.76						3.05	2.97
1g → 4g : 50	4g (c) 76 4g (t) 3	4.26	4.41		5.50		3.70	3.17	2.98
1g → 5g : 14	5g (c) 18 5g (t) 3		5.29	3.98	3.88	4.22	4.15	2.97	2.89
Total 64		5.41							
1h → 4h : 73	4h (c) 100	4.19	4.31		5.17	3.68	3.68	3.14	2.93
1j → 4j : 47	4j (c, c') 100	4.26	4.38		5.30	3.70	3.67	3.14(5)	2.96
1j → 5j : 13	5j (c, c') 100		4.97	3.95	3.84	4.22	3.57	3.01	2.88
Total 60									

^aBased on effective amounts isolated by column chromatography or direct crystallisation as a single fraction (**4a** + **5a**, **4c**, **4g** + **5g**, **4h**) or two fractions (**4f** vs. **5f** and **4j** vs. **5j**). ^bPercentages deduced from the ¹H NMR spectra. ^cIn series 4: doublets with ²J_{H,H} = 6.0-6.5 Hz^{2b, 15c, 16b, 16c, 18} but singlets in series 5.^dIn series 4 as singlets but doublets with ²J_{H,H} = 11.1-11.3 Hz in series 5.^eDoublets with ²J_{H,H} = 8.5-9.0 Hz. ^fDoublets with ²J_{H,H} = 11.5-12.0 Hz.

1,3-oxazolidine counterpart, δ_c (>N-CH₂-O-) was located at ~ 86 ppm but at ~ 95 ppm appeared the >N-CH(Ar)-O- sequence. Next, the ²J_{H,H} coupling patterns at C-4 displayed values typical for *cis*-fused 1,3-oxazolidine systems DOABO (Scheme 1), 8.5 – 9.0 Hz^{15b, 15c, 17b, 17c, 18} (8.5 Hz in the parent compound **V**, R³ = H, Scheme 2).^{2a, 2b} Finally, the ²J_{H,H} values at C-6, 12 Hz were identical with those in the reference **V** (R³ = H, Scheme 2).^{2a, 2b}

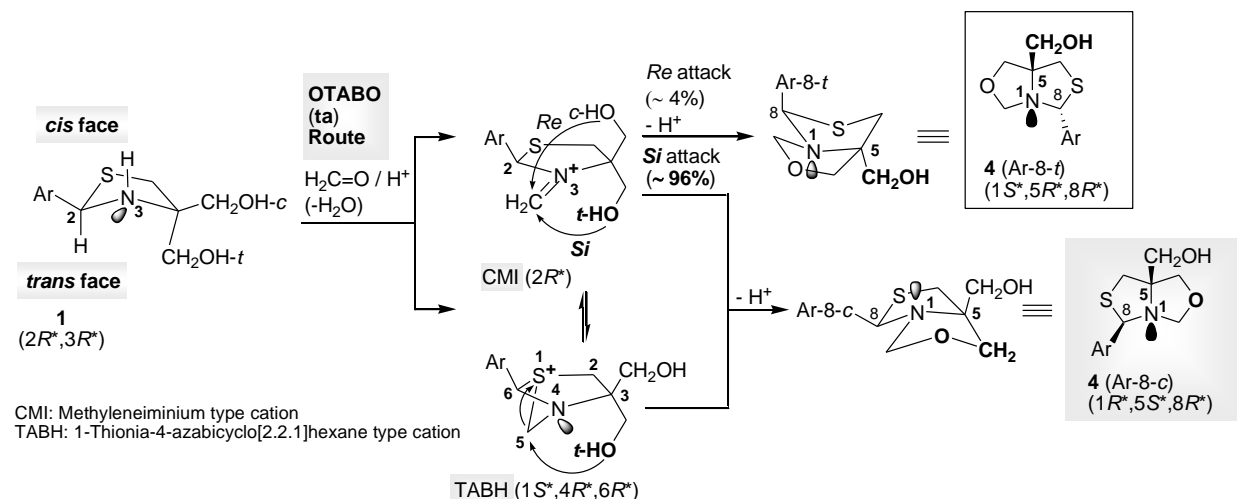
We determined the stereochemistry of the diastereomers starting from the 2D-¹H,¹H-NOESY data for compounds **4d** (c) + **5d** (c) [Chart 5, **4j** (c, c') and **5j** (c, c')]. Overall, the configurational assignments listed in Chart 5 agreed with our previous findings for the *cis*-fused 1,3-oxazolidine systems DOABO type derivatives,^{2c, 16b, 16c, 18} (Scheme 1); the “all-*cis*” spatial arrangements of the ligands lpN(1), C(5)-CH₂OH and Ar-2(8) predominated.

2.2. Rationalisation of the synthetic results

With the above assignments in mind, we dealt with providing plausible mechanistic explanations,

which will be referred to as *routes i - iv*, for the regio- and diastereoselectivities listed in Chart 6.

(i) Route towards thiazolidin-oxazolidines **4** as the main direction (Scheme 8)



Scheme 8

The major regioisomers **4a**, **4c**, **4f-h** and **4j** were obtained via this route. This route required the preliminary formation of the expected *N*-substituted methyleneiminium cations (CMI) with $>\text{N}^+=\text{CH}_2$ diastereotopic faces. The *Si* face was more exposed to the nucleophile addition of $\text{CH}_2\text{OH}-t$, and this addition afforded mostly the **4** (Ar-8-c) series. The reaction with $\text{CH}_2\text{OH}-c$ on the *Re* face would encounter the Ar ligand as a steric obstruction; this geometry was reinforced by the change of the *N*-hybridisation, from sp^3 in **1** to sp^2 in CMI. Formation of the minor diastereomers **4** (Ar-*t*) involved the partial inversion of the thiazolidine **1** ($2R^*,3R^*$) relative configuration to $1S^*,5R^*,8R^*$ in series **4** (Ar-*t*).

The diastereoselectivity for **4** (Ar-8-c) : **4** (Ar-8-*t*) was approximately 96:4, which we could also justify by considering a more appropriate cationic intermediate, i.e., 1-thionia-4-azabicyclo[2.2.1]hexane (TABH). With this intermediate, the bridged C-5 methylene group was placed within the exclusive vicinity of the $\text{CH}_2\text{OH}-t$ nucleophile. We viewed the generation of species TABH to be another consequence of the diminished nucleophilicity of the NH group in the 1,3-thiazolidines **1**, as well as the increase in nucleophilicity furnished by using sulfur, due to the anomeric effect (Section 1.2. c, Scheme 6).^{5b} The main **4** (Ar-8-c) diastereomers preserved the initial relative configuration of the thiazolidine **1** ($2R^*,3R^*$), but the configuration of the bicyclic skeleton ($1R^*,5S^*$) was inverted with respect to **4** (Ar-8-*t*).

Compound **4h** (c) produced diffractable crystals suitable for X-ray analysis. This derivative crystallises as a racemate (Figure 2) with four molecules in the unit cell.

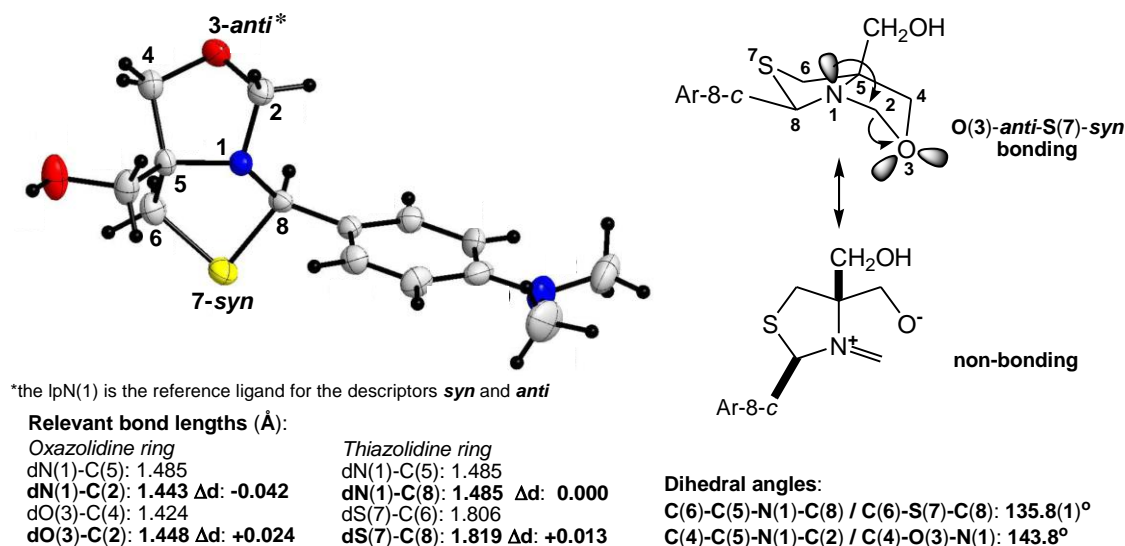


Figure 2. Molecular structure of compound **9h** as the ($1R,5S,8R$) enantiomer, with 40% probability ellipsoids

CONCLUSIONS

- The thiaminalisation of 2-amino-2-(mercaptomethyl)propane-1,3-diol with aryl(di)aldehydes afforded a new series of chiral 4,4-bis(hydroxymethyl)-1,3-thiazolidines with medium to satisfactory yields. The overall results are caused by the redox instability of the thioamino-1,3-diol.
- On the ¹H NMR timescale, the above 2-aryl(bis)-1,3-thiazolidines exhibited no detectable epimerisation at the C-2 position, no *N*-pyramidal inversion and no NH acid-base interchange.
- In the thiaminalic >N-C-S- part of these compounds, the ¹H NMR data, when combined with DFT calculations, revealed an *endo* anomeric effect assigned as lpN → σ* C-S hyperconjugation.
- The IR spectroscopy in the solid state indicated that these structures exist in their ring forms. However, the condensates of salicylaldehyde and terephthalaldehyde displayed weak ring (1,3-thiazolidine) → chain (Schiff Base) tautomerism, due to their spontaneous partial ring opening in solution.
- After treating our 4,4-bis(hydroxymethyl)-1,3-thiazolidines with a stoichiometric amount of formaldehyde, a new class of C-2,8-substituted-3-oxa-7-thia-*r*-1-azabicyclo[3.3.0]-*c*-5-octanes, which are singly functionalised at the C-5-position with an exploitable hydroxymethyl group, were obtained in satisfactory to good yields, regio- and diastereoselectivities.
- Depending on the nature of the *p*-, *m*- or *o*-substituent of the phenyl ring in the initial 2-aryl-1,3-thiazolidines, a C-8 → C-2 migration of the aromatic group occurred during the oxaminalisation. Several mechanistic models were proposed relating to this unexpected reactivity; the proposals consisted of the formation of (C-substituted)-methyleneiminium and 1-thionia-4-azabicyclo[2.2.1]hexanes cations as non-isolable intermediates.
- The first molecular structure of a 3-oxa-7-thia-*r*-1-azabicyclo[3.3.0]-*c*-5-octane derivative, which bears a *p*-dimethylaminophenyl group in position C-8, exhibited an anomeric effect that manifested as hyperconjugation between the lpN(1) (donor) → σ*O(3)-C-(2) (acceptor) orbitals, i.e., occurring in the 1,3-oxazolidine ring only. In contrast, entire thiazolidin-oxazolidine units were involved in four types of (supramolecular) interactions, homochiral >O...H-(OCH₂) and (NC)H₃...π but heterochiral (NC)H₃...O< and (CH)H...S<.

SELECTIVE REFERENCES

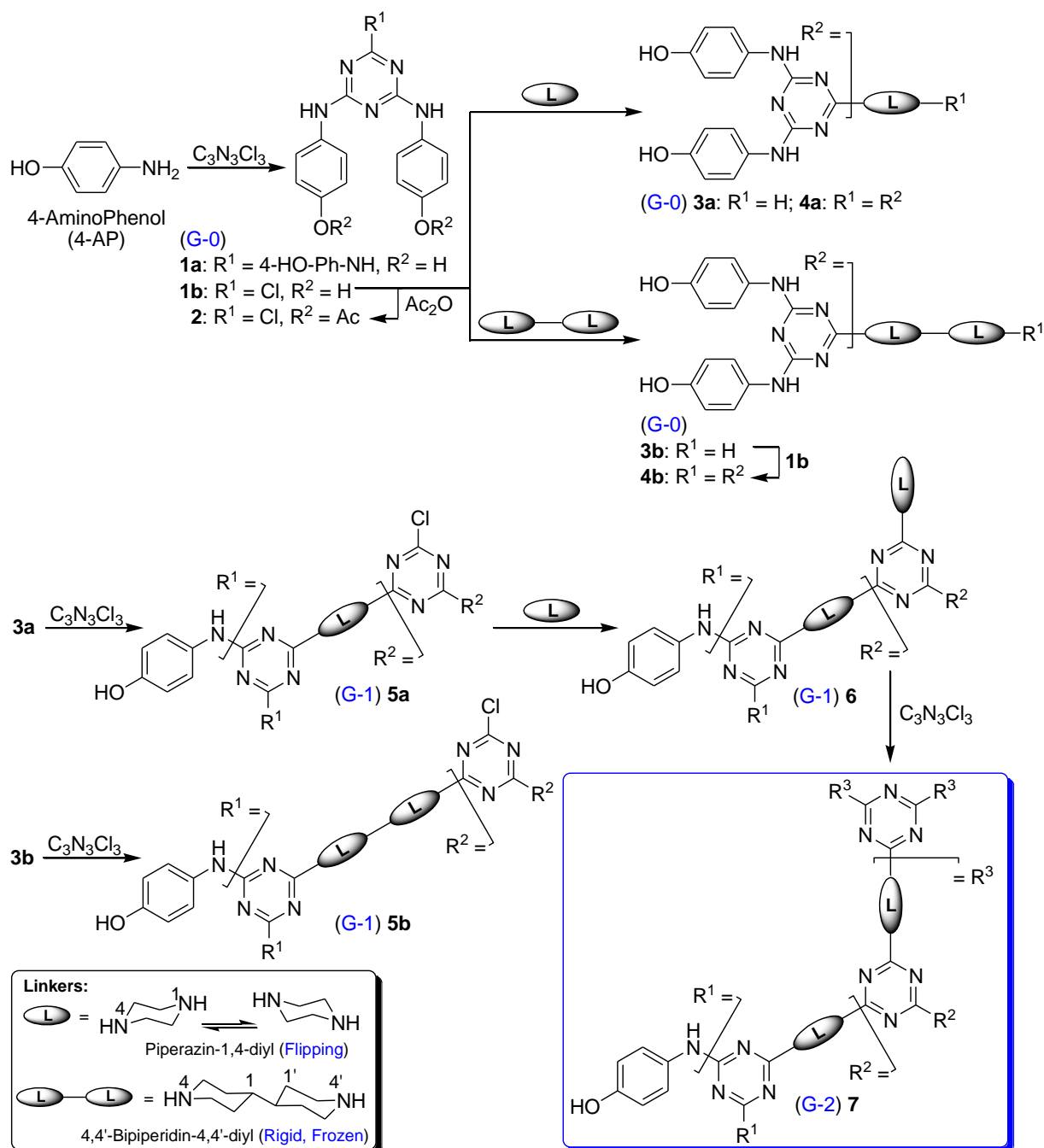
- ¹ a) H. S. Broadbent, W. S. Burnham, R. M. Sheely, R. K. Olsen, *J. Heterocyclic Chem.*, **1976**, *13*, 337-348; b) G. G. Habernel, W. Ecsy, *Heterocycles*, **1977**, *7*, 1027-1032.
- ² a) A. But, C. Batiu, Y. Ramondenc, M. Darabantu, *Rev. Roum. Chim.*, **2009**, *54*, 127-133; b) A. But, P. Lameiras, I. Silaghi-Dumitrescu, C. Batiu, S. Guillard, Y. Ramondenc, M. Darabantu, *Lett. Org. Chem.*, **2010**, *7*, 283-290; c) for a review of the (condensed)-1,3-oxazolidine systems **3** (Scheme 1), see M. Darabantu, *Curr. Org. Synth.*, **2010**, *7*, 235-275.
- ³ a) W. Enz, M. Cecchinato, *Helv. Chim. Acta*, **1961**, *44*, 706-709; b) T. A. Crabb, M. J. Hall, R. O. Williams, *Tetrahedron*, **1973**, *29*, 3389-3398; c) D. Seebach, T. Weber, *Tetrahedron Lett.*, **1983**, *24*, 3315-3318; d) D. Seebach, T. Weber, *Helv. Chim. Acta*, **1984**, *67*, 1650-1661; e) R. Lohow, F. Meneghini, *J. Am. Chem. Soc.*, **1979**, *101*, 420-426; f) A. Hamril, M-H. Péra1, H. Fillion, *J. Het. Chem.*, **1987**, *24*, 1629-1633; g) A. Gonzales, R. Lavilla, J. F. Piniella, A. Alvarez-Larena, *Tetrahedron*, **1995**, *51*, 3015-3024; h) A. N. Skvortsov, V. M. Uvarov, D. S. de Vekki, E. P. Studentsov, N. K. Skvortsov, *Russ. J. Gen. Chem.*, **2010**, *80*, 2007-2021 (cf. *Zh. Obsch. Khim.*, **2010**, *80*, 1697-1711).
- ⁴ For this chemistry highlighting the importance derivatives of type **IIa** (Scheme 2) as scaffolds a) total synthesis of *Biotin* (vitamin H, coenzyme R), F. D. Deroose, P. J. De Clercq, *J. Org. Chem.*, **1995**, *60*, 321-330; b) total synthesis of the antimicrobial *Micococcidin*, A. Ino, Y. Hasegawa, A. Murabayashi, *Tetrahedron Lett.*, **1998**, *39*, 3509-3516; c) synthesis of segments of *Farnesyl Transferase*, H. Yang, X. C. Sheng, E. M. Harrington, K. Ackerman, A. M. Garcia, M. D. Lewis, *J. Org. Chem.*, **1999**, *64*, 242-251.
- ⁵ a) J. Sélambaron, F. Carré, A. Fruchier, J. -P. Roque, A. A. Pavia, *Tetrahedron*, **2002**, *58*, 4439-4444; b) for a similar diagnosis in 1,3-oxazolidine systems see: J. Sélambaron, S. Monge, F. Carré, J. -P. Roque, A. A. Pavia, *Tetrahedron*, **2002**, *58*, 9559-9566.
- ⁶ a) as masked sulfhydryl agents for inhibition of melanogenesis, see A. Napolitano, M. d'Ischia, G. Prota, M. Havens, K. Trampusch, *Biochim. Biophys. Acta.*, **1991**, *1073*, 416-422; b) as anti-inflammatory agents, see: D. Chiarino, F. Ferrario, F. Pellacini, A. Sala, *J. Het. Chem.*, **1989**, *26*, 589-593.
- ⁷ a) C. Saiz, P. Wipf, E. Manta, G. Mahler, *Org. Lett.*, **2009**, *11*, 3170-3173; b) C. Saiz, P. Wipf, G. Mahler, *J. Org. Chem.*, **2011**, *76*, 5738-5746; c) for heteroanalogs and their applications see: M. M. González, M. Kosmopoulou, M. F. Mojica, V. Castillo, P. Hinchliffe, I. Pettinati, J. Brem, C. J. Schofield, G. Mahler, R. A. Bonomo, L. I. Llarrull, J. Spencer, A. J. Vila, *ACS Infect. Dis.*, **2015**, *1*, 544-554; d) as a typical example see: J. H. Tocher, D. I. Edwards, *Biochem. Pharmacol.*, **1995**, *50*, 1367-1371.

- ⁸ a) J. E. Baldwin, *J. Chem. Soc. Chem. Commun.*, **1976**, 18, 734-736; b) J. E. Baldwin, J. Cutting, W. Dupont, L. Kruse, L. Silberman, R. C. Thomas, *J. Chem. Soc. Chem. Commun.*, **1976**, 18, 736-738.
- ⁹ A. Cruz, A. Vasquez-Badillo, I. Ramos-Garcia, R. Contreras, *Tetrahedron: Asymmetry*, **2001**, 12, 711-717.
- ¹⁰ a) G. E. Wilson Jr., T. J. Bazzone, *J. Am. Chem. Soc.*, **1974**, 96, 1465-1470; b) as a new class of non-narcotic antitussive agents (*N*-acylated forms), see C. A. Gandolfi, R. Di Domenico, S. Spinelli, L. Gallico, L. Fiocchi, A. Lotto, E. Menta, A. Borghi, C. D. Rossa, S. Tognella, *J. Med. Chem.*, **1995**, 38, 508-525; c) as new ligands for Hg^{II} complexation (*N*-acyl derivatives, analogous of the corresponding penicillin moiety), see S. Chandrasekhar, D. Chopra, K. Gopalaiah, R. Guru, N. Tayur, *J. Mol. Struct.*, **2006**, 837, 118-131.
- ¹¹ a) R. Valters, W. Flitsch, "Ring-Chain Tautomerism", Plenum: New York, **1985**; b) F. Fülöp, J. Mattinen, K. Pihlaja, *Tetrahedron*, **1990**, 46, 6545-6552; c) V. V. Alkseyev, K. N. Zelenin, *Khim. Geterosikl. Soedin.*, **1998**, 1068-1071; d) L. Lázár, F. Fülöp, *Eur. J. Org. Chem.*, **2003**, 16, 3025-3042; e) M. Darabantu, *Curr. Org. Synth.* **2010**, 7, 120-152.
- ¹² E. L. Eliel, H. S. Wilen, *Stereochemistry of the Organic Compounds*, John Wiley & Sons, New York, NY, Chichester, UK, Brisbane, Toronto, Singapore, **1994**, p. 758, 1199, 1200.
- ¹³ H. Friebolin, *Basic One- and Two Dimensional NMR Spectroscopy*, VCH Verlagsgesellschaft/VCH: Weinheim/New York, NY, **1991**, p. 93, 263-291; b) R. M. Silverstein, F. X. Webster, D. J. Kiemle, *Spectrometric Identification of Organic Compounds*, John Wiley and Sons, New Jersey, U.S.A., **2005**, p. 106, 153-155; c) e.g. 10⁻¹⁰ s for the acid-base interchange and 10⁻⁸ s for the *N*-pyramidal inversion in the case of *N*-substituted piperidines, see: P. J. Crowley, M. J. T. Robinson, M. G. Ward, *Tetrahedron*, **1977**, 33, 915-925.
- ¹⁴ a) M. Karplus, *J. Chem. Phys.*, **1959**, 30, 11-15; b) M. Karplus, *J. Am. Chem. Soc.*, **1963**, 85, 2870-2871.
- ¹⁵ a) P. Vanelle, M. P. De Meo, J. Maldonado, R. Nougier, M. P. Crozet, M. Laget, G. Dumenil, *Eur. J. Med. Chem.*, **1990**, 25, 241-250; b) M. Darabantu, G. Plé, S. Mager, E. Cotor, L. Gaina, L. Costas, A. Mates, *Tetrahedron*, **1997**, 53, 1873-1890; c) C. Maieranu, M. Darabantu, G. Plé, C. Berghian, E. Condamine, Y. Ramondenc, I. Silaghi-Dumitrescu, S. Mager, *Tetrahedron*, **2002**, 58, 2681-2693. d) I. Ghiviriga, D. C. Oniciu, *Chem. Commun.*, **2002**, 2718-2719 and the literature cited therein.
- ¹⁶ a) S. Monge, J. Sélambaron, F. Carré, J. Verducci, J-P. Roque, A. A. Pavia, *Carbohydrate Res.*, **2000**, 328, 127-133; b) M. Darabantu, C. Maieranu, I. Silaghi-Dumitrescu, L. Toupet, E. Condamine, Y. Ramondenc, C. Berghian, G. Plé, N. Plé, *Eur. J. Org. Chem.*, **2004**, 12, 2644-2661; c) C. Berghian, P. Lameiras, L. Toupet, E. Condamine, N. Plé, A. Turck, C. Maieranu, M. Darabantu, *Tetrahedron*, **2006**, 62, 7319-7338.
- ¹⁷ a) A. Star, B. Fuchs, *J. Org. Chem.*, **1999**, 64, 1166-1172; b) A. Star, I. Goldberg, N. G. Lemcoff, B. Fuchs, *Eur. J. Org. Chem.*, **1999**, 9, 2033-2043.
- ¹⁸ a) M. Darabantu, G. Plé, S. Mager, L. Gaina, E. Cotor, A. Mates, L. Costas, *Tetrahedron*, **1997**, 53, 1891-1908; b) M. Darabantu, G. Plé, I. Maieranu, I. Silaghi-Dumitrescu, I. Ramondenc, S. Mager, *Tetrahedron*, **2000**, 56, 3799-3816.

RESULTS AND DISCUSSION

1. Synthesis

The chemistry we followed is resumed in Scheme 2 and the reaction conditions are presented in Table 1.



Scheme 2

First, we tested the chemoselectivity in the amination of cyanuric chloride by *p*-AminoPhenol (*p*-AP) in the synthesis of melamine **1a** (Table 1, entry 1) vs. that of chlorodiamino-*s*-triazine **1b** (Table 1, entries 2 and 3). Although the preparation of **1a** was of applied interest for several authors,^{1a-d, 3} in our hands only the procedure of Negoro and Kawata^{1c, 1d} gave satisfaction as excellent and reproducible yield, 91%.⁷

In similar but milder conditions (Table 1, entry 2), amination of cyanuric chloride performed with two molar equiv. of *p*-aminophenol yielded compound **1b** contaminated with traces of melamine **1a**. Hence, **1b** required purification by column chromatography when an important loss of material due to its relative retention on silica gel was observed, affecting the yield. Our option of choice was

Table 1. Reaction conditions and results in the synthesis of compounds **1-7** (see Scheme 2)

Entry	Reaction	Conditions	Products, yields (%) and isolation: direct crystallization (d.c.), column chromatography on silica gel (c.c.) ^a
1	<i>p</i> -AP → 1a	i) 0.30 equiv. C ₃ N ₃ Cl ₃ , butanone / 0-5 °C (30 min.); ii) 1.00 equiv. AcONa, H ₂ O / 5-9 °C (30 min.); iii) reflux (3 h)	1a : 91 (d.c.)
2	<i>p</i> -AP → 1b	i) 0.50 equiv. C ₃ N ₃ Cl ₃ , butanone / 0-5 °C (30 min.); ii) 1.00 equiv. AcONa, H ₂ O / 5-9 °C (30 min.); iii) r.t. (24 h)	1b : 56 (c.c.)
3	<i>p</i> -AP → 1b	i) 0.50 equiv. C ₃ N ₃ Cl ₃ , acetone / 0-5 °C (2 h); ii) 1.00 equiv. NaHCO ₃ , H ₂ O / 5-9 °C; iii) 45 °C (3 h); r.t. (15 h)	1b : 73 (d.c.) ^b
4	1b → 2	2.23 equiv. Ac ₂ O, 1.00 equiv. K ₂ CO ₃ , THF / r.t. (4 h); reflux (10 h)	2 : 90 (d.c.)
5	1b → 3a	4.00 equiv. piperazine, 1.00 equiv. K ₂ CO ₃ , THF / r.t. (15-20 h)	3a : 83 (c.c.); 85 (d.c.)
6	1b → 3a , 4a	1.00 equiv. piperazine, 1.00 equiv. K ₂ CO ₃ , 1,4-dioxane / reflux (8 h)	3a : 17 (c.c.); 4a 83 (c.c.) ^c
7	1b → 3b	4.00 equiv. 4,4'-bipiperidine, 1.00 equiv. K ₂ CO ₃ , THF / r.t. (36-42 h)	3b : 45 (c.c.); 86 (d.c.)
8	3b → 4b	1.00 equiv. 1b , 1.00 equiv. K ₂ CO ₃ , 1,4-dioxane / reflux (13 h)	4b : 64 (d.c.)
9	3a → 5a	i) 1.00 equiv. 3a , 1.00 equiv. K ₂ CO ₃ , THF / -15 °C (20-24 h); ii) 1.00 equiv. 3a , 1.00 equiv. K ₂ CO ₃ , THF / r.t. (20-24 h); iii) 1,4-dioxane, reflux (36 h)	5a : 90 (d.c.)
10	3b → 5b	i) 1.00 equiv. 3b , 1.00 equiv. K ₂ CO ₃ , THF / -15 °C (22 h); ii) 1.00 equiv. 3b , 1.00 equiv. K ₂ CO ₃ , THF / r.t. (24 h); iii) 1,4-dioxane, reflux (36 h)	5b : 47 (c.c.); 86 (d.c.)
11	5a → 6	i) 4.00 equiv. piperazine, 1.00 equiv. K ₂ CO ₃ , THF / r.t. (20-30 h); ii) reflux (12 h)	6 : 55 (c.c.); 88 (d.c.)
12	6 → 7	i) 0.30 equiv. C ₃ N ₃ Cl ₃ , 1.00 equiv. K ₂ CO ₃ , 1,4-dioxane / r.t. (24 h); ii) reflux (48 h)	7 : 85 (d.c.)

^aOn partially deactivated silica gel (eluent EtOH : aq. NH₃ 25%) for compounds **3a**, **4a**, **3b** and **6**. ^b67% Yield according to Ref. [4b] and [4c]. ^cPartial conversions of **1b** into the depicted compounds, calculated based on effective amounts isolated by column chromatography.

then the method of Bhat and co-workers⁴ (Table 1, entry 3) which produced **1b** with good yield, 73%, in an expeditious manner. Compound **1b** exhibited moderate solubility in organic solvents usually recommended for the synthesis of amino-*s*-triazines (THF, 1,4-dioxane, acetone etc.),⁶ most likely because of its high polarity. That is, in order to adopt a protective-deprotective strategy, **1b** was diacetylated (Table 1, entry 4) in high yield, 90% with complete *O,O'*-chemoselectivity. Unfortunately, the resulted *O,O'*-diacetyl derivative **2** was inappropriate for our envisaged iterative syntheses (Scheme 2). Thus, the reaction between **2** and piperazine (not depicted in Scheme 2), besides the expected amination of the *s*-triazine chlorine, consisted as well of the partial transfer of the acetyl group (*O*-phenol → *N*-piperazine) affording a multicomponent reaction mixture. By contrast, compound **2** was of crucial relevance in electrochemical investigations (Section 3.1.). To conclude, for the present report, we had to manage our strategy limited to (G-0) chlorodendron **1b**.

Based our earlier published methodology,^{5a-d} the chemoselective mono-attachment of piperazine, as the first linker, to **1b** (Table 1, entry 5) gave the (G-0) melamine **3a**. Thus, during the portionwise addition of **1b** to a 300% molar excess of piperazine, the TLC monitoring of the amination revealed a very clean evolution towards **3a** only, i.e. the complete absence of the dimeric melamine **4a** as side product (Scheme 2). As shown in Table 1 (entry 5), it was the single situation, that of **3a**, in which both techniques for its purification (direct crystallisation or column chromatography on partially deactivated silica gel) provided good and comparable quantitative

results. Our attempt to prepare compound **3a** by applying the method of Bath and co-workers^{4c} (equimolar ratio **1b** : piperazine, 82% claimed yield of **3a**) failed (Table 1, entry 6). The resulted mixture **3a** (minor) and **4a** (major) could be successfully separated by column chromatography.

The protocol for the non-symmetric anchorage of the 4,4'-bipiperidine linker to **1b** (Table 1, entry 7) producing melamine **3b**, was the same as in the case of piperazine against **1b** but the amination reached completion in a much longer time. The yield of **3b** was critically influenced by the work-up used for its isolation as pure analytical sample, 86% (direct crystallisation from boiling ethanol) vs. 45% (column chromatography on partially deactivated silica gel). Our tentative explanation relates, once again, to the high relative retention on column chromatography of **3b** (see also the next examples). The symmetric analogue **4b** of **3b** was also prepared from the latter in reaction with **1b** (Table 1, entry 8).

As expected, the one-pot synthesis of (G-1) chlorodendrons **5a** and **5b** (Table 1, entries 9 and 10 respectively) required mild conditions for the first step amination. However, the second step was mandatory to taxing reaction parameters (36 h in refluxing 1,4-dioxane), suggesting the low reactivity of the intermediates due to their strong solvation in the depicted solvents. Except for DMF and DMSO, both compounds **5a** and **5b** manifested low solubility in common organic volatile solvents. Therefore, in order to avoid the loss of material on column chromatography (i.e. compound **5b**, 47% yield), purifications were successfully realised by crystallisations from boiling ethanol (86% optimised yield of **5b**). Even so, the (G-1) chlorodendron **5b** showed an unexpected weak reactivity in subsequent aminations attempted with piperazine or 4,4'-bipiperidine. Therefore, for the present work, we had to limit the study by using henceforth (G-1) chlorodendron **5a** only.

In so doing, we effected, in accordance with the same methodology as that in the case of (G-0) melamine **3a**, the selective anchorage of the next piperazine linker on **5a** (Table 1, entry 11) and obtained (G-1) melamine **6**. We detected no dimeric melamine as side product and isolated **6** by column chromatography on partially deactivated silica gel or, as an optimal decision, by crystallisation (88% yield).

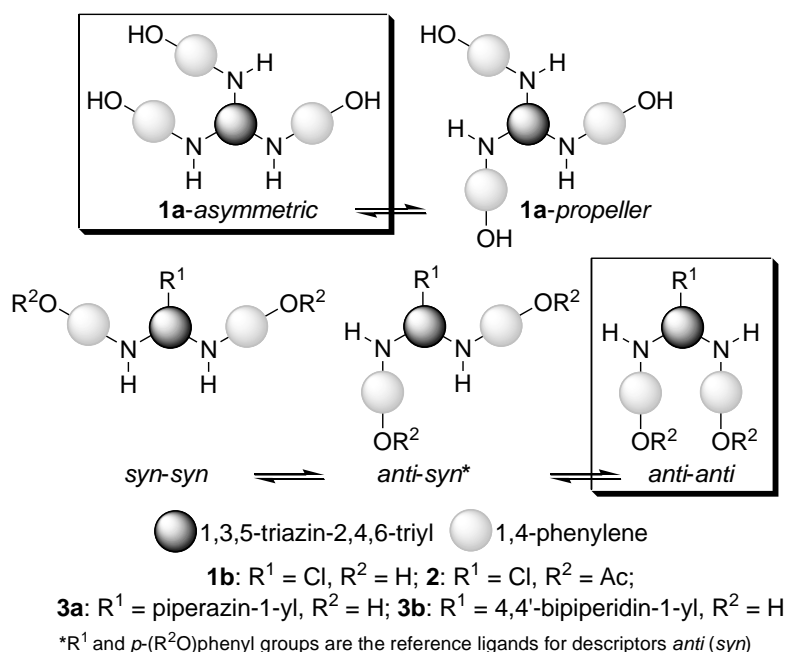
The final installation of the trivalent *s*-triazine core on **6** (Table 1, entry 12) was performed in a one-pot procedure with good global yield (85%). Compound **7**, the first (G-2) dendrimer comprising *p*-aminophenol as peripheral unit, could not be eluted on TLC due to its low solubility in common organic solvents. Its identity was fully confirmed by spectral methods.

2. Preliminary structural assignments

As early as 1971,^{8a} it was established that the C(*s*-triazine)-N(exocyclic) linkages in amino-*s*-triazines have a partial double bond character due to the $p(N) \rightarrow \pi(C=N)$ conjugation between the lone pair of the exocyclic *N*-atom in conjunction with the high π -deficient *s*-triazine ring.⁸ There is a restricted rotation thus induced. Variable temperature NMR spectroscopy is an appropriate technique for monitoring this stereodynamism,⁹ including examples of arylamino-*s*-triazines.^{9d-f, 9h} As for other amino-*s*-triazines, in the case of monomeric (G-0) dendrons **1a**, **1b**, **2**, **3a** and **3b**, at room temperature, a topological idealised model^{5a-d, 9g} predicted, for **1a**, a two terms rotational diastereomerism (*asymmetric* \rightleftharpoons *propeller*) and three terms (*syn-syn* \rightleftharpoons *anti-syn* \rightleftharpoons *anti-anti*) for **1b**, **2**, **3a** and **3b** (Scheme 3).

Therefore, before any electrochemical investigation, a study by means of DFT,¹⁰⁻¹⁷ calculation in solution (DMSO) was implemented for compounds **1a**, **1b**, **2**, **3a**, **3b** and **7**, selected as representative. The results are shown in Tables 2, 3 and Figure 1 together with those referring to the starting *p*-AminoPhenol (*p*-AP) and its *N*-acetyl derivative, the well-known anti-inflammatory drug *ParAcetamol* (PA). They deserved the below comments:

(i) The optimised geometry of melamine **1a** was found of type *asymmetric*, meanwhile *anti-anti* was the preferred rotameric arrangement adopted by the *p*-(R²O)phenyl units in compounds **1b**, **2**, **3a** and **3b** in DMSO (Table 2). The same *anti-anti* stereochemistry was *local* at the periphery



Scheme 3

of dendrimer **7** which disclosed a vaulted *global* shape¹⁸ (Figure 1).

(ii) The increasing order of ϵ_{HOMO} energies (Table 2) correlated with the decreasing strength of the EWG $N(\text{O})$ -substituting the $p\text{-(R}^2\text{O)phenyl}$ amino units (Scheme 2), namely acetyl and variable π -deficient *s*-triazine ring, i.e. **2** < Paracetamol ~ **1b**. However, an equalisation of ϵ_{HOMO} energies in melamine series **1a** ~ **3a** ~ **3b** resulted from calculation. Obviously, the highest ϵ_{HOMO} level was that of *p*-aminophenol.

(iii) The partial double bond nature of connexions C(*s*-triazine)-N(exocyclic) was disclosed by Bond Order (BO) values ranging between 1.20-1.25, anyhow much greater than those of connexions C(Ph)-NH. The calculated Bond Lengths (BL) fully supported their inverted dependence with respect to the corresponding BO indexes (Table 3).

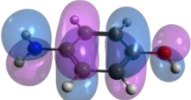
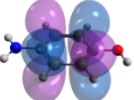
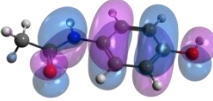
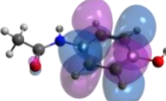
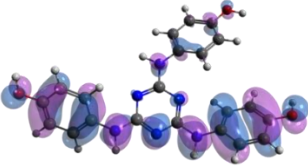
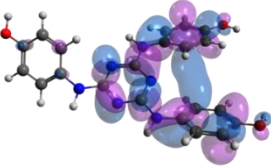
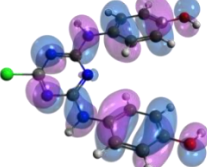
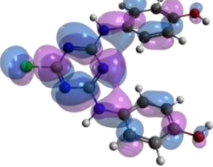
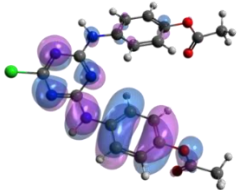
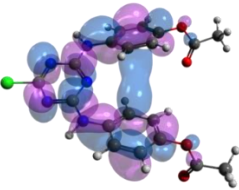
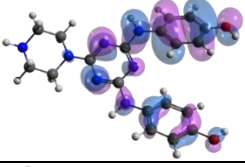
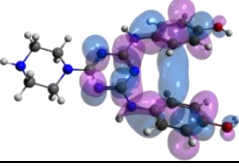
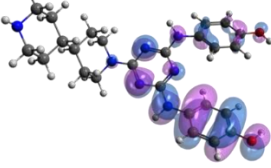
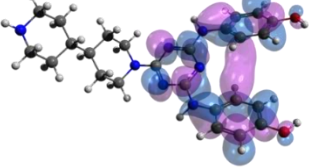
(iv) The lowest nitrogen Lone Pair (LP) orbital populations (1.64-1.68) were found in LPN(H) $\rightarrow\pi(\text{C}=\text{O})$ (*Paracetamol*) and LPN(exocyclic) $\rightarrow\pi(\text{s-triazine})$ conjugated compounds **1a**, **1b**, **2**, **3a** and **3b**. The LP orbital population of the phenolic oxygen was less diminished (3.76-3.88) as a consequence of the LPO(H, Ac) $\rightarrow\pi(\text{Ph})$ or LPO $\rightarrow\pi(\text{C}=\text{O})$ delocalisation.

Furthermore, data issued from (VT) ¹H NMR investigations (Table 4) completed those provided by theoretical anticipations. Unsurprisingly, the most π -deficient diamino-chloro-*s*-triazines **1b** and **2** displayed, at room temperature, the most convincing ¹H NMR spectral appearance, consistent with the nearly frozen nature of their rotational equilibria (Scheme 3) on the NMR time scale.

In contrast, in the same conditions, the rotamerism of all melamines (G-0, -1, -2) was identified by NMR as a classically entitled “slow exchange status between (un)equally populated sites”.¹⁹ Upon heating to 80-90 °C (Table 4), all compounds became single mediated structures, in a fast freely rotating status about all C(*s*-triazine)-N(exocyclic) bonds.

Temperature Gradients (TGs) of the NH protons were also indicative because they revealed the influence of different types of *N*-ligands on solvation. Although this parameter is appropriate for amide $\text{-N(H)-C(=O)-} \leftrightarrow \text{-N}^+(\text{H})=\text{C}(\text{O}^-)\text{-}$ protons in peptides and proteins,²⁰ it can also be applied to amino-*s*-triazines, $\text{-N(H)-C(=N-)-} \leftrightarrow \text{-N}^+(\text{H})=\text{C}(\text{-N}^-)\text{-}$ as established by Simanek and Moreno.^{18b} Following this extrapolation, if TG values of “amide-like” protons in amino-*s*-triazines are more negative than -4 ppb/K in strong hydrogen bond acceptor solvents, such as DMSO-*d*₆,^{9g} the NH groups are exposed to the solvent rather than forming intramolecular hydrogen bonds. On the other hand, a TG value less negative than -4 ppb/K indicates that the NH group preferentially forms

Table 2. Full geometry optimization and calculated ϵ_{HOMO} , ϵ_{LUMO} in *p*-AminoPhenol (*p*-AP), *ParAcetamol* (PA) and monomeric (G-0) dendrons **1a**, **1b**, **2**, **3a** and **3b** in DMSO^a

No.	HOMO	LUMO	ϵ_{HOMO} (eV)	ϵ_{LUMO} (eV)	Gap (eV)
<i>p</i> -AP			-6.24	+0.68	6.92
PA			-7.00	+0.50	7.50
1a			-6.81	+0.31	7.12
1b			-6.99	-0.03	6.96
2			-7.47	-0.23	7.24
3a			-6.80	+0.35	7.15
3b			-6.81	+0.35	7.16

^aThe full geometry optimisation have been carried out at the DFT level of theory considering the M06-2X¹⁰ exchange-correlation functional together with the def2-TZVP¹¹ basis set in the presence of solvent environment implemented in the Gaussian 09¹² program package. The solvent effects have been taken into account via the Polarizable Continuum Model (PCM) using the integral equation formalism variant (IEFPCM)¹³ considering the DMSO ($\epsilon=46.826$) as the solvent environment.

Table 3. Indicative Bond Order (BO) indexes, Bond Lengths (BL) and Lone Pair (LP) orbital populations in *p*-AminoPhenol (*p*-AP), *ParAcetamol* (PA) and (G-0) dendrons **1a**, **1b**, **2**, **3a** and **3b** in DMSO

No.	C(s-triazine)-N(H)		C(Ph)-N(H)		C(s-triazine)-N<		Lone Pair (LP) orbital populations (<i>e</i>) ^a			
	BO ^b	BL (Å) ^c	BO	BL (Å)	BO	BL (Å)	N(H)	O(H, Ac)	-N<	s-triazine N(1, 3, 5)
<i>p</i> -AP	-		1.15	1.375	-		1.82	3.88	-	-
PA	-		1.05	1.410	-		1.64	3.86	-	-
1a	1.21	1.353	1.04	1.411	-		1.68	3.86	-	1.90
1b	1.25	1.351	1.03	1.410	-		1.64	3.86	-	1.90
2	1.24	1.343	1.04	1.406	-		1.64	3.76	-	1.90
3a	1.20	1.360	1.04	1.407	1.23	1.353	1.68	3.86	1.67	1.90-1.91
3b	1.20	1.361	1.04	1.407	1.23	1.352	1.68	3.86	1.67	1.90-1.91

^aObtained by considering the NBO electron population analysis at M06-2X/def2-TZVP level of theory where *e* is the elementary electric charge carried by a single electron. ^bCalculated at M06-2X/def2-TZVP level of theory considering the Wiberg definitions of bond order (see ref. [19]) implemented in the NBO analysis module. ^cCalculated at M06-2X/def2-TZVP level of theory.

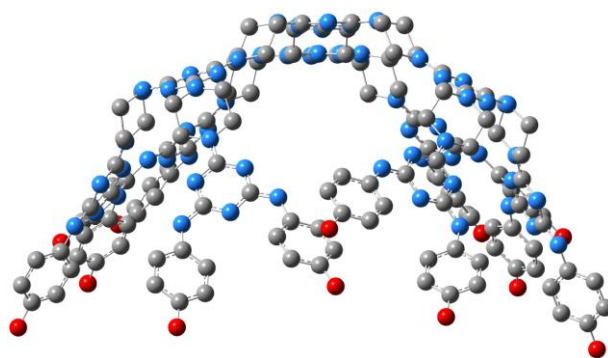


Figure 1. The optimized geometry structure of compound **7** obtained at M06-2X/def2-TZV level of theory¹¹ (the H atoms were omitted for reasons of simplicity)

Table 4. Relevant (VT) ¹H and 2D-¹H-DOSY-NMR data (500 MHz, DMSO-*d*₆) of compounds **1a**, **1b**, **2**, **3-5a**, **3-5b**, **6** and **7**

No.	Relevant δ_H values (ppm) (298 K)		Relevant δ_H values (ppm) (363 K)		Temperature Gradients (TGs) as $(\Delta\delta_{NH}/\Delta T)\times 10^3$ (ppb/K) ^a	<i>D</i> ($\mu\text{m}^2/\text{s}$)	<i>d</i> _H ^b (nm)
	NH	OH	NH	OH			
1a	8.74	9.06	8.37	8.74	-5.69	152	1.44
1b	9.70 9.83 9.91 ^c	9.27	9.46	8.91	-3.69 -5.69 -6.92	218	1.00
2	10.18 10.34 ^c	-	9.97 ^d	-	-3.82 -6.73	230	0.95
3a	8.71	9.01	8.34	8.68	-5.69	152	1.44
4a	8.81	9.04	8.41	8.69	-6.15	137	1.59
3b	8.72	9.02	8.33	8.66	-6.00	131	1.67
4b	8.72	9.01	8.36 ^d	8.70	-6.55	125	1.75
5a	8.83	9.04	8.54	8.79	-4.46	90	2.43
5b	8.72	9.01	8.32 ^d	8.66	-7.27	72	3.03
6	8.78	9.04	8.47	8.78	-4.77	82	2.66
7	8.79	9.05	8.39	8.70	-6.15	70	3.12

^aCalculated as $[(\delta_H^{298\text{K}} - \delta_H^{363\text{K}})/(298\text{K} - 363\text{K})]\times 10^3 < 0$. ^b*d*_H (Hydrodynamic diameter) issued from *D* [diffusion coefficient observed in 2D-¹H-DOSY NMR charts in 5 mM DMSO-*d*₆ (η , dynamic viscosity $2.00\times 10^{-3}\text{ kg m}^{-1}\text{ s}^{-1}$) at 298 K] by applying the Stokes-Einstein equation. ^cMultiple δ_H values due to more than one (*anti-anti*) species found in a frozen rotational equilibrium in agreement with the highest π -deficiency of the *s*-triazine ring in the analysed series (Scheme 3). ^dAt 353 K

intramolecular hydrogen bonds at room temperature. If so, besides the normal aptitude for binding of *p*-HO phenolic functionalities, the contribution to solvation of NH groups, i.e. Me₂S=O...H...N<, was also significant. Indeed, as one can see, almost all TGs in Table 4 were more negative than -4 ppb/K in conjunction with an *anti-anti* arrangement of phenolic (peripheral) units (Scheme 3, Table 2) in all types of compounds.

To what extent the above structural findings have a corresponding electrochemical impact, we will discuss hereafter.

3. Electrochemical characterisation

3.1. Cyclic voltammetry

Next, the electrochemical behaviour of our *p*-aminophenol based amino-*s*-triazines was investigated by means of cyclic voltammetry. The cyclic voltammograms recorded on Pt electrode in DMSO, 0.1M KCl solution are presented in Figure 2.

Except for compounds **2** and **7**, all voltammograms revealed the presence of a single well-defined anodic oxidation peak A1 closely located around 0 V vs. Ag/AgCl, KCl_{sat}. By contrast, 1-3 cathodic reduction peaks, C1-3, were disclosed as C1 and C3 (*Paracetamol* and compounds **1b**, **3b**, **6**), C2 and C3 (compound **1a**) or C1, C2 and C3 (compounds **3a**, **4a**, **4b**, **5a** and **5b**). The variable incidence of the reduction peaks C1 and/or C2 was attributed to the successive reduction

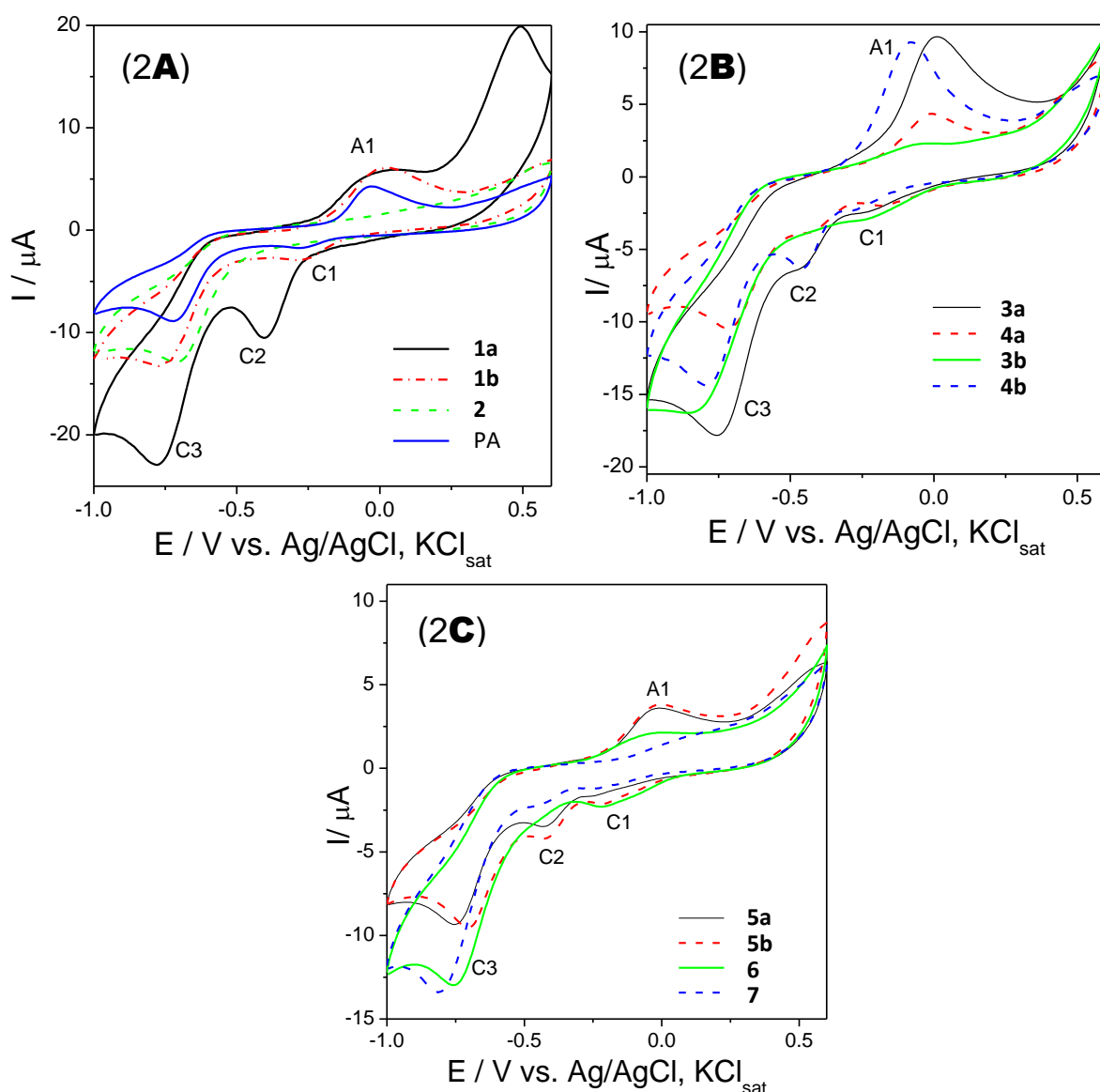


Figure 2. Cyclic voltammograms of 10^{-3} M *Paracetamol* (PA), **1a**, **1b**, **2** (**2A**), **3a**, **3b**, **4a**, **4b** (**2B**) and **5a**, **5b**, **6**, **7** (**2C**). Experimental conditions: electrolyte, anhydrous and ultrasonicated DMSO/0.1M KCl_{sat} solution deaerated with Ar; starting potential -1 V vs. Ag/AgCl, KCl_{sat} ; scan rate, 0.050 Vs^{-1} ; the 25th cycle is shown.

of the species produced during electrochemical oxidation. We note that the reduction peak C3, observed even in anhydrous DMSO 0.1M KCl ultrasonicated solution in the absence of any organic compound, was related to the activity of Pt electrode²¹ and will be not discussed here. The potential values E_p corresponding to peaks A1, C1 and C2, issued from the voltammetric response, are listed in Table 5.

Table 5. Values of A1, C1, C2 peaks potential of compounds *Paracetamol* (PA), **1a**, **1b**, **2**, **3a-5a**, **3b-5b**, **6** and **7** (for Experimental conditions, see Figure 2)

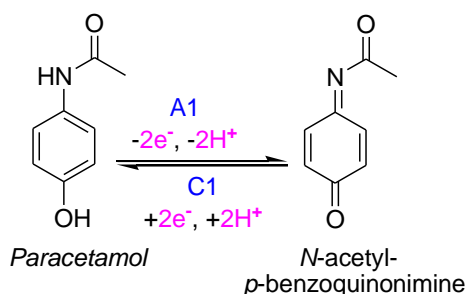
	Compound											
	1b	1a	3a	4a	5a	5b	PA	6	3b	4b	2	7
A1	0.020	0.015	0.013	-0.015	-0.021	-0.024	-0.027	-0.048	-0.052	-0.090	-	^a
C1	-0.270	-	-0.230	-0.180	-0.245	-0.210	-0.275	-0.205	-0.220	-0.275	-	-0.240
C2	-	-0.400	-0.440	-0.415	-0.430	-0.420	-	-	-	-0.460	-	-0.440

^aToo weak to be measured

Since the A1 anodic potentials values were indicative of the electron donating strength of the compounds, we considered that these potentials also reflect their oxidation easiness, i.e. increasing

with the decrease of the oxidation potential value.

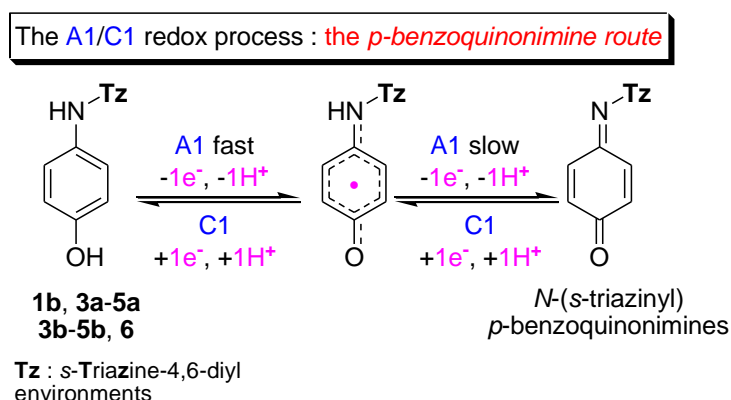
Our attention was primarily focused on the pair of peaks A1/C1. Thus, by comparing voltammograms of the bis(*p*-aminophenol) based diamino-chloro-*s*-triazine **1b** with its *O,O*-diacetyl analogue **2** (Figure 2A), the disappearance of peak A1, around 0.020 V vs. Ag/AgCl, KCl_{sat}, proved that this was due to absence of the free *p*-HO-phenolic group in **1b**, involved in the first step of oxidation. That is, the replacement of *p*-HO (from **1b**) by *p*-AcO group (in **2**) lead to peak A1 vanishing, i.e. single the NH group in **2** was unable to trigger any oxidation process. We note that, in the case of *Paracetamol*, containing just one *p*-aminophenol unit, a recent well-documented *N*-acetyl-*p*-benzoquinonimine oxidation product is mentioned in the literature as the result of a reversible A1/C1 two-electron transfer process (Scheme 4).²²



Scheme 4

The above redox pathway occurs in spite of the low ϵ_{HOMO} level (Table 2) and low LPN(H) orbital population of *Paracetamol* (Table 3). As shown in Table 5, in our conditions, the peak A1 of *Paracetamol* was located at a negative value, -0.027 V vs. Ag/AgCl, KCl_{sat}.

Therefore, concerning the oxidation stage, we postulated a similarity between the EW influence of the variable π -deficient *s*-triazine ring linked to NH group in our compounds and that of EW Ac group in *Paracetamol*. If so, as for *Paracetamol*, the pair of peaks A1/C1 also disclosed an overall and reversible two-electron transfer process / *p*-aminophenol unit even for compounds **1b** and **3a** exhibiting positive E_p A1 values (Table 5). Thus, in a two steps oxidation process, a novel extended π - π -conjugated system of type (*s*-triazinyl)-*p*-benzoquinonimine was formed (Scheme 5).



Scheme 5

One should observe that the decreasing order of the A1 peak potentials (Table 5), for example in (G-0) dendrons series as **1b** > **1a** > **3a** > **3b**, was parallel with the decreasing strength of the π -deficiency of the EWG *s*-triazine expressed as ϵ_{HOMO} values (Table 2) or LPN(H) orbital populations (Table 3). They crucially determined the adjacent NH group ability for oxidation. Therefore, we assumed the *p*-benzoquinonimine route (Scheme 5) to be valid for all derivatives exhibiting the pair of peaks A1/C1 (Figure 2) and the unique electronic transfer for compounds **1b**, **3b** and **6** (Table 5). Nevertheless, to what amount this route involved, simultaneously, all *p*-aminophenol peripheral units could not be established because of the iterative nature of the oxidation process.

Furthermore, the influence of several other factors concerning the redox process A1/C1 (Scheme 5) was also observed. Thus, (G-0) dimeric melamines **4a** and **4b** disclosed significantly lower anodic oxidation potentials against (G-0) monomeric melamines **3a** and **3b**, respectively, most probably because of a better NH-solvation in DMSO expressed by TG values (Table 4).

A comparison between the CVs of (G-0) melamines **3a** and **3b** (Figure 2B) showed that the replacement of the piperazine-1-yl ligand with the more electron-donor 4,4-bipiperidin-1-yl dramatically decreased the anodic oxidation potential, i.e. from +0.013 V to -0.052 V vs. Ag/AgCl, KCl_{sat}. We associated this behaviour with the higher basicity of **3b** vs. **3a** together with the different conformational nature of their diaza-linkers, flipping in **3a** but anancomeric in **3b**. Consequently, the adsorption on the electrode surface of **3b** was more intimate in comparison with that of **3a**. Presumably for the same conformational reason, a similar fluctuation was observed in the case of dimeric (G-0) melamines **4a** (-0.015 V) and **4b** (-0.090 V). *Mutatis-mutandis*, the CVs of the (G-0) melamine **3a** against its dimer **4a** from one hand or of **3b** against **4b** on the other hand (Figure 2B) exhibited a comparable enhancement of the oxidation current in the case of dimers due, very likely, to the doubling of the number of peripheral phenolic groups and to the symmetry of the molecule.

Similar concepts applied in the case of angularly built (G-1) dendrons **5a**, **5b** and **6**.

The oxidation potential values corresponding to peak A1 in these compounds revealed that **5a**, **5b** and **6** (Figure 2C) behave similarly in what the easiness of the oxidation was concerned. However, the oxidation current intensity was much smaller in the case of (G-1) melamine **6** with respect to its (G-1) chlorodendron precursor **5a**, presumably because of the blocking of the electrode surface by adsorption of the compound **6** oxidation products.

It is important to notice that, for compound **7** (Figure 2C), the oxidation peak A1 almost disappeared, suggesting that the dendrimer was much more difficult to oxidize than all its precursors. This behaviour could be motivated by the vaulted spatial arrangement (Figure 1) of **7**, which impeded the contact between the redox centres of the dendrimer and the Pt electrode surface.

3.2. Influence of the starting potential

In order to investigate the influence of the starting potential on the electrochemical response of compounds, dimeric G-0 dendron **4a** was selected as a typical example (Figure 3).

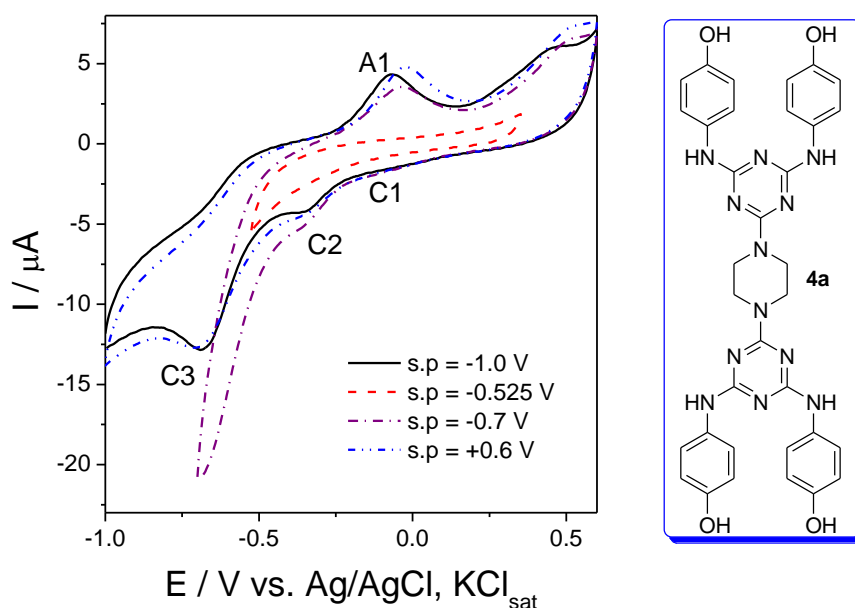


Figure 3. Cyclic voltammogram of 10^{-3} M **4a** at different values of starting potential. Experimental conditions: electrolyte, anhydrous and ultrasonicated DMSO/0.1M KCl_{sat} solution deaerated with Ar; scan rate, 0.050 V s⁻¹; the 7th cycle is shown.

As expected, the width of the scanned potential domain was proven to be of great importance.

Starting from an enough negative value of potential (e.g. at least -0.7 V vs. Ag/AgCl, KCl_{sat}), the appearance of the oxidation peak A1 and of the subsequent reduction processes responsible for reduction peaks C1 and C2 was noticed. When we limited the potential range to a narrow domain (e.g. -0.525 V to +0.300 V vs. Ag/AgCl, KCl_{sat}) no characteristic oxido-reduction peaks appeared. Generally, the starting potential for the electrochemical measurements was -1 V vs. Ag/AgCl, KCl_{sat}. If the experiment was done within a large potential window (-1.0 V - +0.6 V), reversing the scan direction (e.g. starting from +0.6 V vs. Ag/AgCl, KCl_{sat}), no influence on the shape of the voltammogram was observed (Figure 3).

3.3. Reproducibility

The reproducibility of the voltammetric measurements was investigated by recording 3 successive voltammograms for the same electrode with cleaning of its surface between measurements. The reproducibility of cyclic voltammetric measurements for compound **4a** was good. Thus, for a mean value of the peak current intensity of 9.48×10^{-6} A, for 3 successive measurements the relative standard deviation (RSD) was 11.9% (results not shown).

3.4. Influence of repetitive potential cycling

Dimeric (G-0) melamine dendrons **4a** and **4b**, having a low *s*-triazine π -deficiency, were selected in order to study the influence of repetitive potential cycling on the electrochemical response under potentiodynamic conditions by continuous cycling of the electrode potential (25 cycles) in the potential range of -1 V ÷ +0.6 V vs. Ag/AgCl, KCl_{sat}, in DMSO solution, on Pt electrode. The results are shown in Figure 4.

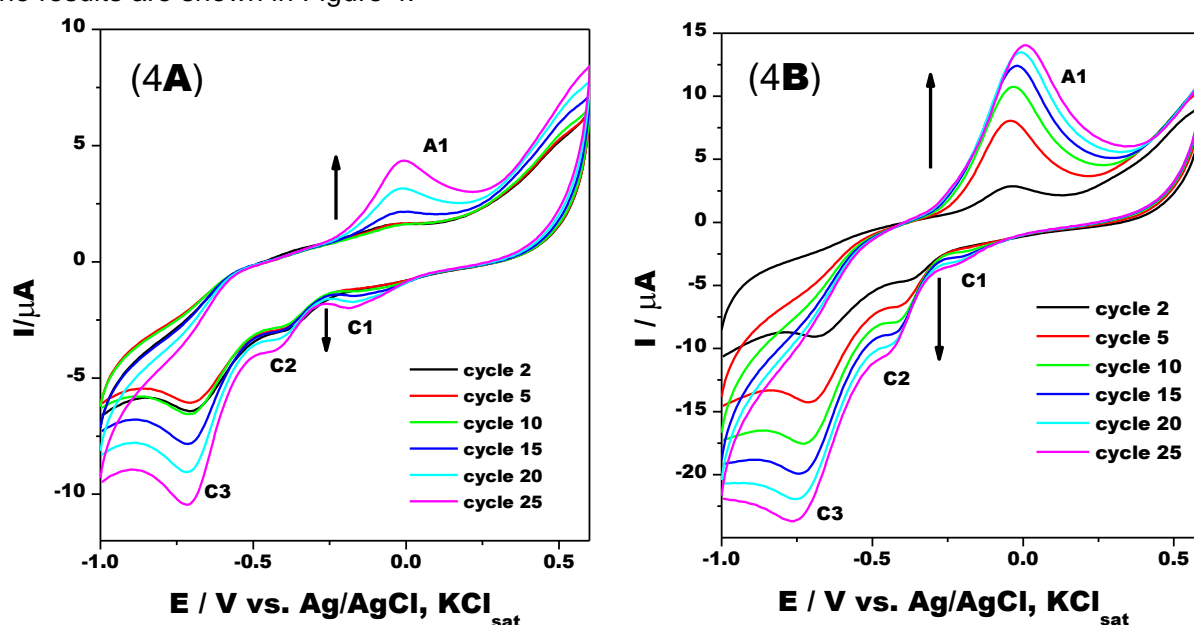


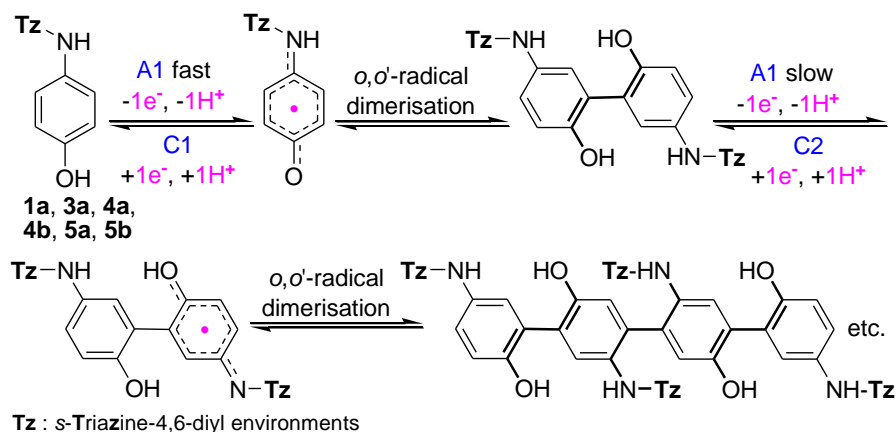
Figure 4. Cyclic voltammograms of 10^{-3} M **4a** (4A) and **4b** (4B) on Pt electrode. Experimental conditions: electrolyte, anhydrous and ultrasonicated DMSO/0.1M KCl_{sat} solution deaerated with Ar; starting potential, -1 V vs. Ag/AgCl, KCl_{sat}; scan rate, 0.050 V s^{-1}

A progressive increase of the peak current was observed suggesting a possible polymerization taking place on the Pt electrode surface.

As proposed in Scheme 6, in our case, the electrochemical pathway should be (i) similar with that of *p*-aminophenol, irrespective the presence of the *s*-triazinyl fragment and (ii) related with that of *Paracetamol*.^{22d}

Thus, the electrochemical significance of peak A1 was almost the same as that in Scheme 5, fast *p*-HO phenolic against slow NH oxidation, the last one being the most sensitive to the EWG *s*-triazine vicinity. As a result, a radical *o,o'*-coupling, similar with that previously reported for

The A1/C2 redox process: *the electropolymerization route*



Scheme 6

Paracetamol,^{22d} occurred to produce dimeric and then linear tetrameric species respectively with a *s-trans* arrangement of the *s*-triazine bulky motifs. One must observe that the cathodic peak potential C2 (Table 5) was located at much more negative values in comparison with C1, in agreement with the decreasing order of stability against reduction of the involved π - π -conjugated system, aromatic (C2) > *p*-benzoquinoniminic (C1).

Besides **4a** and **4b**, the *electropolymerization route* could be extrapolated to all melamines exhibiting the reduction peak C2 namely (G-0) **1a** and **3a**, (G-1) **5a** and **5b**. The *electropolymerization route* appeared to be the single one in the case of (G-0) melamine **1a** (Figure 2A), however not observed for melamines (G-0) **3b** (Figure 2B) and (G-1) **6** (Figure 2C).

CONCLUSIONS

- Avoiding any protective-deprotective step, the iterative synthesis of a new ten members family of (G-0, -1, -2) dendritic melamines comprising *p*-aminophenol (peripheral unit) and piperazine or 4,4'-bipiperidine (linkers) was reported.
- The chemoselective amination of cyanuric chloride performed with the above amino-nucleophiles was more accessible if piperazine was the internal linker of choice.
- Overall, the low solubility of these amino-*s*-triazines in common volatile organic solvents combined with their high relative retention on column chromatography were the two main obstacles to be overcome, successfully, with good yields.
- DFT calculation in DMSO (with global energy minima, indicative bond order indexes, bond lengths and lone pair orbital populations) helpfully established and discriminated the rotational diastereomerism of *p*-aminophenol peripheral units about the partial double bonds C(*s*-triazine)-N(exocyclic) as being of type *asymmetric* or *anti-anti*. The last one was also localised at the periphery of the first *p*-aminophenol based (G-2) dendritic melamine which adopted a vaulted global shape.
- Calculation revealed a lower N-lone pair orbital population in Ph-NH units in comparison with that of the phenolic oxygen atom.
- (VT) ¹H NMR spectroscopy disclosed, by means of temperature gradients, our *p*-aminophenol based amino-*s*-triazines being not only OH but also strongly >N...H...O=SMe₂ solvated molecules.
- Solvation was higher if the internal linker was anancomeric (4,4'-bipiperidin-1,1'-diyl) against flipping (piperazine-1,4-diyl), however less dependent on the molecular dimension (*d_H*).
- Almost all the above structural assignments had an impact on electrochemical characterisation of our amino-*s*-triazines by cyclic voltammetry (Pt electrode/DMSO).
- A two-electron transfer process was observed.

- Depending on the variable strength of π -deficiency of the s-triazine ring acting as EWG on the adjacent NH group and the modulate ability of the latter to undergo redox processes in tandem with the phenolic *p*-HO group, two electrochemical pathways, similar with those already reported for *Paracetamol* and *p*-aminophenol were proposed, (i) *the p-benzoquinonimine route* and (ii) *the electropolymerization route*.

SELECTIVE REFERENCES

- ¹ a) A. Petri, European Patent 0 208 376 A2/January 14, **1987**; b) A. Petri, European Patent 0 208 376 B1/September 15, **1993**; c) M. Negoro, K. Kawata, US Pat. 2005/0209453 A1/September 22, **2005**; d) M. Negoro, K. Kawata, US Pat 7 135 567/November 14, **2006**.
- ² a) S. Shabbir, S. Zulfiqar, Z. Ahmad, M. I. Sarwar, *Tetrahedron*, **2010**, *66*, 1389-1398; b) S. S. Mahapatra, S. Rana, J. W. Cho, *J. Appl. Polym. Sci.*, **2011**, *120*, 474-483.
- ³ P. de Hoog, P. Gamez, W. L. Driessen, J. Reedijk, *Tetrahedron Lett.*, **2002**, *43*, 6783-6786.
- ⁴ a) S. K. Ghosh, A. Saha, B. Hazarika, U. P. Singh, H. R. Bhat, P. Gahtori, *Lett. Drug Des. Discov.*, **2012**, *9*, 329-335; b) H. R. Bhat, U. P. Singh, P. Gahtori, S. K. Ghosh, K. Gogoi, A. Prakashe, R. K. Singh, *New J. Chem.*, **2013**, *37*, 2654-2662; c) H. R. Bhat, U. P. Singh, P. Gahtori, S. K. Ghosh, K. Gogoi, A. Prakash, R. K. Singh, *RSC Adv.*, **2013**, *3*, 2942-2952.
- ⁵ a) M. Darabantu, M. Pinte, M. Fazekas, P. Lameiras, C. Berghian, I. Delhom, I. Silaghi-Dumitrescu, N. Plé, A. Turck, *Lett. Org. Chem.*, **2006**, *3*, 905-910; b) F. Popa, P. Lameiras, O. Moldovan, M. Tomoaia-Cotisel, E. Hénon, A. Martinez, C. Sacalis, A. Mocanu, Y. Ramondenc, M. Darabantu, *Tetrahedron*, **2012**, *68*, 8945-8967; c) O. Moldovan, P. Lameiras, I. Nagy, T. Opruta, F. Popa, C. Antheaume, Y. Ramondenc, M. Darabantu, *Tetrahedron*, **2013**, *69*, 2199-2213; d) O. Moldovan, I. Nagy, P. Lameiras, C. Antheaume, C. Sacalis, M. Darabantu, *Tetrahedron: Asymmetry*, **2015**, *26*, 683-701; e) V. Lates, D. Gligor, M. Darabantu, L. M. Muresan, *J. Appl. Electrochem.*, **2007**, *37*, 631-636.
- ⁶ a) W. Zhang, E.E. Simanek, *Org. Lett.*, **2000**, *2*, 843-845; b) A.E. Enciso, F. Ramirez-Crescencio, M. Zeiser, R. Redón, E.E. Simanek, *Polym. Chem.*, **2015**, *6*, 5219-5224; c) R.S. Sreepurambuduru, Z.M. Abid, K.M. Claunch, H.-H. Chen, S.M. McGillivray, E.E. Simanek, *RSC Adv.*, **2016**, *6*, 8806-8810.
- ⁷ C. Morar, L. Cost, P. Lameiras, C. Antheaume, M. Darabantu, *Synthetic Commun.*, **2015**, *45*, 1688-1695.
- ⁸ a) T. Drakenberg, S. Forsen, *Chem. Commun.*, **1971**, *21*, 1404-1405; b) S. S. Mirvish, P. Gannett, D. M. Babcock, D. Williamson, S. C. Chen, D. D. Weisenburger, *J. Agric. Food Chem.*, **1991**, *39*, 1205-1210.
- ⁹ a) I. Willner, J. Rosengaus, Y. J. Eichen, *Phys. Org. Chem.*, **1993**, *6*, 29-43; b) A. R. Katritzky, I. Ghiviriga, D. C. Oniciu, A. Barkock, *J. Chem. Soc., Perkin Trans. 2*, **1995**, *4*, 785-792; c) A. R. Katritzky, I. Ghiviriga, P. G. Steel, D. C. Oniciu, *J. Chem. Soc., Perkin Trans. 2*, **1996**, *3*, 443-447; d) P. Amm, N. Platzer, J. Guilhem, J. P. Bouchet, J. P. Volland, *Magn. Reson. Chem.*, **1998**, *36*, 587-596; e) H. E. Birkett, R. K. Harris, P. Hodgkinson, K. Carr, M. H. Charlton, J. C. Cherryman, A. M. Chippendale, R. P. Glover, *Magn. Reson. Chem.*, **2000**, *38*, 504-511; f) M. Amm, N. Platzer, J. P. Bouchet, J. P. Volland, *Magn. Reson. Chem.*, **2001**, *39*, 77-84; g) I. Ghiviriga, D. C. Oniciu, *Chem. Commun.*, **2002**, *22*, 2718-2719; h) H. E. Birkett, J. C. Cherryman, A. M. Chippendale, J. O. S. Evans, R. K. Harris, M. James, I. J. King, G. Mc Pherson, *Magn. Reson. Chem.*, **2003**, *41*, 324-336.
- ¹⁰ Y. Zhao, D. G. Truhlar, *Theor. Chem. Acc.*, **2008**, *120*, 215-241.
- ¹¹ F. Weigend, R. Ahlrichs, *Phys. Chem. Chem. Phys.*, **2005**, *7*, 3297-3305.
- ¹² Gaussian 09, Revision D.01, M. J. Frisch, G. W. Trucks, H. B. Schlegel, G. E. Scuseria, M. A. Robb, J. R. Cheeseman, G. Scalmani, V. Barone, B. Mennucci, G. A. Petersson, H. Nakatsuji, M. Caricato, X. Li, H. P. Hratchian, A. F. Izmaylov, J. Bloino, G. Zheng, J. L. Sonnenberg, M. Hada, M. Ehara, K. Toyota, R. Fukuda, J. Hasegawa, M. Ishida, T. Nakajima, Y. Honda, O. Kitao, H. Nakai, T. Vreven, J. A. Montgomery Jr., J. E. Peralta, F. Ogliaro, M. Bearpark, J. J. Heyd, E. Brothers, K. N. Kudin, V. N. Staroverov, R. Kobayashi, J. Normand, K. Raghavachari, A. Rendell, J. C. Burant, S. S. Iyengar, J. Tomasi, M. Cossi, N. Rega, J. M. Millam, M. Klene, J. E. Knox, J. B. Cross, V. Bakken, C. Adamo, J. Jaramillo, R. Gomperts, R. E. Stratmann, O. Yazyev, A. J. Austin, R. Cammi, C. Pomelli, J. W. Ochterski, R. L. Martin, K. Morokuma, V. G. Zakrzewski, G. A. Voth, P. Salvador, J. J. Dannenberg, S. Dapprich, A. D. Daniels, Ö. Farkas, J. B. Foresman, J. V. Ortiz, J. Cioslowski, D. J. Fox., Gaussian, Inc.: Wallingford CT, **2009**.
- ¹³ J. Tomasi, B. Mennucci, R. Cammi, *Chem. Rev.*, **2005**, *105*, 2999-3093.
- ¹⁴ J. P. Foster, F. Weinhold, *J. Am. Chem. Soc.*, **1980**, *102*, 7211-7218.
- ¹⁵ A. E. Reed, R. B. Weinstock, F. Weinhold, *J. Chem. Phys.*, **1985**, *83*, 735-746.
- ¹⁶ K. A. Wiberg, *Tetrahedron*, **1968**, *24*, 1083-1096.
- ¹⁷ GaussView, Version 5.0.9, R. Dennington, T. Keith, J. Millam, *Semichem Inc.*, Shawnee Mission, KS, **2009**.
- ¹⁸ a) F. Vögtle, G. Richard, N. Werner, *Dendrimer Chemistry*, WILEY-VCH Verlag GmbH & Co. KGaA: **2009**, p. 7-22, 25-44; b) X. K. Moreno, E. E. Simanek, *Macromolecules*, **2008**, *41*, 4108-4114.
- ¹⁹ a) H. Friebolin, *Basic one- and two dimensional NMR spectroscopy*; VCH Verlagsgesellschaft: Weinheim, New York, **1991**, pp 93, 263-291; b) E. L. Eliel, H. S. Wilen, *Stereochemistry of the Organic Compounds*; John Wiley & Sons, New York, **1994**, p. 642, 1191.
- ²⁰ H. Kessler, *Angew. Chem. Int. Ed. Engl.*, **1982**, *21*, 512-523.
- ²¹ V. Tanasković, I. Pašti, S. Mentus, *Int. J. Electrochem. Sci.*, **2013**, *8*, 6243-6251.
- ²² a) M. Zidan, T. W. Tee, A. H. Abdullah, Z. Zainal, G. J. Kheng, *Int. J. Electrochem. Sci.*, **2011**, *6*, 279-288; b) A. Asghari, M. Ameri, A. A. Ziarati, S. Radmannia, A. Amoozadeh, B. Barfi, L. Boutorabi, *Chinese Chem. Lett.*, **2015**, *26*, 681-684; c) C. Engin, S. Yilmaz, G. Saglikoglu, S. Yagmur, M. Sadikoglu, *Int. J. Electrochem. Sci.*, **2015**, *10*, 1916-1925; d) V. Fischer, P.R. West, L.S. Harman, R.P. Mason, *Environ. Health Persp.*, **1985**, *64*, 127-137.

Chapter III

*Design, synthesis and structure of novel G-2 melamine-based dendrimers incorporating 4-(*n*-octyloxy)aniline as a peripheral unit*

INTRODUCTION

N-substituted melamine (2,4,6-triamino-1,3,5-triazine)-based dendrimers¹ are a class of macromolecules reported as early as 2000 by E. E. Simanek and co-workers^{1a} as part of an innovative development of convergent^{1a, 1f} and divergent^{1a, 1f, 1g, 1o} strategies towards iterative dendritic synthesis. Along with their expansion, both the biological impact of the above arborescent structures, mainly as drug delivery systems,² and their utilisation as organic materials have constantly been highlighted. In the latter context, dendritic liquid crystals defines a well-established area in the organic materials domain,³ including few examples of *s*-triazine dendrimers exhibiting mesogenic behaviour. The first cases known so far refer to *N*-substituted G-0-3 dendritic melamines with *n*-octyl peripheral groups as unconventional columnar liquid crystals and G-0 tris(triazolyl)triazines (available via the “click” reaction between 2,4,6-tris(ethynyl)-*s*-triazine and various icosanyloxyphenylazides) with liquid crystalline and luminescent properties.

On the other hand, mesogenic supramolecular perylene bisimide assemblies with a number of 2-amino-4,6-bis[(4-alkoxy)phenylamino]-*s*-triazines,^{4, 4a} amphiphilic azobenzene-containing linear-dendritic block copolymers^{4b} and G-0 monomeric or dimeric dendritic liquid crystals with photochromic azobenzene mesogens^{4b, 4c} called attention on the use of 4-(*n*-octyloxy)aniline as key building block in the above macromolecules' elaboration.

Following up our contributions in the field of dendritic melamines' synthesis, structural analysis⁵ and electrochemistry,⁶ we recently become interested in the inclusion of 4-aminophenol, playing the role of peripheral unit, in G-0-2 dendritic melamines' preparation, by applying the classic S_N2-Ar amination of cyanuric chloride in iterative-convergent strategies. Depending on several factors such as (i) the variable π -deficiency of the *s*-triazine branch-cells, (ii) basicity and conformational nature of the diaza-six-membered saturated heterocycle as linker and (iii) the global molecular shape, the resulted 4-aminophenol-based melamines displayed relevant redox properties^{6c} and, in some cases, selective aptitudes to produce MOFs (metal-organic frameworks).^{6b}

All the above information prompted us towards an *ab initio* exploration of 4-(*n*-octyloxy)aniline (seen as the *n*-octyl ether derivative of 4-aminophenol) as starting material towards new melamine-based dendrimers as synthesis (feasibility and limits), structure and self-assembly propensity. To the best of our knowledge, no similar approach has been reported so far.

RESULTS AND DISCUSSION

1. Design

The key elements for construction and the design of the targeted G-2 dendrimers are shown in Chart 1. Cyanuric chloride,^{1, 2} trimesic acid trichloride⁷ and 1,3,5-tris(bromomethyl)benzene⁸ are commercial chemicals, classically known as reactive *m*-trivalent (hetero)aryl halo-compounds, that are easily convertible into dendritic cores in reactions with various dendrons as *N*- and *O*-nucleophiles.

The preparation of the central building block **A** [1,3,5-tris(piperazinomethyl)benzene] consisted of the amination of 1,3,5-tris(bromomethyl)benzene with commercially available *N*-Boc piperazine followed by deprotection, and was achieved according to the literature⁹ (97% overall yield in our hands). Similarly, 2,4,6-tris[(4-hydroxy)phenylamino]-*s*-triazine **B**, a known starting material for plastics manufacturing^{10, 10d} and divergent G-1 dendritic synthesis,^{10c} was obtained using 4-aminophenol as amine nucleophile and reacting it with cyanuric chloride by applying a previously patented protocol^{10c} completed with our own subsequent improvements.^{6c} With regard to (4-aminophenoxy)alkanoic acid-based tripodal melamines **C1** and **C3**, we recently reported their synthesis in three steps via convergent (starting from *N*-acetyl-4-aminophenol, also known as *Paracetamol*) and divergent (via **A**) strategies¹¹ which are summarised in Scheme 1.

All central building blocks (**A-C**) already contain a standard *m*-trivalent core (benzene-1,3,5-triyl or *s*-triazin-2,4,6-triyl) connected to 1,4-disubstituted six-membered (hetero)cycle linkers. These linkers were

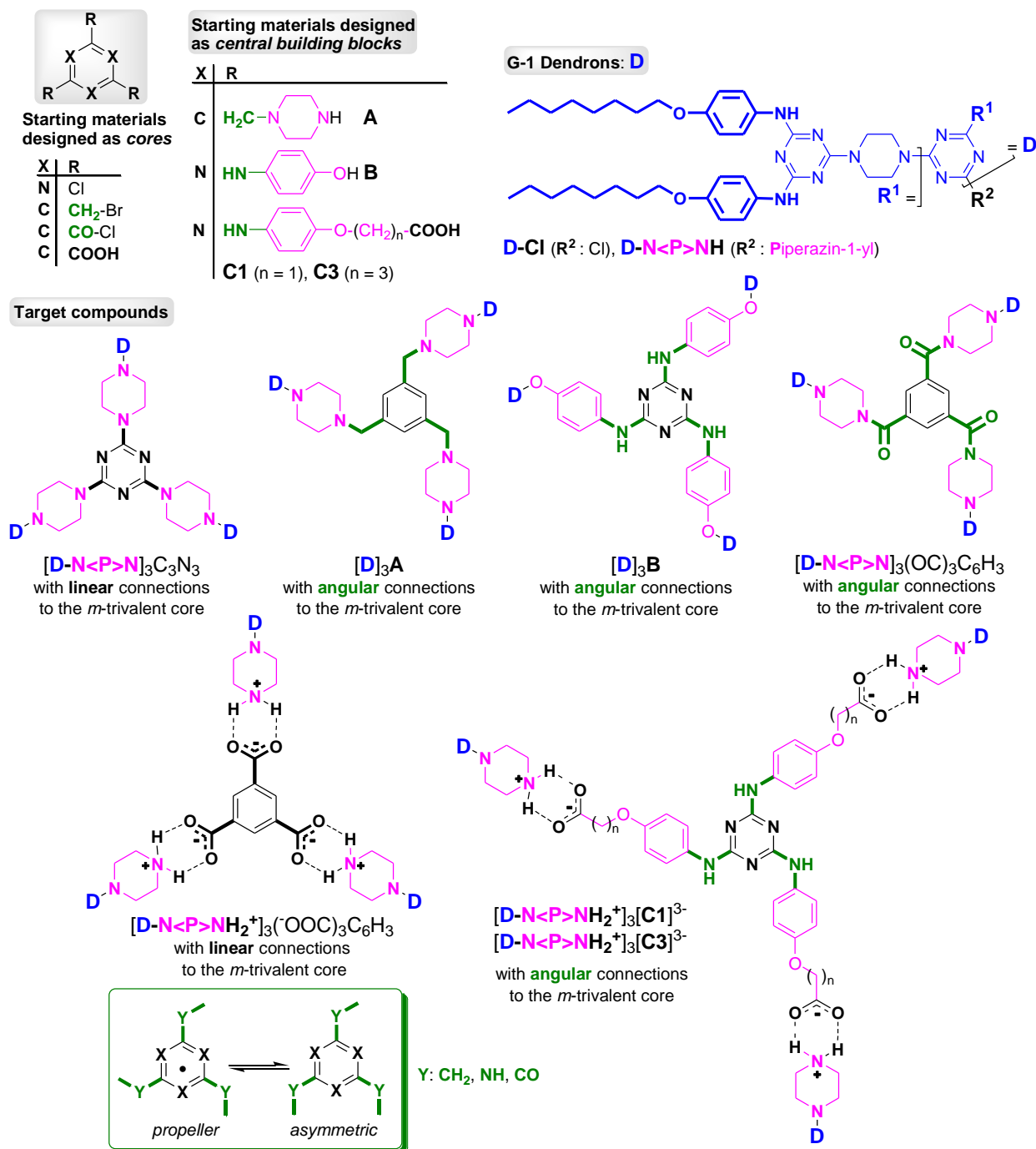
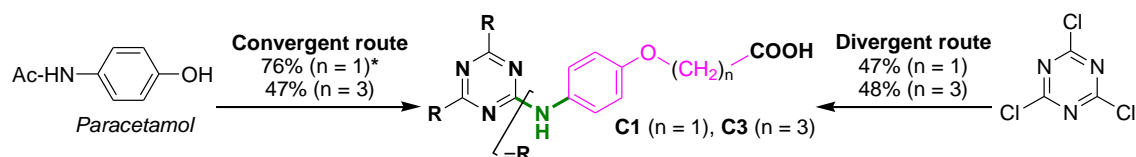


Chart 1: The key elements for construction and design of the targeted G-2 dendrimers



Convergent route: a) Br-(CH₂)_n-COOEt / K₂CO₃ (Williamson); b) H⁺ / H₂O; c) C₃N₃Cl₃ / AcONa, K₂CO₃

Divergent route: a) *p*-H₂N-C₆H₄-OH / AcONa; b) Br-(CH₂)_n-COOEt / K₂CO₃ (Williamson); c) H⁺ (n = 1), HO⁻ (n = 3) / H₂O

*Overall (a → c) yields

Scheme 1: Convergent versus divergent three steps (a-c) synthesis of central building blocks **C1** and **C3**

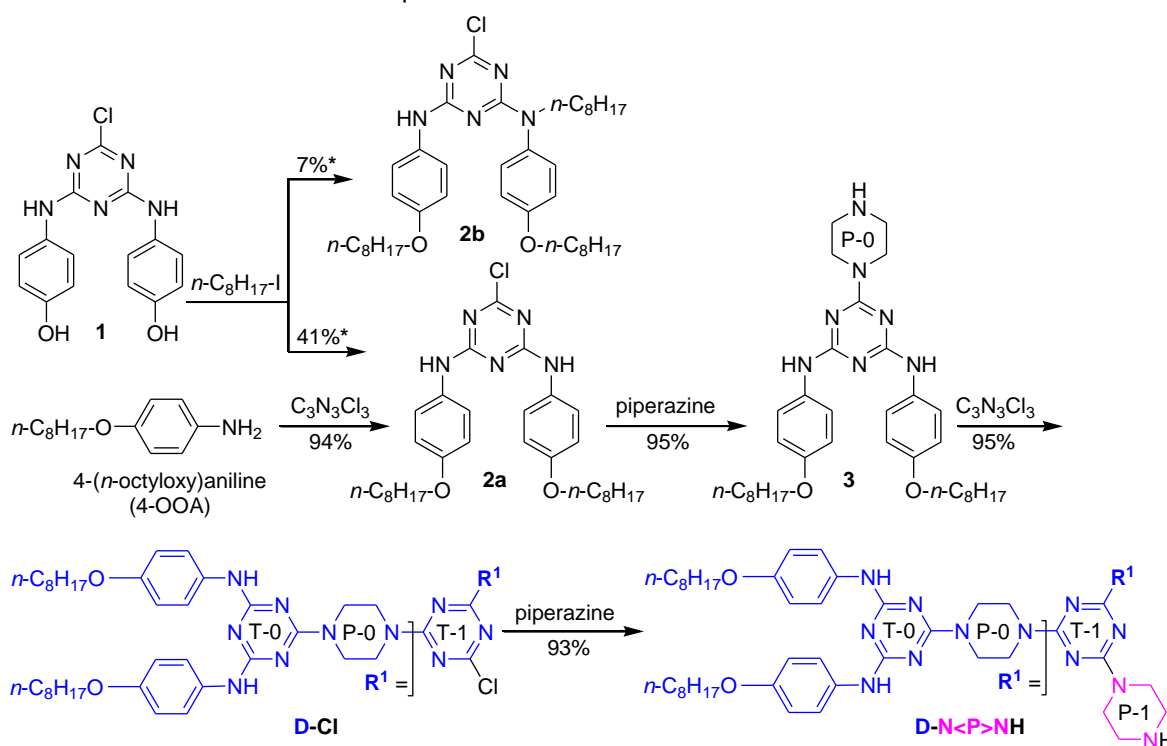
chosen based on their intimate nature: flexible (piperazin-1-yl)methyl (in **A**), rigid 1,4-phenylene (in **B**) and rigid 1,4-phenylene with adjustable alkoxy-spacers (n = 1, 3, in **C1** and **C3**, respectively). G-1 chloro- and piperazine-dendrons, **D-Cl** and **D-N<P>NH**, as well as central building blocks **B**, **C1** and **C3**, had *s*-triazine rings linked by C(*s*-triazine)-N(exocyclic) partial double bonds, which exist due to classic LP(N^{sp2}, exocyclic)

→ $\pi(\text{C}=\text{N}, s\text{-triazine})$ delocalisation. A well-documented restricted rotation effect that causes diastereomerism is thus induced.¹² In the case of some dendritic melamines, this intrinsic feature can promote specific spatial arrangements at room temperature in solution, for example, *asymmetric* vs. *propeller* (C_3 -symmetric),^{5a-b, 5e, 12e, 13} “dendritic choreography”,^{6j} “open-gates \rightleftharpoons closed-gates” frontier rotamerism^{5b} and “in \rightleftharpoons out” axial chirality.^{5d}

In addition, in the targeted G-2 dendrimers (Chart 1), different connections of branches around the core (or central building blocks) were imagined, i.e., *linear* or *angular* (*covalent* vs. *ionic* by carboxyl/amino neutralisation) and were seen as a complementary focus to our work towards structural diversity.

1.2. Synthesis of G-1 dendrons

G-1 dendrons **D-CI** and **D-N<P>NH** (Chart 1) were prepared according to the chemistry depicted in Scheme 2. Reaction conditions and quantitative results are listed in Table 1.



*As partial conversions of 1 into 2a and 2b based on the effective amounts of these products isolated after column chromatography

Scheme 2: Synthesis of G-1 dendrons **D-CI** and **D-N<P>NH**

Table 1: Reagents and conditions in the synthesis of compounds **2a**, **2b**, **3**, **D-CI** and **D-N<P>NH**

Entry	Reaction	Conditions ^a
1	1 → 2a , 2b	(i) 1.00 equiv. <i>n</i> -C ₈ H ₁₇ -I, 8.00 equiv. K ₂ CO ₃ , acetone, -13 °C, 3 h; r.t., 12 h; (ii) 1.00 equiv. <i>n</i> -C ₈ H ₁₇ -I, r.t., 72 h; 50 °C, 8 h / N ₂
2	4-OOA → 2a ^b	(i) 0.50 equiv. C ₃ N ₃ Cl ₃ , acetone, 0-5 °C, 2 h; (ii) 1.00 equiv. NaHCO ₃ , H ₂ O, 0-5 °C; 45 °C, 3 h; r.t., 18 h / N ₂
3	2a → 3	4.00 equiv. piperazine, 1.00 equiv. K ₂ CO ₃ , THF, r.t., 34 h
4	3 → D-CI	0.50 equiv. C ₃ N ₃ Cl ₃ , 1.00 equiv. K ₂ CO ₃ , THF, -10 °C, 3 h; r.t., 36 h; reflux, 24 h
5	D-CI → D-N<P>NH	4.00 equiv. piperazine, 1.00 equiv. K ₂ CO ₃ , THF, r.t., 40 h; reflux, 15 h

^aFor comments about these conditions, see Section 3.1. ^bThe same double amination of cyanuric chloride with 4-(*n*-octyloxy)aniline was reported by S. Yagai and co-workers in 2012.^{9a} with no isolation of 2a, as it was submitted *in situ* to ammonolysis to give 2-amino-4,6-bis[4-(*n*-octyloxy)phenylamino]-s-triazine (75% overall yield).

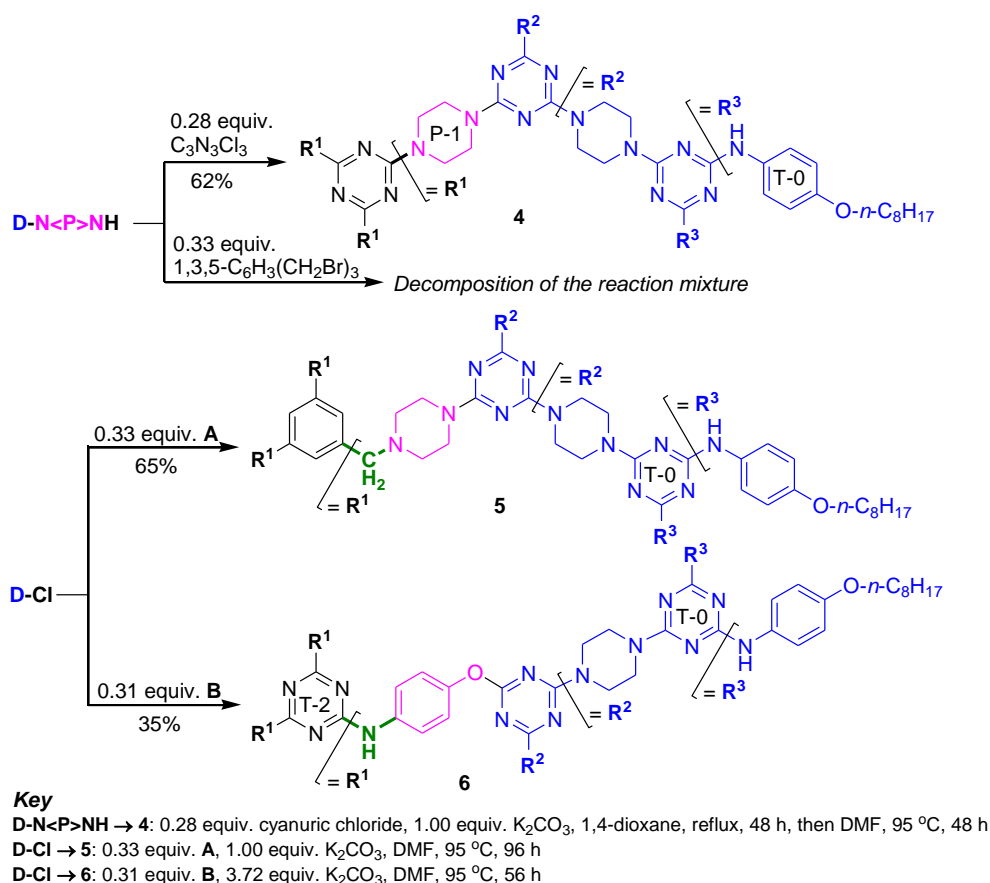
We initially considered using the previously reported 4-hydroxyphenyl *N*-substituted 2-chloro-4,6-diamino-s-triazine **1**^{6c, 14} as starting material. To our disappointment, the attempted *O,O'*-bis-alkylation of **1** with 1-iodooctane (Williamson etherification, Table 1, entry 1), afforded a multicomponent reaction mixture (TLC monitoring, 100% conversion of **1**), from which we succeed in isolating only G-0 chloro-dendron **2a**

and the *O,O',N*-tris-alkylated side product **2b** by column chromatography. Other efforts (not detailed in the present report), such as manipulation under dark conditions or replacing the iodine in the alkylating reagent by bromine, provided even more unsatisfactory results, e.g., the *O*-mono-alkylated product. By contrast, the double amination of cyanuric chloride with commercial 4-(*n*-octyloxy)aniline (Table 1, entry 2) gave the desired G-0 chloro-dendron **2a** with excellent yield.

Using G-0 dendron **2a**, we synthesised G-1 dendrons in two (\rightarrow **D-Cl**) or three (\rightarrow **D-N<P>NH**) orthogonal transformations,¹⁵ with excellent overall yields (90% and 84% from **2a** respectively). The complete chemoselectivity observed during the installation of the piperazine linkers on **2a** (Table 1, entry 3) and on **D-Cl** (Table 1, entry 5) was ensured by the use of a 300% molar excess of this inexpensive reagent.

1.3. Synthesis of G-2 dendrimers

The synthesis of G-2 dendrimers **4-6** (Scheme 3) revealed a moderate reactivity of G-1 dendrons **D-N<P>NH** and **D-Cl** with cyanuric chloride and central building blocks **A** and **B**. Therefore, in addition to TLC, all reactions were monitored by HRMS as well. They were stopped when no further reaction was observed by TLC and when the expected molecular peak was identified by HRMS (ESI+, ACN+TFA).



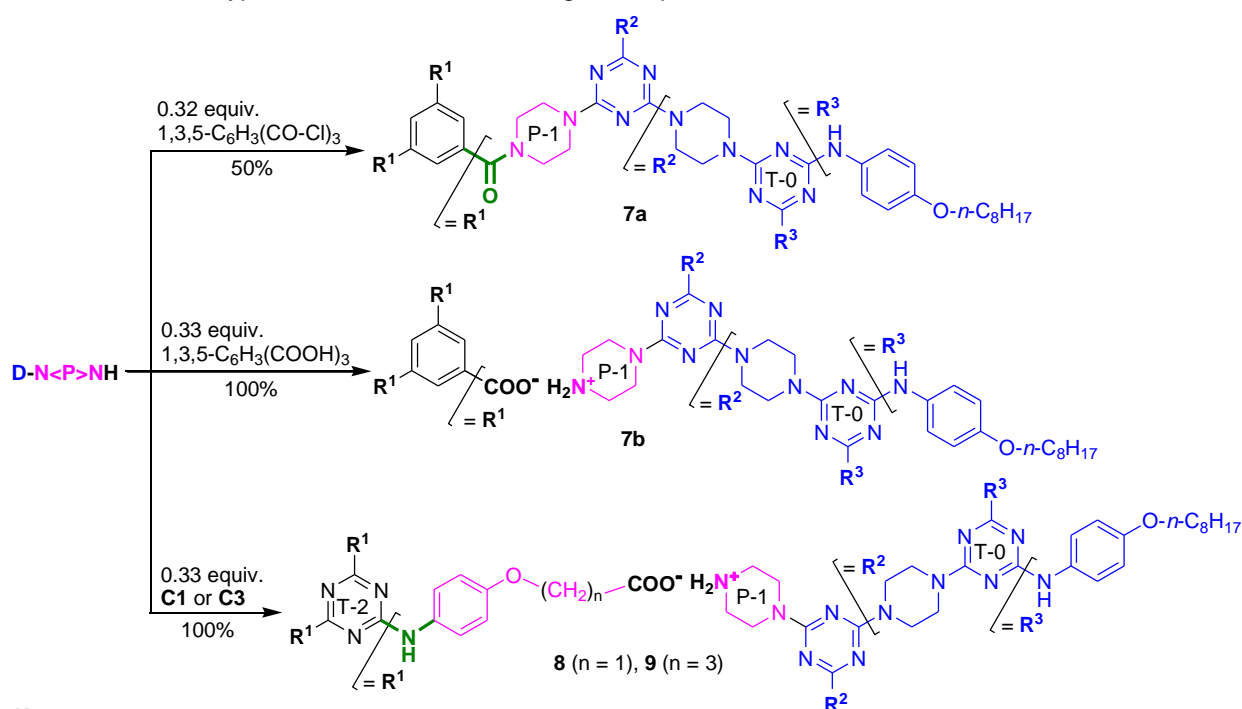
Scheme 3: Synthesis of G-2 dendrimers **4-6** by *m*-trimerisations of G-1 dendrons **D-Cl** and **D-N<P>NH**

Under demanding thermal conditions, the complete amination of cyanuric chloride by **D-N<P>NH** gave the G-2 dendrimer **4** with satisfactory yield. By contrast, treatment of 1,3,5-tris(bromomethyl)benzene with **D-N<P>NH** (3 equiv., 72 h in refluxing 1,4-dioxane in the presence of K_2CO_3 as proton scavenger) resulted in no dendrimer formation; decomposition of **D-N<P>NH** was observed instead (as determined by additional NMR monitoring). Nevertheless, the desired G-2 dendrimer **5** could be obtained through an alternative route, namely, by amination of G-1 chloro-dendron **D-Cl** with building block **A** (Chart 1) under harsh conditions.

To obtain dendrimer **6**, we expected to exploit the nucleophilicity of the phenoxide groups in the *N,N'*

,*N'*-tris(4-hydroxyphenyl)melamine **B** (Chart 1) based on the previous example of P. Gamez and co-workers,^{10c} which involved reaction with 2-chloro[4,6-di(pyridin-2-ylamino)]-s-triazine in the presence of DIPEA (69% yield after 48 h at 85 °C in pyridine). However, when dendrimer **6** was obtained by reacting **B** (0.31 equiv.) with **D-Cl** (1.00 equiv.), the reaction only proceeded properly when 4.00 equiv. K₂CO₃ per phenolic OH group in **B** was used as the proton scavenger and deprotonating reagent, i.e., in an identical acid/base molar ratio as that used earlier in the triple Williamson etherification of **B** (Chart 1, Scheme 1, *Divergent route*) with bromoalkanoic acid ethyl esters.¹³ Even so, the yield of **6** was modest, 35%.

Furthermore, we obtained G-2 dendrimers **7a** and **7b** (Scheme 4) by the triple amidation of trimesic acid trichloride upon treatment with G-1 dendron **D-N<P>NH** (covalent *m*-trimerisation → **7a**) or by simple neutralisation of the latter with trimesic acid (ionic *m*-trimerisation → **7b**), the product of which was symbolised as [D-N<P>NH₂⁺]₃(⁻OOC)₃C₆H₃ (Chart 1). In the synthesis of **7a**, unexpectedly difficult conditions for this type of reaction were, once again, required.



Key

D-N<P>NH → **7a**: 0.33 equiv. trimesic acid trichloride, 1.00 equiv. K₂CO₃, THF, 0 °C, r.t., 72 h then reflux, 48 h / N₂

D-N<P>NH → **7b**: 0.33 equiv. trimesic acid, THF, 60 °C, 15 min. then evaporation to dryness

D-N<P>NH → **8** and **9**: 0.33 equiv. **C1** (or **C3**), DMSO, 95 °C, 15 min. then lyophilisation

Scheme 4: Synthesis of G-2 dendrimers **7-9** by *m*-trimerisations of G-1 dendron **D-N<P>NH**

Similar amidations run in triplicate using instead the acid chlorides of **C1** and **C3** provided negative results.

Therefore, we had to limit our efforts to the stoichiometric salts (Chart 1), symbolised as [D-N<P>NH₂⁺]₃[**C1**]³⁻ (**8**) and [D-N<P>NH₂⁺]₃[**C3**]³⁻ (**9**). These dendritic constructions by ionic *m*-trimerisations occurred smoothly and in quantitative yields (Scheme 4).

2. Structural assignments

Our research continued with a structural study, implemented by means of DFT calculations, solution (VT) NMR techniques, IR (KBr) spectroscopy and TEM analysis.

2.1. Assignments based on DFT calculations of G-0 and G-1 dendrons: optimal geometry and solvation effects

First, we attempted to explain the generally difficult conditions encountered during synthesis (Schemes 2-4) based on DFT calculations (Table 2).

As in the case of other amino-*s*-triazines,^{5a-c, 12e, 13} for G-0 dendrons **2a** and **3**, a topologically

Table 2: Full geometry optimisation of G-0 dendrons **2a**, **3**,¹⁶⁻¹⁹ solvation energies of G-0 and G-1 dendrons **2a**, **3**, **D-Cl**, **D-N<P>NH**²⁰ and Lone Pair (LP) electron occupation of piperazine N^{sp3} nitrogens in dendrons **3** and **D-N<P>NH**¹⁶⁻¹⁸

No.	Relative conformational total electronic Energy ΔE (kJ mol ⁻¹) ^a In the gas phase In DMSO			ΔG of solvation (kJ mol ⁻¹) for the (<i>a-a</i>) major rotamer ^a		LP electron occupation of piperazine N ^{sp3} nitrogens (<i>e</i>) ^b	
	(<i>s-s</i>)	(<i>a-s</i>)	(<i>a-a</i>)	THF ^c	1,4-Dioxane ^d	THF	1,4-Dioxane
2a	10.464 17.371	8.329 15.558	0.000 0.000	-146.37	-104.39	-	-
3	4.395 5.923	4.730 4.504	0.000 0.000	-167.54	-122.51	1.92	1.92
D-Cl	-	-	-	-378.66	-284.28	-	-
D-N<P>NH	-	-	-	-401.81	-301.36	1.93	1.92

^aSee Experimental and SI (pp. SI40) for details of this DFT calculation. ^bElementary electric charge carried by a single electron.

^cDielectric constant, $\epsilon = 7.4257$. ^dDielectric constant, $\epsilon = 2.2099$.

idealised model predicted a three terms (*syn-syn* \rightleftharpoons *anti-syn* \rightleftharpoons *anti-anti*) rotational equilibrium about the C(*s*-triazine)-N^{sp2}(exocyclic) (Chart 2) partial double bonds, at room temperature. Similar to simpler 4-hydroxyphenyl-based amino-*s*-triazine analogues of **2a** and **3**,^{6b-6c} the optimised (*a-a*) geometry was found to be largely dominant, both in the gas phase as well as in solution, e.g., DMSO, which was the most appropriate solvent for (VT) ¹H NMR and TEM investigations (see Section 2.3). As expected, the relative ΔE values for the rotational diastereomerism decreased (i) with the decrease of the steric hindrance between the three (hetero)aryl rings in rotamers (*s-s*) > (*a-s*) > (*a-a*), and (ii) with the weakening of the π -deficiency of the *s*-triazine, **2a** > **3**. The same optimal geometry (*a-a*) was found in duplicate, (*a-a*)/(*a-a*), in G-1 dimers **D-Cl** and **D-N<P>NH** (Chart 2).

Furthermore, for the major (*a-a*) rotamers, calculations also revealed high solvation energies in the case of all four G-0 and G-1 dendrons. For a single compound, the solvation energy was 33-40% higher in THF vs. 1,4-dioxane. Unsurprisingly, piperazine-dendrons were more solvated than their chloro-precursors, e.g., **3** vs. **2a** (+14% in THF, +17% in 1,4-dioxane), and **D-N<P>NH** vs. **D-Cl** (about +6% in both solvents). Taking into account the negligible decrease in LP electron occupation of the piperazine N^{sp3} nitrogens in **3** and **D-N<P>NH** as well, we ascribed the low reactivity of G-1 dendrons **D-Cl** and **D-N<P>NH** in our S_N2-Ar amination conditions to the increased solvation of their (*a-a*)/(*a-a*) rotamers (+140-170%, i.e., more than double) compared to those of the (*a-a*) rotamers of G-0 **3** and **2a**.

In addition to all the above, due to the steric accommodation of 12 *n*-octyloxy chains, the occurrence of a *starburst* effect^{3a, 18b} during the covalent *m*-trimerisations (Scheme 3), was also presumed (see Section 2.2.1.).

2.2. Assignments by means of NMR and IR spectroscopy

The ¹H NMR data deserving of comment are listed in Table 3.

2.2.1. Rotational diastereomerism at dendritic level

As expected, due to it having the highest π -deficient *s*-triazine group, at room temperature only G-0 chloro-dendron **2a** exhibited the nearly frozen nature of the *anti* \rightleftharpoons *syn* (Chart 2) rotational equilibrium on a 500 MHz ¹H NMR timescale. In contrast, under the same conditions, the rotational diastereomerism of all other compounds (G-0, G-1 and G-2) was identified, as the classically entitled “slow exchange status between unequally populated sites”.²² At room temperature, dendrimers **5**, **7a**, **8** and **9** displayed unique signals for the topologically equivalent ¹H and ¹³C nuclei of the *m*-trivalent core and their adjacent angular connections, i.e., consistent with a *propeller* as *local* dominant arrangement (Chart 1). Except for G-2 dendrimer **5**, upon heating to 90 °C, all compounds became single mediated structures, in states with rapid and free rotation about all the C(*s*-triazine)-

Table 3: Relevant (VT) ^1H NMR, Temperature Gradients and 2D- ^1H -DOSY NMR data (500 MHz, DMSO- d_6) of G-0 dendrons **2a**, **3**, G-1 dendrons **D-CI**, **D-N<P>NH** and G-2 dendrimers **4-6**, **7a**, **7b**, **8**, **9**

No.	δ_{H} (ppm) values of indicative NH protons (see Chart 2)				Temperature Gradients (TGs) as $(\Delta\delta_{\text{H}}/\Delta T)\times 10^3$ (ppb K $^{-1}$) ^a		D^{b} ($\mu\text{m}^2 \text{s}^{-1}$)	d_{H}^{b} (nm)
	NH adjacent to s-triazine T-0		NH adjacent s-triazine T-2		NH adjacent to s-triazine T-0	NH adjacent s-triazine T-2		
	298 K	363 K	298 K	363 K				
2a^c	10.03 9.96 9.85	9.63	-	-	-6.15 -5.08 -3.38		198	1.10
3	8.87	8.50	-	-	-5.69		191	1.14
D-CI	9.08	8.70	-	-	-5.85		129	1.69
D-N<P>NH	8.93	8.57	-	-	-5.54		110	1.98
4	9.71	8.93	-	-	-12.00		89	2.45
5	8.92	8.51 8.53 8.55 8.60	-	-	-6.31 -6.00 -5.69 -4.92		88	2.48
6^d	-	8.55	-	9.02	-		-	-
7a	8.94	8.55	-	-	-6.00		107	2.04
7b	8.93	8.53	-	-	-6.15		105 225	2.08 0.97
8	8.93	8.54	8.93	8.60	-6.00	-5.08 ^e	113	1.93
9	8.94	8.54	8.70	8.57	-6.15	-2.00 ^f	115	1.90

^aTGs calculated as $[(\delta_{\text{H}}^{298 \text{ K}} - \delta_{\text{H}}^{T \text{ K}})/(298 \text{ K} - T)]\times 10^3 < 0$ (where $T = 363 \text{ K}$). ¹, ²¹ ^b d_{H} (hydrodynamic diameter) issued from D [diffusion coefficient observed in 2D- ^1H -DOSY NMR charts as 5.0 mM (**2a**, **3**, **D-CI**, **D-N<P>NH**, **5**, **8** and **9**) or 2.5 mM (**4**, **7a** and **7b**) in DMSO- d_6 (η , dynamic viscosity $2.00\times 10^{-3} \text{ kg m}^{-1} \text{ s}^{-1}$) at 298 K] by applying the Stokes-Einstein equation. ^cMultiple δ_{H} and TG values due to more than one (*anti-anti* major 64% vs. *anti-syn* minor 36%) species found in a frozen rotational equilibrium in agreement with the highest π -deficiency of the s-triazine ring in the analysed series (Chart 2). ^dDue to the low solubility of compound **6** in DMSO- d_6 , its convincing NMR spectra could be obtained at 363 K only. ^eTG as -6.92 ppb K^{-1} in the starting material **C1**. ^fTG as -6.07 ppb K^{-1} in the starting material **C3**.

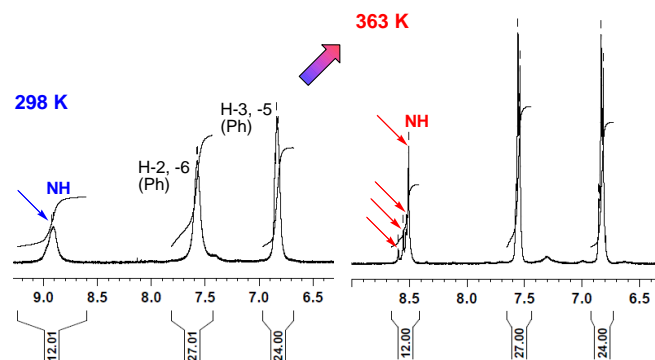


Figure 1. Comparative details from ^1H NMR spectra of G-2 dendrimer **5** (500 MHz, 5.0 mM in DMSO- d_6)

N(exocyclic) bonds. In contrast, in the ^1H NMR spectrum of dendrimer **5** recorded at 90 °C, multiple resonances (Table 3 and Figure 1) were displayed by the indicative NH protons, suggesting the occurrence of a significant peripheral steric hindrance, *starburst* effect,^{3a, 3b} against authentic free rotation upon heating. This fact was not quite surprising because we previously reported a related situation in the case of some G-0 dendrons as *N,N'*-disubstituted 2-chloro-4,6-diamino-s-triazines with bulky azaspirodecane and propane-1,3-diol ligands and entitled this “abnormal” behaviour “*pseudo freely rotating*” status.^{5c}

2.2.2. Dendritic solvation

In line with solvation energy calculations (Table 2), the temperature gradients (TGs) of the indicative NH protons provided additional information on the solvation in the regions surrounding

the s-triazine units (branch-cells, T-0 or cores T-2, Schemes 3 and 4).

If so, the compounds under investigation (Table 3) exhibited TG values denoting significant (peripheral) >N–H...O=SMe₂ hydrogen bond interactions. TGs moderately increased, from -5.55 ppb K⁻¹ in G-1 **D-N<P>NH** to about -6.00 ppb K⁻¹ in G-2 dendrimers, together with the hydrodynamic diameters, *d*_H, except dendrimers **4** and **5**. Dendrimer **4** was by far the most NH/DMSO solvated of the series (TG around -12.00 ppb K⁻¹) in conjunction with one of the highest *d*_H values, of 2.45 nm.

On the other hand, an evaluation of the TG values of the inner (T-2) vs. the peripheral (T-0) NH groups in ionic dendrimer **8** showed a comparable aptitude for NH/DMSO H-binding, -5.08 ppb K⁻¹ (-6.92 ppb K⁻¹ in the starting material **C1**) vs. -6.00 ppb K⁻¹, respectively. Furthermore, the replacement of the central methylene spacer (*n* = 1, in **8**) with a trimethylene one (*n* = 3, in **9**) had no influence on the peripheral (T-0) NH groups/DMSO solvation as they maintained almost the same TG (-6.00 ppb K⁻¹ in **8** vs. -6.15 ppb K⁻¹ in **9**). In contrast, the inner (T-2) NH groups of **9** appeared “protected” against DMSO (as a hydrogen bond acceptor) because their TG was only -2.00 ppb K⁻¹, much less negative than in the starting material **C3** (-6.00 ppb K⁻¹), i.e., the three identical intramolecular >N–H...LP(N-1, -3, -5 of s-triazine T-2 core) interactions prevailed, being, most likely, a consequence of the aforementioned C₃ symmetric *propeller* as *local* arrangement.

2.2.3. Assignment of ionic interactions in dendrimers **7b**, **8** and **9**

On the ¹H NMR timescale in DMSO-*d*₆, the triple ionic interactions in dendrimers **7b**, **8** and **9** (Scheme 4) could only be indirectly assigned, due to rapid proton interchange, symbolised as: 3 **D-N<P>NH** + (HOOC)₃R ⇌ [**D-N<P>NH₂⁺** · OOC]₃R

As a consequence of the triple ionisation of the carboxyl groups in tripodal melamines **C1** and **C3**, only a remote upfield shift of their ¹H δ_{NH} values was observed: from 9.47 ppm (in **C1**,¹³) to 8.93 ppm (in the tris-anion of **8**) and from 8.95 ppm (in **C3**,¹³) to 8.70 ppm (in the tris-anion of **9**) (Table 3). A different diagnosis, based on aliphatic carboxyl group ionisation thus promoting ¹H shielding of proximal (α and β) methylene protons, was reported in the case of some G-2 PAMAM ionic dendrimers obtained by –COOH / H₂N– neutralisation (NMR solvent, CDCl₃).²³

However, in the case of the cationic counterpart, if a more illustrative series was examined, i.e., **D-N<P>NH**, **4**, **7a**, **7b**, **8** and **9** (Table 4), δ_H resonances of the methylene protons α-to the N^{sp3} nitrogen of P-1 piperazine linker (in **D-N<P>NH** vs. **7b**, **8** and **9**) revealed minor fluctuations, between 2.97 and 3.15 ppm. These resonances were found much further upfield with respect to the

shifts of the methylene protons α-situated vs. the piperazine P-1 N^{sp2} nitrogen involved in p→π LP(N) → π(C=N, s-triazine; C=O, amide) conjugation (3.78-3.91 ppm). To conclude, except the well-documented deshielding promoted by the magnetic anisotropy of π-delocalised systems, such as s-triazines and amides,²⁴ no such vicinal effect created by a quaternary EWG of type >N^{sp3}H₂⁺ was detected in the piperazine P-1 linker of compounds **7b**, **8** and **9**, even in the case of the strongest proton donor, the trimesic acid (p*K*_a = 3.12, 3.89 and 4.70).²⁵

Table 4: ¹H NMR discrimination of methylene protons in piperazine P-1 linkers of compounds **D-N<P>NH**, **4**, **7a**, **7b**, **8** and **9**

Methylene locations	Compound					
	δ _H (ppm) (500 MHz, DMSO- <i>d</i> ₆ , 298 K)					
	D-N<P>NH	4	7a	7b^a	8^a	9^a
α-to N ^{sp3}	3.13	-	-	3.09	2.97	3.15
α-to N ^{sp2}	3.91	3.80	3.78	3.78	3.78	3.78

^aDownfield shifted resonances (Δδ as +0.25 and +0.33 ppm) of α-CH₂ protons to –NH₃⁺ group were reported in the case of some G-2 PAMAM dendrimers obtained by –COOH / H₂N– neutralisation (CDCl₃).²³

In addition, only in G-1 amino-dendron **D-N<P>NH** the ^1H NMR integration of its termini piperazine P-1 linker disclosed the presence of just 4 methylene protons (instead of 8) at room temperature as well as at 90 °C, presumably due to their longer T_1 value (longitudinal relaxation time).^{22a} No such spectral appearance was observed in the case of G-0 precursor **3**. Subsequent to the use of **D-N<P>NH** in covalent (\rightarrow **4**, **7a**, **5**) or ionic (\rightarrow **7b**, **8** and **9**) *m*-trimerisations, the same ^1H NMR integration evidenced, throughout, the existence of expected 8 H / P-1 unit.

On the IR timescale (Figures 2a-d), the comparative spectra of compounds **7a/7b**, **7b**/trimesic acid, **8/C1** and **9/C3** fully proved the presence of only the tris-carboxylate anions.²⁶

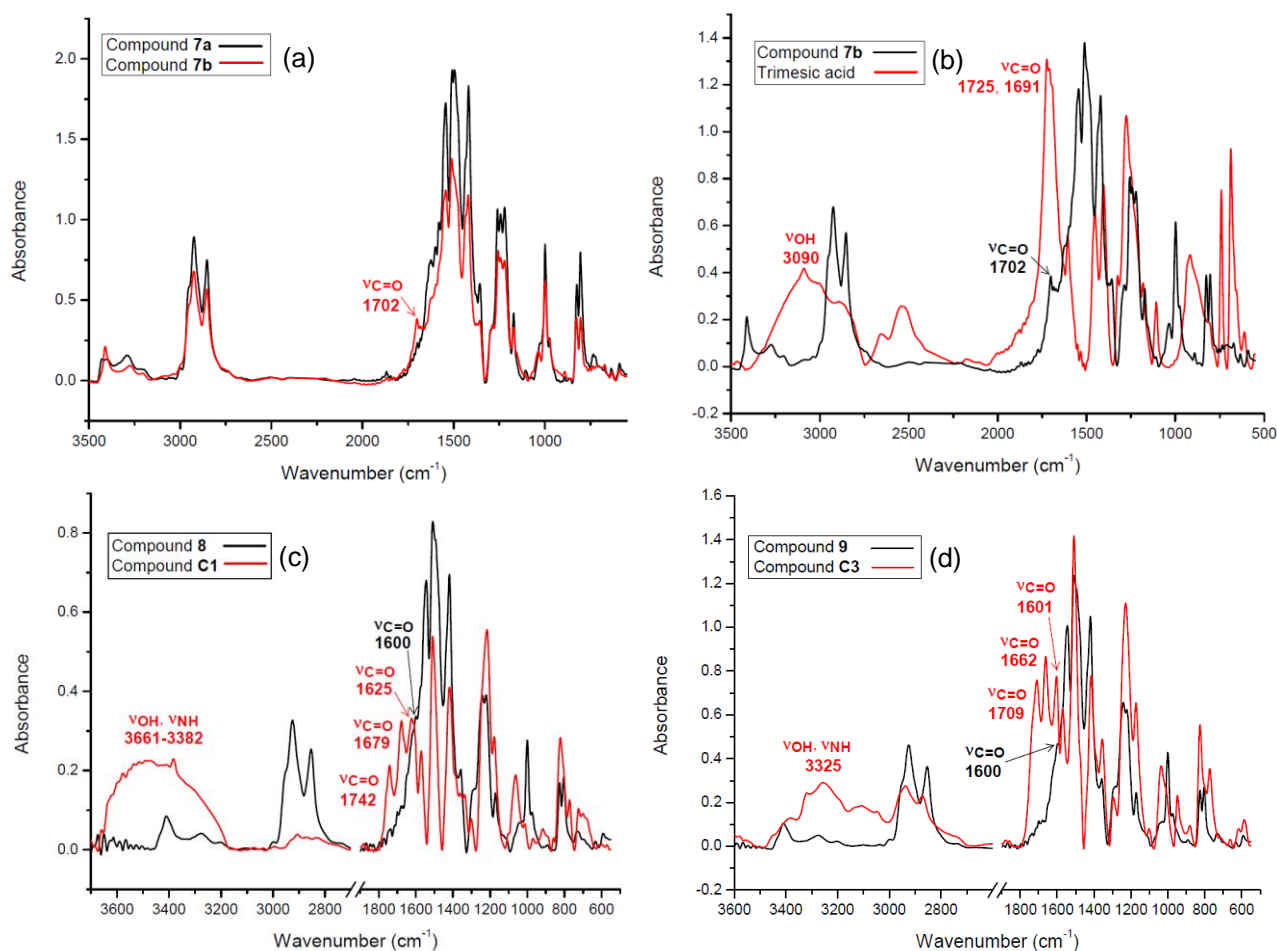


Figure 2. Comparative IR spectra (KBr) of compounds **7a/7b** (a), **7b**/trimesic acid (b), **8/C1** (c) and **9/C3** (d)

(i) The spectrum of dendritic salt **7b** was almost the duplicate of that of covalent **7a** (Figure 2a), except for the presence of a weak band located at 1702 cm⁻¹ which was attributed to the ν_{C=O} stretching absorption of the tris-carboxylate anion in **7b**.^{26a, 26b}

(ii) Indeed (Fig. 2b), the shift to a lower field and weaker intensity of the strong ν_{C=O} band (from 1725 cm⁻¹ for the COOH groups of trimesic acid to 1702 cm⁻¹ for the COO⁻ groups of **7b**), together with the disappearance of the ν_{OH} stretching band (3090 cm⁻¹) of the carboxyl groups (strongly H-associated in trimesic acid) confirmed the existence of the trimesic tris-carboxylate anion in **7b**. Nevertheless, the stretching (ν_{NH}, 3000-2700 cm⁻¹) or deformation (δ_{NH}, 1620-1560 cm⁻¹) bands^{26b, 26c} of the protonated >NH₂⁺ group of the P-1 piperazine linker could not be definitely allocated due to the overlapping in the above regions between the absorptions of the piperazine methylene groups (ν_{CH₂}), carbonyl bonds (ν_{C=O}) in the COO⁻ groups, aryl bonds (ν_{C=C}) and *s*-triazine bonds (ν_{C=N}).

(iii) Similar attributions were applied in the case of ionic dendrimers **8** (Figure 2c) and **9** (Figure 2d). The vanishing of the carboxyl ν_{OH} bands from **C2** and **C3** in the dendritic environment of **8** and **9** established the ionic nature of the latter. Due to their overall lower symmetry in comparison with trimesic acid, tripodal

aminophenoxy-acids-based *N*-substituted melamines **C2** and **C3** exhibited multiple (3-4) carboxyl $\nu_{C=O}$ stretching absorptions, in agreement with their different degrees of H-bond association, i.e., dimers (1742 and 1709 cm^{-1}), polymers (1679, 1625, 1622 and, presumably, even 1600 cm^{-1}). Succeeding the ionic trimerisations, all these bands were absent in the IR spectra of **8** and **9**, with the remaining carboxylate $\nu_{C=O}$ stretching band being located most likely at approximately 1600 cm^{-1} .

In conclusion, the exact protonated site in ionic dendrimers **7b**, **8** and **9** could not be attributed accurately either in solution (^1H NMR), or in the solid state (IR). Consequently, their proposed cationic structures shown in Chart 1 and Scheme 4 (linker P-1 as piperazin-1-ium moiety) should be seen intuitively, a proton sponge-like comportment of G-1 piperazine dendron **D-N<P>NH** being not entirely ruled out.^{2j} In line with this hypothesis, we recently described^{11b} the aptitude of the non-*O*-*n*-octylated analogue of G-2 dendrimer **4** (Scheme 3) to deprotonate Hemin completely (1:5 molar ratio, pK_a 6.63²⁷, 4.8-5.7²⁸), thus generating a new MOF for H_2O_2 amperometric detection. More insights on this debate we obtained by means of DFT calculations only (see Section 3.3.).

2.2.4. Assignments by means of 2D- ^1H -DOSY NMR in tandem with DFT calculations at dendritic level

Except for dendrimers **4** (d_H 2.45 nm) and **5** (d_H 2.48 nm) (Table 3), in the series of trimers **7-9** the expected increase in the hydrodynamic diameters (d_H) with respect to their G-1 monomeric precursor, **D-N<P>NH** (1.98 nm), was negligible (1.90-2.04 nm).

2D- ^1H -DOSY NMR charts of G-2 dendrimers **7a** (covalent) vs. ionic **7b**, **8** and **9** (Figure 3) displayed unique structures, with a partial dissociation of **7b**, presumably due to the sterically induced imperfect accommodation of the three G-1 cationic dendrons **D-N<P>NH₂⁺** around the smallest central tris-anion of the series, trimesic tris-carboxylate. In other words, the 2D- ^1H -DOSY NMR charts were consistent with the envisaged 3(**D-N<P>NH**):1 (acid trimesic, **C1** or **C3**) stoichiometric assembly of dendrimers **7b**, **8** and **9**. That is, we had to assume that in series **D-N<P>NH**, **7-9**, the correlation between *D* values (by means of hydrodynamic diameters d_H , Table 3) and the macromolecular size was not direct, i.e., dendritic structures with different molecular weight displaced related volumes of solvent. The above encountered situation was comparable to that of some PAMAM dendrimers exhibiting *D* values around 100 $\mu\text{m}^2 \text{s}^{-1}$.²⁹

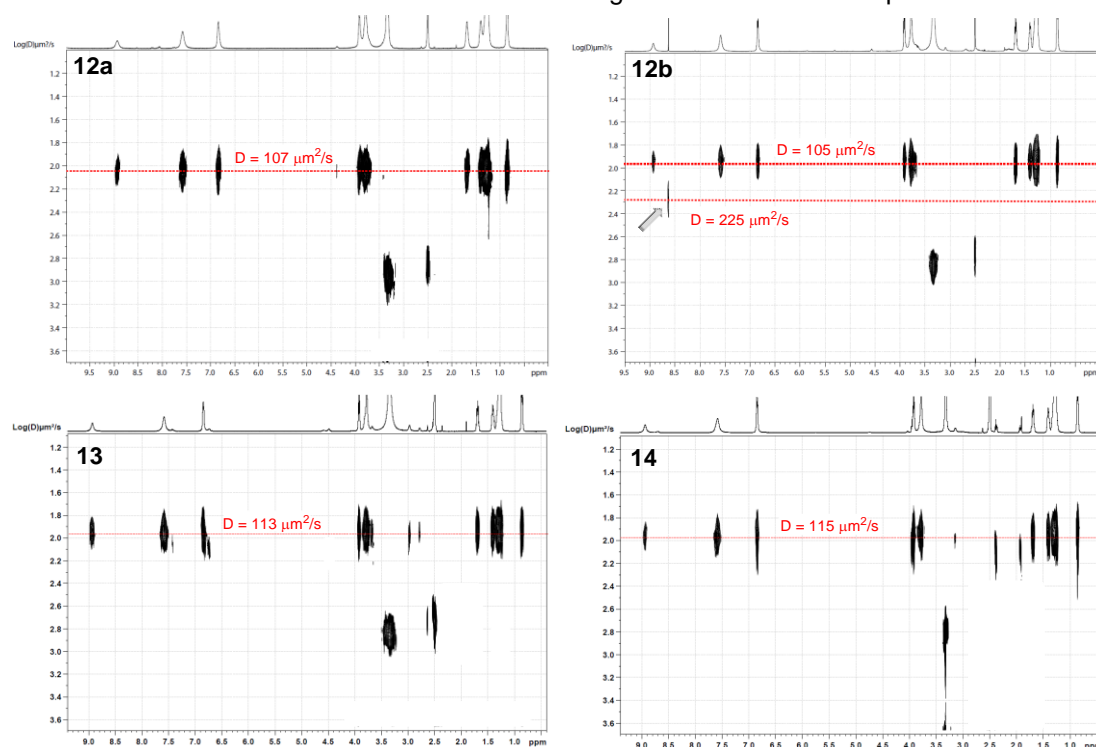
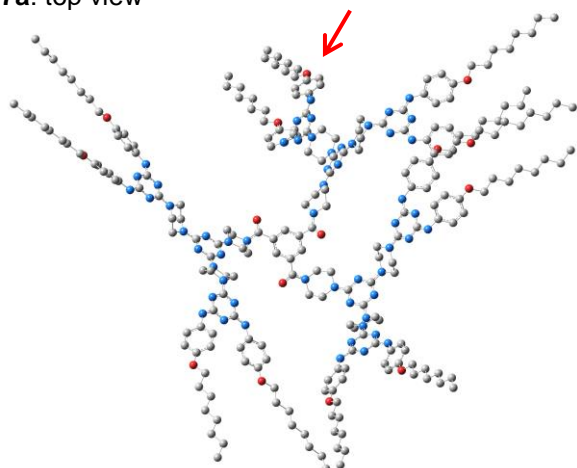


Figure 3. 2D- ^1H -DOSY NMR charts (DMSO- d_6 , 500 MHz, 298 K) of compounds **7a**, **7b** (2.5 mM), **8** and **9** (5.0 mM)

Therefore, an additional effort to estimate the above situation in the case of dendrimers 7-9, by means of DFT calculations in solution (DMSO) (Figures 4-6), was straightforward.

7a: top view



7a: side view

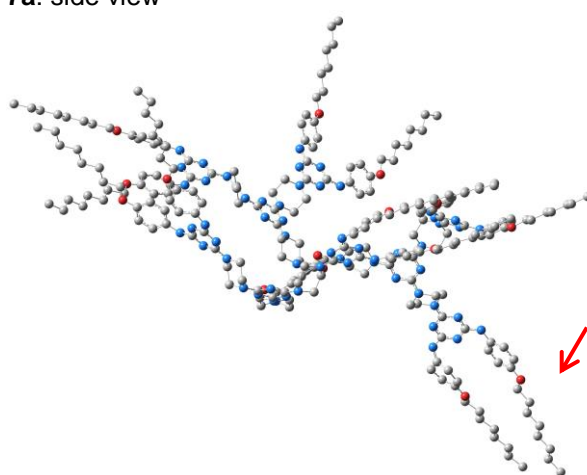
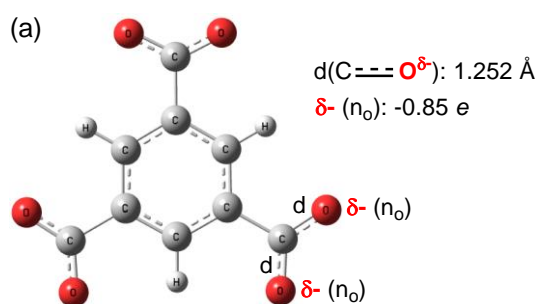


Figure 4. The DFT optimised geometry at M062X/def2-TZVP level of theory of G-2 dendrimer **7a** in DMSO (hydrogen atoms were omitted for reasons of simplicity)



7b: top view

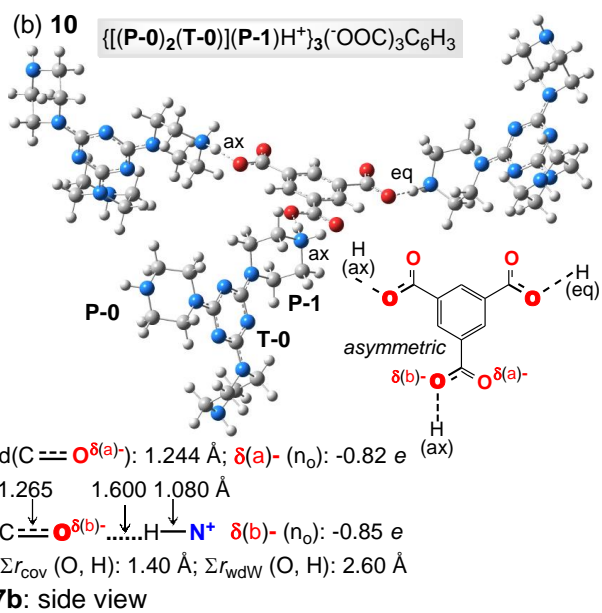
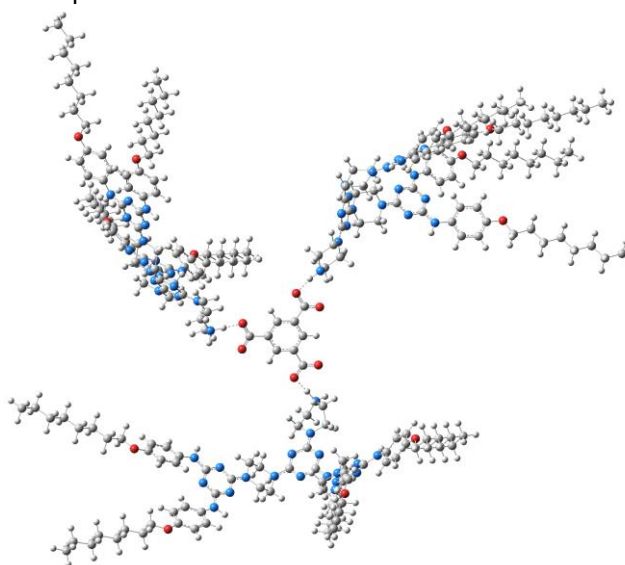


Figure 5. The DFT optimised geometry at M062X/def2-TZVP level of theory of trimesic tris-carboxylate

anion (a), of model G-1 dendrimer **10** (b) and of G-2 dendrimer **7b** in DMSO

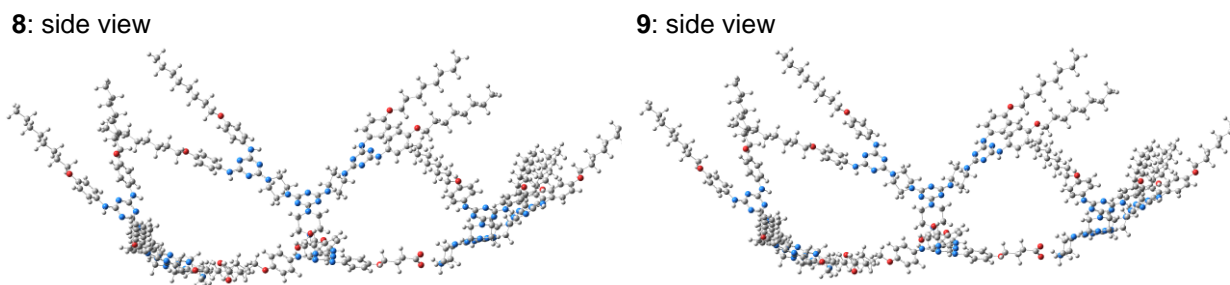


Figure 6. The DFT optimised geometry at M062X/def2-TZVP level of theory of G-2 dendrimers **8** and **9** in DMSO

First, the optimisation of the geometry of G-2 dendrimer **7a** (Figure 4) identified its global form to be almost vaulted although the degree of freedom of the six G-1 dendritic units appeared restricted. Indeed, one of them (marked by the red arrow) had an opposite direction to the other five, caused, probably, by the *propeller* orientation (Chart 1) of the three covalent junctions around the benzene core.

In contrast, the energetic minimum of the ionic analogue **7b** could be accessed in a gradual approach only. Thus, we had to start from a preliminary DFT calculation of the trimesic tris-carboxylate anion (Figure 5a) because its identical partial double bond lengths ($d(C \equiv O^{\delta-})$) and oxygen atoms negative charges values (δ^- , as Natural Population (n_o) according to NBO analysis) were then taken as references with regard to those of the same tris-anion installed in a model G-1 ionic environment, **10** (Figure 5b). We considered dendrimer **10** as a simplified version of **7b** from which the 4,6-bis[4-(*n*-octyloxy)phenylamino]-s-triazin-2-yl G-0 branches were removed. Oxygen atoms negative charges in **10** (Figure 5b), $\delta^{(a)-}$ and $\delta^{(b)-}$, did not differ significantly vs. those of the initial trimesic tris-carboxylate anion (δ^- , Figure 5a). Besides the electrostatic attraction between the tris-carboxylate anion and the P-1 piperazin-1-ium melamine G-1 cations, the occurrence of important H-bonding three interactions ($>C \equiv O^{\delta(b)-} \dots H(ax \text{ or } eq)\text{-NH}^+<$) were identified, being supported by the bond lengths decreasing order as 1.265 \AA ($d(C \equiv O^{\delta(b)-})$ in **10**) $>$ 1.252 \AA ($d(C \equiv O^{\delta-})$ in trimesic tris-carboxylate anion) $>$ 1.244 \AA ($d(C \equiv O^{\delta(a)-})$ in **10**) together with Σr_{cov} (O, H): $1.40 \text{ \AA} < d(O^{\delta(b)-} \dots H)$: $1.60 \text{ \AA} < \Sigma r_{wdw}$ (O, H): 2.60 \AA .³⁰ One must observe that, contrarily to our planned design of **7b**, as $[D-N<P>NH_2^+]_3(\text{OOC})_3C_6H_3$ (Chart 1, *linear* connection, as a six-membered chelate, to the *m*-trivalent core), the H-bonding network in model **10** determined simpler *angular* connections of the P-1 piperazin-1-ium melamine G-1 cations around the trimesic tris-carboxylate anion core in a statistically favoured *asymmetric* manner (Chart 1). In spite of this *local* “irregularity”, entirely re-found in the optimized geometry of **7b** (Figure 5), its *global* profile was of type *propeller* due to the adopted vault shape of its three G-1 branches (**D**, Chart 1), i.e., concavity vs. convexity.

Extrapolation of the ionic relationships found for model **10** to compounds with higher mass **8** and **9** (Figure 6) provided their energetic minima as to correspond to (i) a *local propeller* orientation of the G-1 branches around the s-triazin-2,4,6-triyl core (initial design, Chart 1) and (ii) a *global* vaulted form (“candelabrum” allure) promoted, as in the case of **7b**, by the same arched G-1 branches.

2.3. Assignments by means of TEM analyses

We also considered of interest to corroborate our *ab initio* study with an introductory exploration by means of TEM (Transmission Electronic Microscopy). In this purpose, the sampling was made by dissolving compounds **D-N<P>NH** and **4-9** ($\sim 1\text{ mg}$) in DMSO (1 mL, see Section 3.1.) under sonication. One drop of solution was deposited on a Formvar/Carbon coated copper grid (300 Mesh) and let to free evaporate to dryness at room temperature (24 h). Except for compound **4**, agglomerations of homogeneously packed spherical nano-aggregates (Figures 7 and 8) were thus obtained. They were comparable with those of the recently reported G-2 PAMAM ionic ($-\text{COO}^- / \text{H}_3\text{N}^+$) dendrimers, already mentioned.²³ Each sample preparation was repeated three times and the hereafter discussed numerical data were mediated.

The size of nanospheres (expressed by their average diameters, D) ranged in a large domain (234-1454 nm) with a quite uniform distribution of D values in all situations.

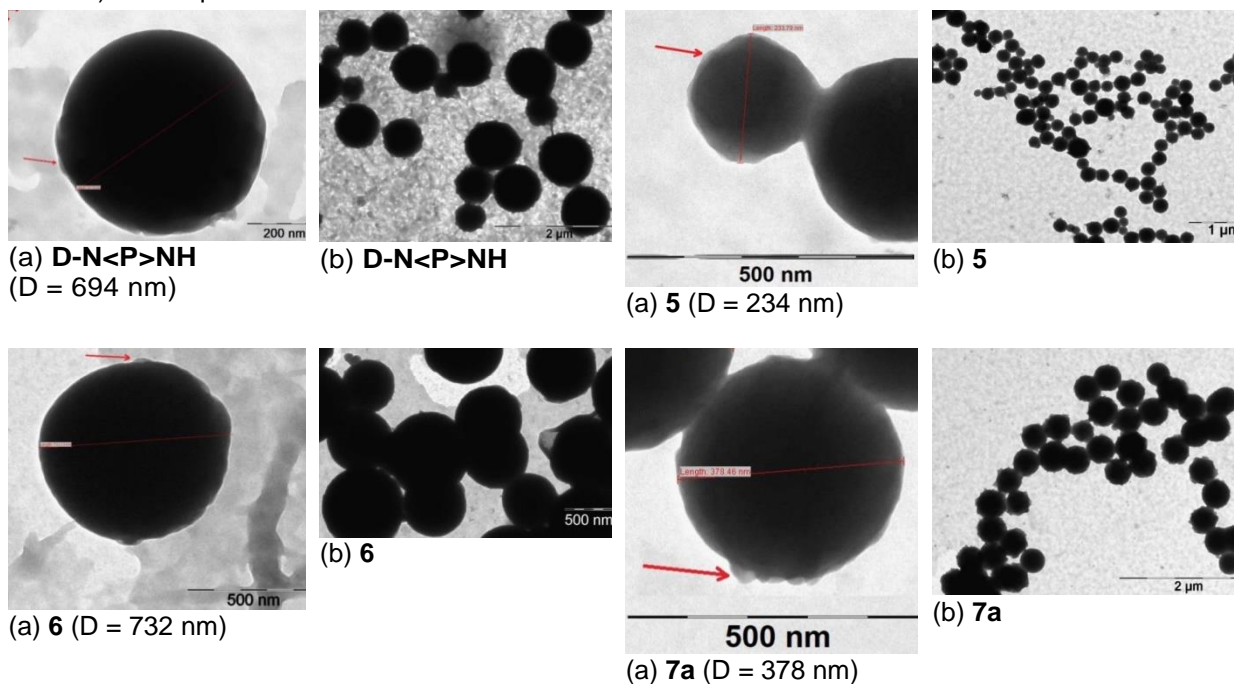


Figure 7. TEM images of homogeneously packed spherical nano-aggregates (a) and their agglomerations (b) in the case of G-1 amino-dendrion **D-N<P>NH** and of covalent G-2 dendrimers **5-7a**. D is the average diameter of nanospheres; the red arrow shows the nano-particles that aggregate.

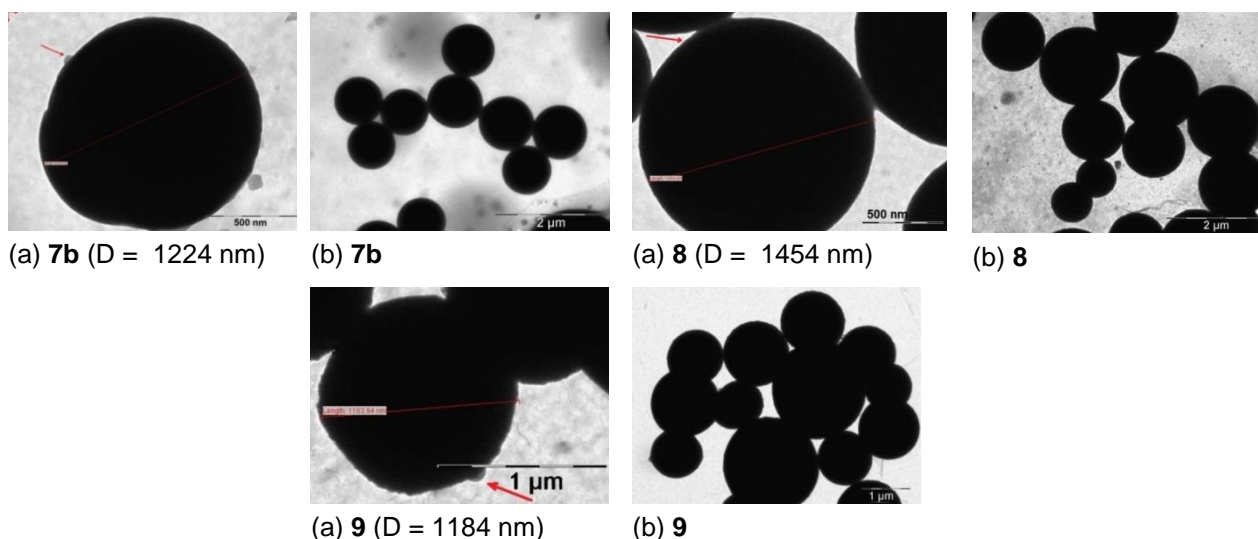


Figure 8. TEM images of homogeneously packed spherical nano-aggregates (a) and their agglomerations (b) in the case of G-2 ionic dendrimers **7b, 8** and **9**; the red arrow indicates the nano-particles that aggregate). D is the average diameter of nanospheres; red arrow shows the particles that aggregate.

With the exception of compound **6**, all other G-2 dendrimers were, in fact, trimers of the same G-1 dendron, **D-N<P>NH**. Therefore, for the present discussion, we will limit our assignments to the structural diversity impact of the central building blocks (or cores) together with that of the dendritic elaboration (covalent vs. ionic), seen both accountable for the observed different propensity for self-assembly as nano-aggregates. Indeed, covalent dendrimers **5-7a** generated nanospheres with much smaller average diameter (259-732 nm, Figure 7) than the ionic **7b-9** (992-1454 nm, Figure 8). Moreover, according to the

literature,³¹ the last ones appeared to be among the greatest previously reported nanosystems as polymeric nanoparticles.

In covalent series, G-1 dendron **D-N<P>NH** itself (as unexpected reference) self-assembled into nanospheres with a high D value (694 nm).

Surprisingly, single trimer **4** (**[D-N<P>N]**₃C₃N₃, Chart 1), containing *s*-triazine as *linearly* linked core, gave no distinct spherical aggregation. In contrast, by replacing the P-1 piperazine linker in **4** with a 4-oxyphenylamino unit, the resulting dendrimer **6** (**[D₃]B**, Chart 1), still encompassing *s*-triazine as core but *propeller angularly* coupled, evidenced a total opposite behaviour, i.e., aggregation under the form of nanospheres with the highest (732 nm) D value.

Trimers of **D-N<P>NH** *angularly-propeller* attached to 1,3,5-trisubstituted benzene cores, as π -electron-enhanced (1,3,5-tris(methylene)benzene, **[D₃]A** (Chart 1), compound **5**, D = 234 nm) or π -poor (1,3,5-tris(formyl)benzene, **[D-N<P>N]**₃(OC)₃C₆H₃ (Chart 1), compound **7a**, D = 378 nm) self-assembled into the smallest spherical nano-aggregates.

By far, due to their electrostatic interactions (attractions vs. repulsions) G-2 ionic dendrimers **7b**, **8** and **9** (Figure 8) produced the most developed spherical nano-aggregates. The ionic relationships masked those deduced in covalent series, namely the π - π and π -H stacking and *angular-propeller* connectivity of the G-1 dendritic branches to the *m*-trivalent core.

CONCLUSIONS

- Starting from 4-(*n*-octyloxy)aniline, the five- step orthogonal convergent synthesis of a new seven terms series of G-2 melamine based-dendrimers was achieved in overall yields ranging between 29 and 79%.
- By means of DFT calculation in solution, the reaction conditions were found mandatory to the high solvation of the G-0 and G-1 dendrons exhibiting a major (*anti-anti*) (parallel) rotamerism of the peripheral 4-(*n*-octyloxy)phenyl units about the C(*s*-triazine)-N(exocyclic) partial double bonds.
- The final iterative synthetic step was realised by covalent and / or (carboxyl / amino) ionic trimerisations, to recommend two G-1 *N*-substituted melamine dendrons with piperzine-1,4-diyl (linkers) and 4-(*n*-octyloxyphenyl)amino (peripheral units), **D-CI** and **D-N<P>NH**, as promising scaffolds for future dendritic elaborations.
- Tandem DFT-(VT) NMR investigations revealed (i) the regular shape in solution of the terminal 4-(*n*-octyloxy)phenyl units (“parallel”, *anti-anti*), (ii) the *propeller* arrangement, in the case of the *angular* connections of G-1 dendrons around the *m*-trivalent core, (iii) the vaulted shapes of G-2 dendrimers and (iv) in one case, the occurrence of a *starburst* effect.
- The “salt”-like nature of the G-2 dendrimers (obtained by a carboxyl : amino 1:3 stoichiometric trimerisation) could be unambiguously assigned by means of ¹H NMR (in solution) and IR (solid state), confirming the existence of the only tris-carboxylate anions.
- TEM analysis indicated the aptitude of our G-2 vaulted melamines for π - π and π -H stacking self-assembly into homogeneously packed spherical nano-aggregates. Their size was tailored primarily by the covalent vs. ionic nature of dendrimers, i.e., the last ones producing nanospheres with more than 1000 nm averaged D values. The structural variety of the covalent dendritic elaboration around the *m*-trivalent cores (1,4-phenylene over piperazin-1,4-diyl adjacent linkers, *propeller* over *asymmetric* rotamerism of the *angular* over *linear* connectivity) modulated the degree of nano-aggregation.

SELECTIVE REFERENCES

¹ a) W. Zhang, E. E. Simanek, *Org. Lett.*, **2000**, 2, 843–845; b) W. Zhang, D. T. Nowlan, L. M. Thomson, M. W. Lackowski, E. E. Simanek, *J. Am. Chem. Soc.*, **2001**, 123, 8914–8922; c) A. P. Umali, E. E. Simanek, *Org. Lett.*, **2003**, 5, 1245–1247; d) M. B. Steffensen, E. E. Simanek, *Org. Lett.*, **2003**, 5, 2359–2361; e) W. Zhang, S. E. Tichy, L. M. Perez, C. G. Maria, P. A. Lindahl, E. E. Simanek, *J. Am. Chem. Soc.*, **2003**, 125, 5086–5094; f) M. B. Steffensen, E. E. Simanek, *Angew. Chem., Int. Ed.*, **2004**, 43, 5178–5180; g) E. Hollink, E. E. Simanek, *Org. Lett.*, **2006**, 8, 2293–2295; h) M. B. Steffensen, E. Hollink, F. Kuschel, M. Bauer, E. E. Simanek, *J. Polym. Sci. Part A: Polym. Chem.*, **2006**,

- 44, 3411-3433; i) A. P. Umali, L. H. Crampton, E. E. Simanek, *J. Org. Chem.*, **2007**, *72*, 9866-9874; j) X. K. Moreno, E. E. Simanek, *Macromolecules*, **2008**, *41*, 4108-4114; k) A. Chouai, E. E. Simanek, *J. Org. Chem.*, **2008**, *73*, 2357-2366; l) V. J. Venditto, K. Allred, C. D. Allred, E. E. Simanek, *Chem. Commun.*, **2009**, *37*, 5541-5542; m) A. Chouai, V. J. Venditto, E. E. Simanek, *Org. Synth.*, **2009**, *86*, 151-160; n) A. Chouai, V. J. Venditto, E. E. Simanek, *Org. Synth.*, **2009**, *86*, 141-150; o) J. Lim, M. A. Mintzer, L. M. Perez, E. E. Simanek, *Org. Lett.*, **2010**, *12*, 1148-1151; p) E. E. Simanek, H. Abdou, S. Lalwani, J. Lim, M. Mintzer, V. J. Venditto, B. Vittur, *Proc. Roy. Soc. A*, **2010**, *466*, 1445-1468; r) A. E. Enciso, F. Ramirez-Crescencio, M. Zeiser, R. Redón, E. E. Simanek, *Polym. Chem.*, **2015**, *6*, 5219-5224.
- ² a) S. A. Bell, M. E. McLean, S. -K. Oh, S. E. Tichy, W. Zhang, R. M. Corn, R. M. Crooks, E. E. Simanek, *Bioconjugate Chem.*, **2003**, *14*, 488-493; b) H. -T. Chen, M. F. Neerman, A. R. Parrish, E. E. Simanek, *J. Am. Chem. Soc.*, **2004**, *126*, 10044-10048; c) M. F. Neerman, W. Zhang, A. R. Parrish, E. E. Simanek, *Int. J. Pharm.*, **2004**, *281*, 129-132; d) J. Lim, E. E. Simanek, *Mol. Pharmaceut (Pharm.)*, **2005**, *2*, 273-277; e) H. L. Crampton, E. E. Simanek, *Polym. Int.*, **2007**, *56*, 489-496; f) M. O. Merkel, M. A. Mintzer, J. Sitterberg, U. Bakowsky, E. E. Simanek, T. Kissel, *Bioconjugate Chem.*, **2009**, *20*, 1799-1806; g) J. Lim, V. J. Venditto, E. E. Simanek, *Bioorg. Med. Chem.*, **2010**, *18*, 5749-5753; h) J. Lim, E. E. Simanek, *Adv. Drug Deliv. Rev.*, **2012**, *64*, 826-835; i) E. E. Simanek, A. E. Enciso, G. M. Pavan, *Expert Opinion on Drug Discovery*, **2013**, *8*, 1057-1069; j) E. E. Simanek, A. E. Enciso, *RSC Polymer Chemistry Series*, **2015**, *13*, 249-267. k) R. S. Sreperumbuduru, Z. M. Abid, K. M. Claunch, H. -H. Chen, S. M. McGillivray, E. E. Simanek, *RSC Adv.*, **2016**, *6*, 8806-8810.
- ³ a) F. Vögtle, G. Richardt, N. Werner, *Dendrimer Chemistry Concepts; Syntheses, Properties, Applications*; WILEY-VCH Verlag GmbH & Co. KGaA, Weinheim, **2009**, pp. 3, 14, 299-300; b) P. G. de Gennes, H. Hervet, *J. Physique Lett. Fr.*, **1983**, *44*, 351-360.
- ⁴ a) S. Yagai, M. Usui, T. Seki, H. Murayama, Y. Kikkawa, S. Uemura, T. Karatsu, A. Kitamura, A. Asano, S. Seki, *J. Am. Chem. Soc.*, **2012**, *134*, 7983-7994; b) Z. Shi, H. Lu, Z. Chen, R. Cheng, D. Chen, *Polymer*, **2012**, *53*, 359-369; c) D. -Y. Kim, S. -A. Lee, Y. -J. Choi, S. -H. Hwang, S. -W. Kuo, C. Nah, M. -H. Lee, K. -U. Jeong, *Chem. Eur. J.*, **2014**, *20*, 5689-5695.
- ⁵ a) M. Darabantu, M. Pinteá, M. Fazekas, P. Lameiras, C. Berghian, I. Delhom, I. Silaghi-Dumitrescu, N. Plé, A. Turck, *Lett. Org. Chem.*, **2006**, *3*, 905-910; b) M. Pinteá, M. Fazekas, P. Lameiras, I. Cadis, C. Berghian, I. Silaghi-Dumitrescu, F. Popa, C. Bele, N. Plé, M. Darabantu, *Tetrahedron*, **2008**, *64*, 8851-8870; c) F. Popa, P. Lameiras, O. Moldovan, M. Tomoia-Cotisel, E. Hénon, A. Martinez, C. Sacalis, A. Mocanu, Y. Ramondenc, M. Darabantu, *Tetrahedron*, **2012**, *68*, 8945-8967; d) O. Moldovan, P. Lameiras, I. Nagy, T. Opruta, F. Popa, C. Antheaume, Y. Ramondenc, M. Darabantu, *Tetrahedron*, **2013**, *69*, 2199-2213; e) O. Moldovan, I. Nagy, P. Lameiras, C. Antheaume, C. Sacalis, M. Darabantu, *Tetrahedron: Asymmetry*, **2015**, *26*, 683-701.
- ⁶ a) V. Lates, D. Gligor, M. Darabantu, L.M. Muresan, *J. Appl. Electrochem.*, **2007**, *37*, 631-636; b) A. R. Deac, C. Morar, G. L. Turdean, M. Darabantu, E. Gál, A. Bende, L. M. Muresan, *J. Solid State Electrochem.*, **2016**, *20*, 3071-3081; c) C. Morar, G. Turdean, A. Bende, P. Lameiras, C. Antheaume, L. M. Muresan, M. Darabantu, *Compt. Rend. Chim.*, **2017**, *20*, 402-414.
- ⁷ B. A. Hernandez, V. Chang, I. Villanueva, M. D. Heagy, *J. Org. Chem.*, **1999**, *64*, 6905-6906.
- ⁸ G. R. Newkome, Z. Yao, G. R. Baker, V. K. Gupta, *J. Org. Chem.*, **1985**, *50*, 2003-2004.
- ⁹ a) S. Ricken, P. W. Osinski, P. Eilbracht, R. Haag, *J. Mol. Catal. A: Chem.*, **2006**, *257*, 78-88; b) M. A. Subhani, K-S. Müller, P. Eilbracht, *Adv. Synth. Catal.*, **2009**, *351*, 2113-2123; c) M. Beigi, S. Ricken, K. S. Müller, F. Koç, P. Eilbracht, *Eur. J. Org. Chem.*, **2011**, *8*, 1482-1492.
- ¹⁰ a) A. Petri, Euro. Pat. 0 208 376 A2/January 14, **1987**; b) M. Negoro, K. Kawata, US Pat 7 135 567/November 14, **2006**; c) P. de Hoog, P. Gamez, W.L. Driessen, J. Reedijk, *Tetrahedron Lett.*, **2002**, *43*, 6783-6786, d) M. Negoro, K. Kawata, US Pat. 2005/0209453 A1/September 22, **2005**.
- ¹¹ a) C. Morar, L. Cost, M. Darabantu, *Stud. U. Babeş-Bol. Che. LX*, **2015**, (*2, Tom I*), 7-14; b) C. Morar, L. Cost, P. Lameiras, C. Antheaume, M. Darabantu, *Synthetic Commun.*, **2015**, *45*, 1688-1695.
- ¹² a) S. S. Mirvish, P. Gannett, D. M. Babcock, D. Williamson, S. C. Chen, D. D. Weisenburger, *J. Agric. Food Chem.*, **1991**, *39*, 1205-1210; b) I. Willner, J. Rosengaus, Y. J. Eichen, *J. Phys. Org. Chem.*, **1993**, *6*, 29-43; c) A. R. Katritzky, I. Ghiviriga, D. C. Oniciu, A. Barkock, *J. Chem. Soc. Perkin Trans.*, **1995**, *2*, 785-792; d) A.R. Katritzky, I. Ghiviriga, P. G. Steel, D. C. Oniciu, *J. Chem. Soc. Perkin Trans.*, **1996**, *2*, 443-447; e) I. Ghiviriga, D. C. Oniciu, *Chem. Commun.*, **2002**, *22*, 2718-2719.
- ¹³ M. Fazekas, M. Pinteá, P. Lameiras, A. Lesur, C. Berghian, I. Silaghi-Dumitrescu, N. Plé, M. Darabantu, *Eur. J. Org. Chem.*, **2008**, *14*, 2473-2494.
- ¹⁴ a) H. R. Bhat, U. P. Singh, P. Gahtori, S. K. Ghosh, K. Gogoi, A. Prakashe, R. K. Singh, *New J. Chem.*, **2013**, *37*, 2654-2662; b) H. R. Bhat, U. P. Singh, P. Gahtori, S. K. Ghosh, K. Gogoi, A. Prakash, R. K. Singh, *RSC Adv.*, **2013**, *3*, 2942-2952.
- ¹⁵ C-H. Wong, S.C. Zimmerman, *Chem. Commun.*, **2013**, *49*, 1679-1695.
- ¹⁶ Y. Zhao, D. G. Truhlar, *Theor. Chem. Acc.*, **2008**, *120*, 215-241.
- ¹⁷ F. Weigend, R. Ahlrichs, *Phys. Chem. Chem. Phys.*, **2005**, *7*, 3297-3305.
- ¹⁸ Gaussian 09, Revision D.01, M. J. Frisch, G. W. Trucks, H. B. Schlegel, G. E. Scuseria, M. A. Robb, J. R. Cheeseman, G. Scalmani, V. Barone, B. Mennucci, G. A. Petersson, H. Nakatsuji, M. Caricato, X. Li, H. P. Hratchian, A. F. Izmaylov, J. Bloino, G. Zheng, J. L. Sonnenberg, M. Hada, M. Ehara, K. Toyota, R. Fukuda, J. Hasegawa, M. Ishida, T. Nakajima, Y. Honda, O. Kitao, H. Nakai, T. Vreven, J. A. Montgomery Jr., J. E. Peralta, F. Ogliaro, M. Bearpark, J. J. Heyd, E. Brothers, K. N. Kudin, V. N. Staroverov, R. Kobayashi, J. Normand, K. Raghavachari, A. Rendell, J. C. Burant, S. S. Iyengar, J. Tomasi, M. Cossi, N. Rega, J. M. Millam, M. Klene, J. E. Knox, J. B. Cross, V. Bakken, C. Adamo, J. Jaramillo, R. Gomperts, R. E. Stratmann, O. Yazyev, A. J. Austin, R. Cammi, C. Pomelli, J. W. Ochterski, R. L. Martin, K. Morokuma, V. G. Zakrzewski, G. A. Voth, P. Salvador, J. J. Dannenberg, S. Dapprich, A. D. Daniels, Ö. Farkas, J. B. Foresman, J. V. Ortiz, J. Cioslowski, D. J. Fox. . Gaussian, Inc.: Wallingford CT, 2009.
- ¹⁹ J. Tomasi, B. Mennucci, R. Cammi, *Chem. Rev.*, **2005**, *105*, 2999-3094.
- ²⁰ A. V. Marenich, C. J. Cramer, D.G. Truhlar, *J. Phys. Chem. B*, **2009**, *113*, 6378-6396.

- ²¹ H. Kessler, *Angew. Chem. Int. Ed. Engl.*, **1982**, *21*, 512-523.
- ²² a) H. Friebolin, *Basic One- and Two-Dimensional NMR Spectroscopy*; VCH Verlagsgesellschaft: Weinheim, New York, **1991**, p. 93, 263-291; b) E. L. Eliel, H. S. Wilen, *Stereochemistry of Organic Compounds*; John Wiley & Sons, New York, **1994**, p. 642.
- ²³ E. Fedeli, S. Hernández-Aínsa, A. Lancelot, R. González-Pastor, P. Calvo, T. Sierra, J. L. Serrano, *Soft Matter*, **2015**, *11*, 6009-6017.
- ²⁴ W. E. Stewart, T. H. Siddall, *Chem. Rev.*, **1970**, *70*, 517-551.
- ²⁵ H. C. Brown, *Determination of organic structures by physical methods*; E. A. Braude, F.C. Nachod editors, **1955** Academic Press, New York.
- ²⁶ a) F. S. Parker, *Applications of Infrared Spectroscopy in Biochemistry, Biology and Medicine*; Plenum Press, New York, **1971**, p. 351; b) R. M. Silverstein, F. X. Webster, D. J. Kiemle, *Identification spectroctrométrique de composés organiques*; De Boeck & Larcier s.a. **2007**, p. 95, 96, 101; c) R.A. Heacock, L. Marion, *Can. J. Chem.*, **1956**, *34*, 1782-1795.
- ²⁷ B. B. Hasinoff, H. B. Dunford, D. G. Horne, *Can. J. Chem.* **1969**, *47*, 3225-3232.
- ²⁸ D. G. Wu, D. Cahen, P. Graf, R. Naaman, A. Nitzan, D. Shvarts, *Chem. Eur. J.* **2001**, *7*, 1743-1749.
- ²⁹ M. A. van Dongen, B. G. Orr, M. M. Banaszak Holl, *J. Phys. Chem. B*, **2014**, *118*, 7195-7202.
- ³⁰ S. Alvarez, *Dalton Trans.*, **2013**, *42*, 8617- 8636.
- ³¹ S. Bhatia, Nanoparticles types, classification, characterization, fabrication methods and drug delivery applications. In *Natural Polymer Drug Delivery Systems*; Springer International Publishing, Switzerland **2016**; pp. 33-93.

List of publications

1. "Design, Synthesis and Structure of Novel G-2 Melamine-Based Dendrimers Incorporating 4-(n-Octyloxy)aniline as a Peripheral Unit"
C. Morar, P. Lameiras, A. Bende, G. Katona, E. Gál and M. Darabantu*
Beilstein. J. Org. Chem., **2018**, accepted with minor revisions (ISI 2016/2017: 2.337)
2. "New p-Aminophenol Based Dendritic Melamines. Iterative Synthesis, Structure and Electrochemical Characterisation"
C. Morar, G. Turdean, A. Bende, P. Lameiras, C. Antheaume, L. M. Muresan* and M. Darabantu*
C. R. Chim., **2017**, *20*, 402-414
<http://dx.doi.org/10.1016/j.crci.2016.07.002> (ISI 2016: 1.879)
3. "Novel N-modified Gycines Based on a (1S,2S)-2-Amino-1-(4-nitrophenyl)propane-1,3-diol Skeleton: 1,3-Dioxanes and Tripodands"
O. Moldovan, K. Albert, I. Nagy, **C. Morar**, C. Sacalis and M. Darabantu*
Tetrahedron Lett., **2016**, *57*(51), 5808-5811
<https://doi.org/10.1016/j.tetlet.2016.11.048> (ISI 2016 : 2.193)
4. "Glassy Carbon Electrode Modified with Hemin and New Melamine Compounds for H₂O₂ Amperometric Detection"
A. R. Deac, **C. Morar**, G. L. Turdean, M. Darabantu, E. Gál, A. Bende and L. M. Muresan
J. Solid State Electr., **2016**, *20*(11), 3071-3081
<http://link.springer.com/article/10.1007/s10008-016-3298-0?view=classic> (ISI 2016: 2.316)
5. "Synthesis of Some Selectively N-protected (1S,2S)-p-Nitrophenylserinol Based Diamino-1,3-dioxanes and Tripodands"
I. Nagy, O. Moldovan, F. Popa, P. Lameiras, **C. Morar**, C. Sacalis and M. Darabantu*
Synthetic Commun., **2015**, *45*(20), 2319-2330
<http://dx.doi.org/10.1080/00397911.2015.1078360> (ISI 2014/2015: 1.065)
6. "Convergent versus Divergent Three Steps Synthesis of the First (4-Aminophenoxy)alkanoic Acids Based Tripodal Melamines"
C. Morar, L. Cost, P. Lameiras, C. Antheaume and M. Darabantu*
Synthetic Commun., **2015**, *45*(14), 1688-1695
<http://dx.doi.org/10.1080/00397911.2015.1041048> (ISI 2014/2015: 1.065)
7. "Synthesis and Stereochemistry of New 1,3-Thiazolidine Systems Based on 2-Amino-2-(mercaptomethyl)propane-1,3-diol: 4,4-Bis(hydroxymethyl)-1,3-thiazolidines and c-5-Hydroxymethyl-3-oxa-7-thia-r-1-azabicyclo[3.3.0]octanes"
C. Morar, C. Sacalis, P. Lameiras, A. Soran, H. Khartabil, C. Antheaume, I. Bratu, O. Moldovan and M. Darabantu*
Tetrahedron, **2013**, *69*(47), 9966-9985
<http://dx.doi.org/10.1016/j.tet.2013.09.070> (ISI 2013: 2.817)